AMPHIPHILIC BLOCK COPOLYMERS ON A DENDRIMER CORE

By

YOUNG HIE KIM

Bachelor of Science
Kangwon National University
Chunchon, Korea
1984

Master of Science
Purdue University
West Lafayette, IN
1997

Submitted to the Faculty of the
Graduate College of the
Oklahoma State University
in partial fulfillment of
the requirements for
the Degree of
DOCTOR OF PHILOSOPHY
May, 2007

AMPHIPHILIC BLOCK COPOLYMERS ON A

DENDRIMER CORE

Thesis Approved:

_____Warren T. Ford_____
Thesis Advisor

_____K. Darrell Berlin_____

_____Richard A. Bunce_____

_____James P. Wicksted_____

_____A. Gordon Emslie_____
Dean of the Graduate College

PREFACE

Polymers are large molecules composed of many smaller units. Dendrimers are a class of highly branched polymers with spherical shape and dimensions in nanometers, i.e., one-billionth of a meter. Amphiphilic molecules contain both water loving (hydrophilic) and water hating (hydrophobic) chains as in soaps and detergents. Dendrimers with amphiphilic end branches may be good for dispersion of nanomaterials. These dendrimers might be used as molecular weight and size standards and as hosts for the transport of biologically important guests due to their small uniform size.

A linear copolymer has chains composed of two or more different monomers linked together. Linear chains that consist of a long sequence of one repeating unit and then a long sequence of a different repeating unit are called block copolymers. By controlled methods, growth of polymer chains from the end groups of a dendrimer would convert a dendrimer of one size to larger molecules with relatively low distribution of sizes of molecules. The controlled method of atom transfer radical polymerization (ATRP) was used to synthesize amphiphilic block copolymers of hydrophobic styrene and hydrophilic acrylic acid from the dendrimer chain ends. The amphiphilic block copolymer dendrimers in water formed aggregates from about 40 nm to > 100 nm in diameter. Atomic force microscopy (AFM) images of spin coated thin films show that the materials have aggregation characteristics of amphiphilic PS-PAA block copolymers,

in general, as shown by morphological transitions either from spherical to worm-like or from worm-like to spherical aggregates.

An emulsion is a finely divided mixture of two immiscible substances, like oil (hydrophobic) and water (hydrophilic). These hydrophobic oil droplets are dispersed in water and are surrounded by amphiphilic surfactant (soap) to prevent coagulation of the oil. Emulsion polymerization is used to produce latexes that are a suspension of rubber or plastic (polymer) particles in water. To produce the dendritic styrene latex, styrene monomer was mixed with a dendrimer and an initiator and polymerized in water either with or without the surfactant. The presence of a surfactant reduced the average diameter of dendritic styrene latexes to approximately 50 nm with broad particle size distribution (PSD). More than 100 nm and narrower PSD were obtained in the absence of surfactant.

ACKNOWLEDGEMENTS

I would like to thank Dr. Warren Ford for being an outstanding advisor. His guidance, patience and insightful knowledge on my research project through my stay at Oklahoma State University have allowed me to gain valuable experiences in organic and polymer science. Under the guidance of him, it has allowed me to become an independent researcher who is able to construct and solve my research related problems.

I would also like to thank my research committee: Dr. Darrell Berlin, Dr. Richard Bunce, Dr. James Wicksted, and Dr. Andrew Mort, for their patience, time and assistance with my dissertation and research proposal. I also thank the following people for instrumental and research assistance: Dr. Margaret Eastman, Gianna Bell-Eunice, Phoebe Doss, Terry Colberg, Dr. Susheng Tan, Dr. Zushen Xu, Drs. Dongqi and Shuhui Qin and Dr. Ziad El Rassi's group.

I also thank the Ford Group for the conversations and memories. I must specifically thank: Dr. Robert Sherman Jr. and Rani Karnati for their friendships and research assistance during my stay.

I would also like to thank my family for their support, patience, and encouragement through all my education.

I would also like to thank the National Science foundation and Petroleum Research Fund for financial assistance to this project and Oklahoma State University for my education and financial support as a teaching assistant.

TABLE OF CONTENTS

LIST OF TABLES

CHAPTER II

CHAPTER III

CHAPTER IV

LIST OF FIGURES

CHAPTER I

CHAPTER II

CHAPTER III

Figure Page

CHAPTER IV

Figure Page

LIST OF SCHEMES

CHAPTER II

CHAPTER III

CHAPTER IV

CHAPTER I

DENDRIMERS AND ATOM TRANSFER RADICAL POLYMERIZATION

Introduction

Dendrimers are large and spherical macromolecules with a highly branched three-dimensional architecture. They are monodisperse, meaning of a consistent size. Their structures consist of core, branches, and end groups.[1-8] The structure of poly(propylene imine) (PPI) dendrimer generations 1-5 is shown in Figure 1.

Dendrimers have attractive structural features that include the nanoscopic sizes of the molecules, spherical surfaces, and spacious interior.[4,6,9] The physical properties of dendrimers are dependent upon their structural features.[1-9]

There are two well-known methods of dendrimer synthesis, divergent and convergent (Figure 2).[1,2,5,6] In either method, the synthesis requires a stepwise process, which is the reason for the monodisperse composition. By the divergent method, the dendrimer grows outward from the core to the periphery. The molar mass of the dendrimer is approximately doubled with each increasing generation. Large dendrimers have been prepared by this approach. Incomplete growth steps and side reactions, however, become unavoidable and leave impurities. In the convergent approach, the

dendrimer is produced from the surface towards the interior by linking surface units together with more monomers step by step. This provides for simple purification as impurities and side products are minimized. [1,2,5,6]

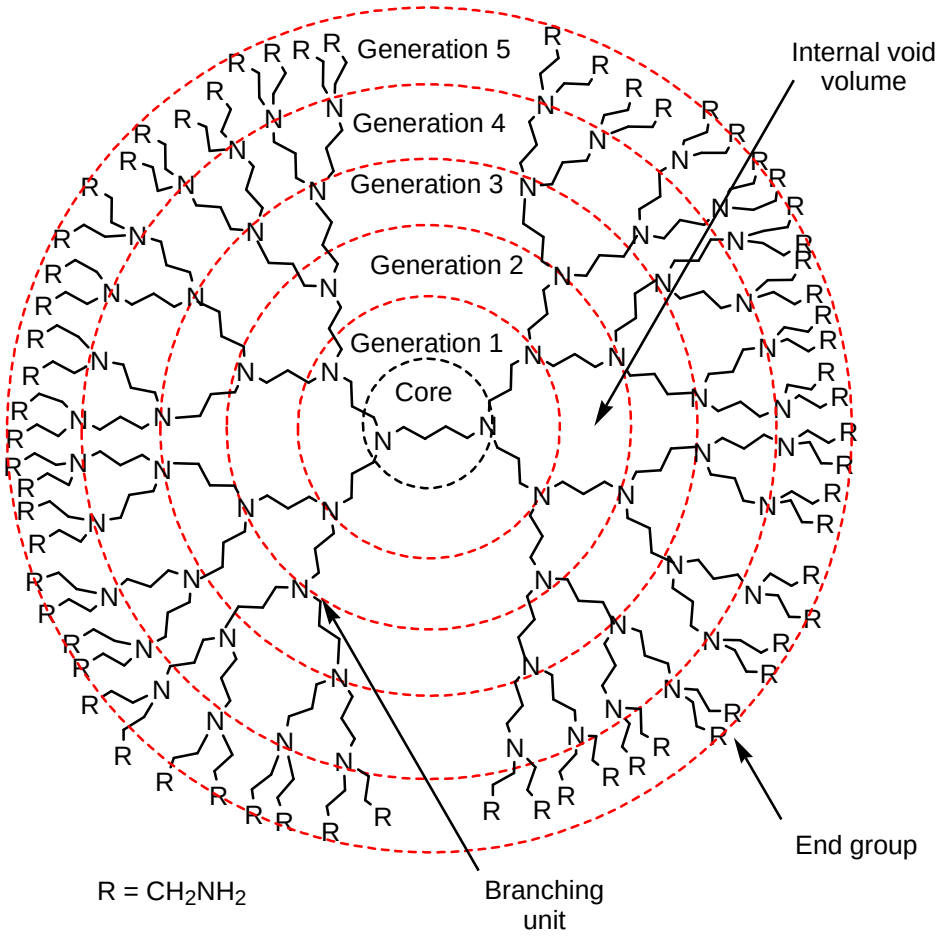

Figure 1. PPI dendrimer generations 1-5 showing the morphological structural aspects that consist of core, branching unit, internal void volume, and end group.

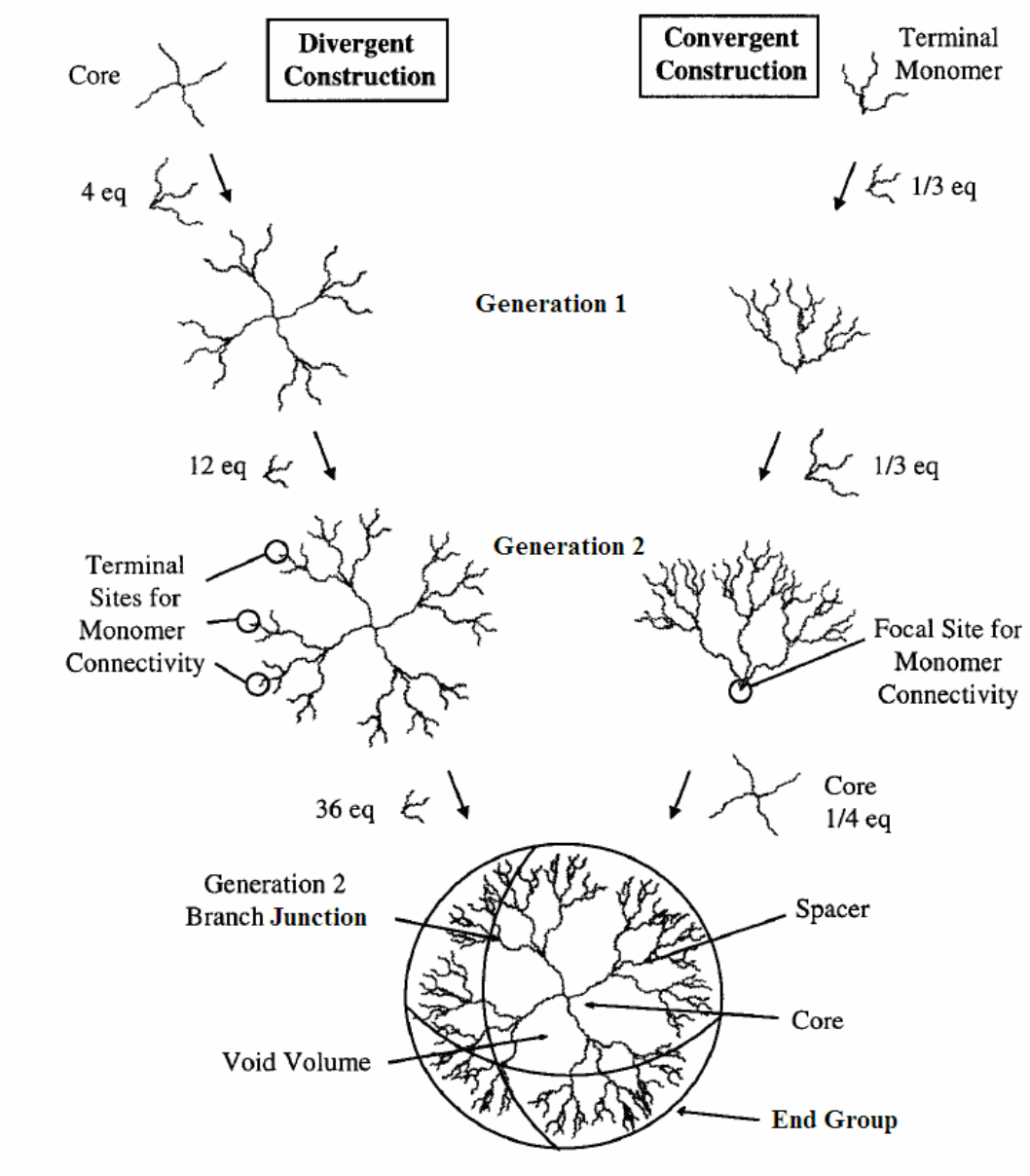

Figure 2. Dendrimer construction with divergent and convergent procedures.[10]

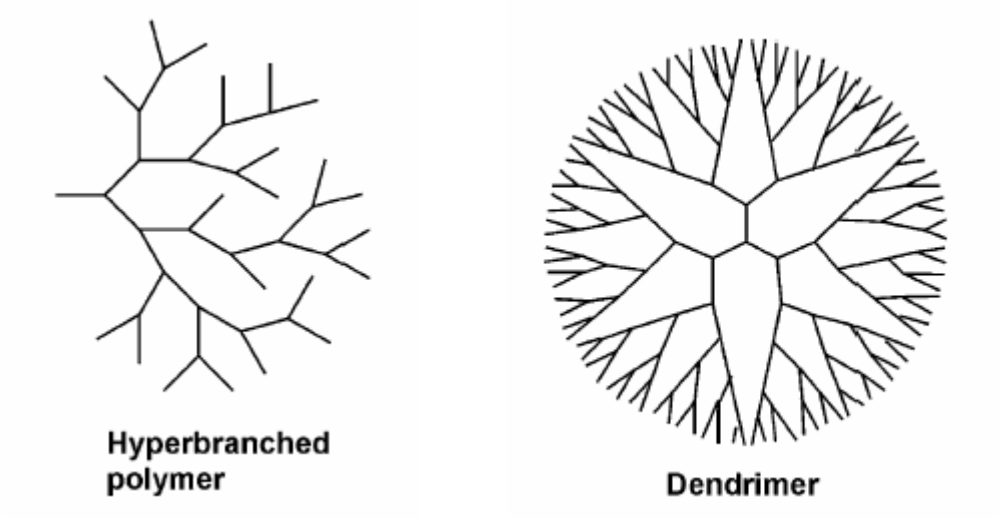

Figure 3. Hyperbranched polymer and dendrimer.[11]

In contrast, the structures of hyperbranched polymers are not as precisely controlled so that it makes them imperfect molecules. Hyperbranched polymers can be obtained by the one-pot polymerization of AB_2 monomers, as long as A reacts only with B from another molecule. Reactions between A and B from the same molecule terminate the polymerization by cyclization. This synthesis method produces broad molecular weight distributions and irregular arm growth.[4,6,12] There are missing parts in the structure and fewer active chemical groups at the surface of these molecules. Such hyperbranched structures provide lower viscosity and more space inside the molecules that leads to an advantage for binding larger molecules.[13]

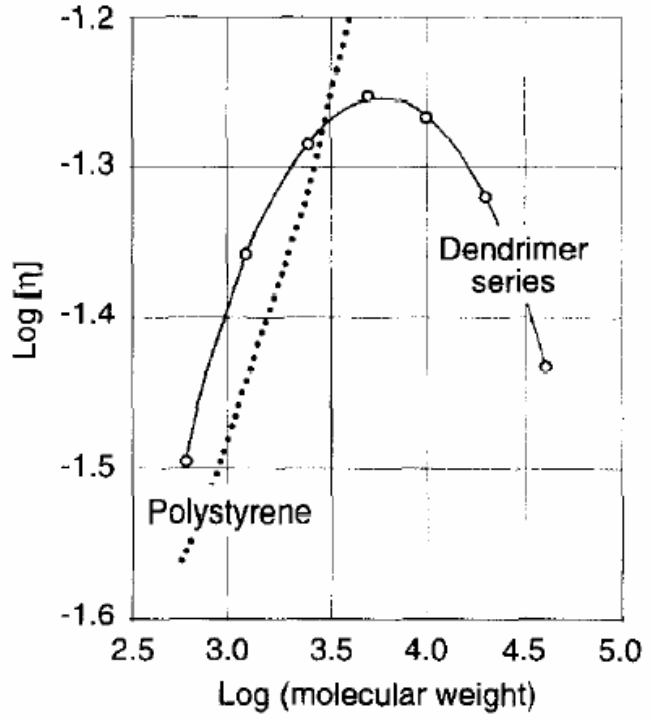

Figure 4. A plot of the intrinsic viscosity [η] against molecular weight for nitrile-terminated PPI dendrimer series and polystyrene.[3,5]

The intrinsic viscosity, glass transition temperature, and solubility of dendrimers are different from those properties of linear polymers.[5,21] In general, the intrinsic viscosity increases the increasing molecular weight of linear polymers (Figure 4). In the case of dendrimers, intrinsic viscosity [η] is inversely proportional to the hydrodynamic density and is proportional to the hydrodynamic volume (V_H)[21,22]

$$[\eta] = 2.5N_aV_H/M = (10\Pi/3)N_aR_H^3/M$$

where R_H is the hydrodynamic radius and N_a the Avogadro number. Intrinsic viscosity $[\eta]$ in dendrimers goes through a maximum as molecular weight (M) of dendrimers increases (Figure 4). This fact may result from the globular shapes of higher generation dendrimers, leaving them unable to tangle with one another such as the case of linear polymers. As the branching points at the peripheral regions get crowded, its steric congestion affects the structural features. Dendrimers at low generations ($1 \rightarrow 3$) have generally open, floppy structures; however, the dendrimers have more globular conformation at higher generations (>4).[23] Spherical dendrimers form until steric crowding of the end groups limits complete reaction at a specific generation and also destroys the monodispersity of molecules.[5]

The glass transition temperature (T_g) of dendrimers is known to be a function of the number of arms and the molecular weight. End group, core, branch unit, and functionality are the parameters to be measured. The theoretical finding by Shutz is that the backbone glass temperature has influence over the T_g.[3,24]

Monodispersity and globular shape of dendrimers provide interesting properties for study of molecular topology. The surface and interior of the dendritic sphere are two distinct chemical environments. Two chemical environments play an important role for guest and host molecules for the existence of voids in the dendrimer chemistry. This unique environment of the dendrimer interior and surface is influenced by hydrophobic/hydrophilic interactions. Dendrimers have been utilized as molecular weight and size standards,[25] as gene transfection agents, as hosts for the transport of biologically important guests,[23,26] and as anti-cancer agents.[23,26,27]

A number of functionalities and high local densities of active sites at the surface areas in a dendrimer molecule have drawn a lot of attention from medicinal chemistry. Multivalency on the surface of the dendrimers allows enhancing the drug-loading capacity of carriers and strengthening of ligand-receptor binding.[23,28]

Dendrimers as catalytic agents have been also utilized for their high surface functionality.[28]

Dendrimers are widely becoming recognized as versatile and well controlled nanoscale building blocks along with metal nanocrystals and nanotubes.[27,29-32] By adjusting chemical properties of the core, the shells, and especially the surface layer, dendrimers can be modified to fit the needs of specific applications in nanotechnology.

Controlled radical polymerization in general produces narrow molecular weight distribution (MWD) and enables synthesis of block copolymers, which can not be accomplished by conventional radical polymerization. In conventional radical polymerization chain termination causes polymers with broad molecular weight distributions.[33]

The Matyjaszewski research group has developed a method of controlled/"living" polymerization that is capable of polymerizing a wide variety of monomers and is tolerant of trace impurities such as water and inhibitor. The system that was developed was termed Atom Transfer Radical Polymerization (ATRP). ATRP is the most widely used of the living polymer methods.[33-41]

In ATRP, a transition metal species abstracts a halogen atom from the organic halide (dormant) to form the oxidized species and a carbon centered radical (active). A radical addition to monomer then occurs. The reaction between oxidized transition metal

and chain radical result in a target polymer and recycles the reduced transition metal species. The small equilibrium constant of the activation step lowers the concentration of growing radicals and reduces the contribution of radical-radical termination significantly, providing well-defined polymers with low polydispersity.[33-41]

(a) Stepwise mechanism[38,39]

Initiation

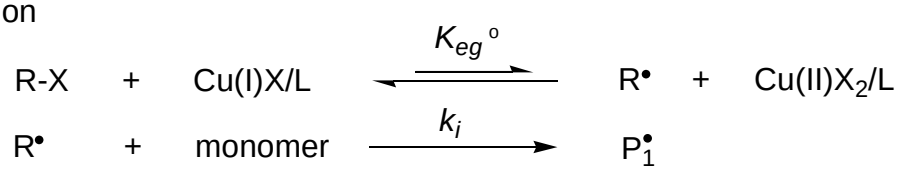

Propagation

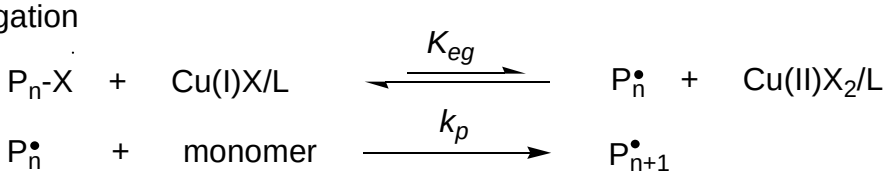

Termination

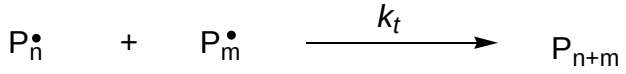

R· = alkyl radical X = Cl or Br

L = complexing ligand monomer = vinyl monomer

P_n-X = dormant P_n· = active polymer chain

P_{n+1}· = growing radical k_i = rate constant of initiation

k_p = rate constant of propagation k_t = rate constant of termination

$K_{eg}{}^{o}$ = equilibrium constant for initiation

K_{eg} = equilibrium constant for propagation

(b) Reversible mechanism[34,37]

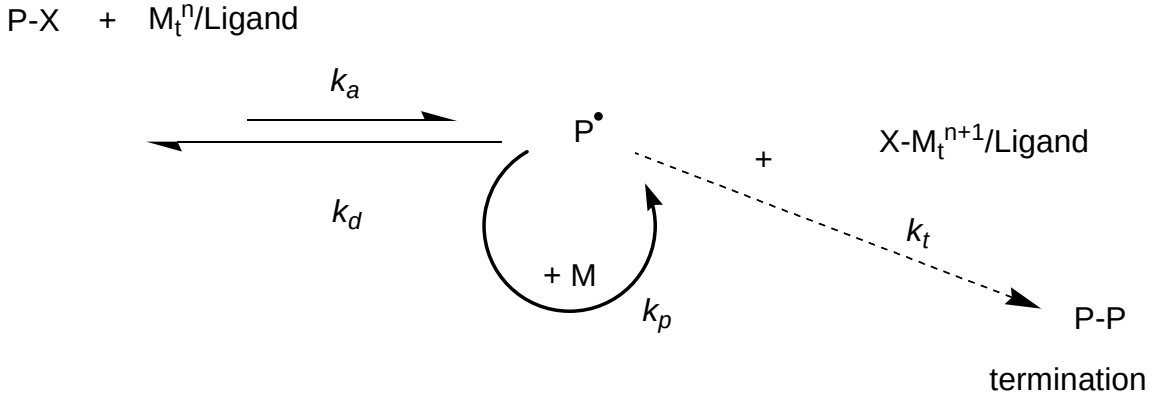

P-X = propagating dormant	M_t^n = transition metal
Ligand = complexing ligand	P· = propagating radical
X = Br or Cl	M = vinyl monomer
k_a = rate constant of activation	k_d = rate constant of deactivation
k_p = rate constant of propagation	k_t = rate constant of termination

Figure 5. Mechanisms of ATRP.

ATRP is based on a reversible exchange between a low concentration of growing radicals and a dormant species. Reactivation of the dormant species allows the polymer chains to grow and deactivate later. The radical is formed by a transition metal catalyst that is abstracting the halogen atom at the chain end of the organic initiator for ATRP. The end group of the organic initiator is usually an alkyl halide. The reversible process results in a polymer chain that grows slowly and gradually and has a well-defined end group due to minimum termination under appropriate conditions.[33-37,41]

The initiator efficiency is possibly dependent upon halogen exchange between the growing chains and the metal center. The order of bond strength in alkyl halide is *R*-Cl >

R-Br > *R*-I. Thus, alkyl chloride should be the least efficient initiator and alkyl iodide the most efficient. The affinities toward metal catalysts are also important. In the case of the affinities toward metal catalysts, if the relative affinity of halide is higher toward carbon, low affinities toward metal catalysts can be still used. The use of alkyl bromides as initiators has additional advantages compared with chlorides because of the faster exchange reaction which results in polymers with lower polydispersities. However, some side reactions occur more readily for *R*-Br/Cu-Br than for the mixed halide systems. Use of alkyl iodides requires special precautions due to their light sensitivity, the low affinity of iodine toward most metals, and the possibility of heterolytic cleavage of the *R*-I bond.[36]

Other types of living polymerizations are more restricted than ATRP by many factors: a limited number of monomers available, sensitivity to moisture, and incompetence to randomly copolymerize with two or more monomers. Radical polymerization is not susceptible to moisture so that emulsions or suspensions can be performed in water.[40] Copolymerization can be accomplished with two or more monomers. Therefore controlled/"living" radical polymerization provides a method to maximize the potential of living polymerizations.

ATRP has been able to polymerize a wide range of monomers including various styrenes, acrylates and methacrylates as well as other monomers such as acrylonitrile, vinylpyridine, and dienes.[34,35] In general, ATRP uses simple alkyl halides as initiators and transition metals such as iron and copper as the catalysts. The transition metal is complexed by one or more ligands. These catalysts can be used in very low amounts,

whereas other ATRP systems require the use of more expensive reagents such as Ru complexes.[34,36,41]

The well-known disadvantage of ATRP is the need to remove and the transition metal complex from the resulting polymer, because the initial transition metal complex can contaminate the polymer and also can be recycled at the end of polymerization.

By ATRP, polymers with controlled molar masses and narrow polydispersities can be obtained. ATRP is readily applicable to dendrimers which are aimed to produce well-defined and narrow polydisperse amphiphilic block copolymers with controlled molecular weights dendrimers. Also, ATRP allows dendrimers to enlarge quickly and retain narrow molecular weight distribution (MWD).

Living radical polymerization was used to obtain well-defined and narrow polydispersity amphiphilic block copolymers with controlled molecular weights. ATRP was the method chosen for the living radical polymerization described in this dissertation, enabling to control the type of amphiphilic polymers. A new class of macroinitiators was developed by using the PPI dendrimer and then used as a precursor for block polymers. Highly branched structural features in the PPI dendrimer allowed us to control of polymer architecture, size and shape, and a multiplicity of chain ends that were functionalized further by polymerization. The diameters of the spherical PPI dendrimers (generation 2 to generation 5) range from 2 to 5 nm.[42] By taking advantage of architecture and size of the PPI dendrimer, the main objective of the project was to synthesize and characterize the monodisperse branched polystyrene with chain lengths of 50 repeat units and poly(*t*-butyl acrylate) with chain lengths of 100-450 repeat units from dendrimer chain ends in the 64- arm PPI dendritic ATRP initiator. These types of

amphiphilic block polymers allowed us to attempt synthesis of the monodisperse polymer particles with 10 to 100 nm in diameters, which can be accomplished by emulsion polymerization of styrene.

References

(1) Newkome, G. R.; Moorefield, C. N.; Vogtle, F. *Dendrimers,* 2nd Edition; Wiley: Chichester, United Kingdom, 2001.

(2) Tomalia, D. A.; Durst, H. D. *Topics in Current Chemistry* **1993**, *165*, 193-313.

(3) van Genderen, M. H. P.; de Brabander-Van Den Berg, E. M. M.; Meijer, E. W. *Advances in Dendritic Macromolecules* **1999**, *4*, 61-105.

(4) Tomalia, D. A. *Materials Today (Oxford, United Kingdom)* **2005**, *8*, 34-46.

(5) Matthews, O. A.; Shipway, A. N.; Stoddart, J. F. *Progress in Polymer Science* **1998**, *23*, 1-56.

(6) Tomalia, D. A. *Progress in Polymer Science* **2005**, *30*, 294-324.

(7) Tomalia, D. A.; Frechet, J. M. *Progress in Polymer Science* **2005**, *30*, 217-219.

(8) Smith, D. K.; Hirst, A. R.; Love, C. S.; Hardy, J. G.; Brignell, S. V.; Huang, B. *Progress in Polymer Science* **2005**, *30*, 220-293.

(9) Bosman, A. W.; Janssen, H. M.; Meijer, E. W. *Chemical Reviews (Washington, D. C.)* **1999**, *99*, 1665-1688.

(10) Newkome, G. R.; He, E.; Moorefield, C. N. *Chemical Reviews (Washington, D. C.)* **1999**, *99*, 1689-1746.

(11) Gao, C.; Yan, D. *Progress in Polymer Science* **2004**, *29*, 183-275.

(12) Hanselmann, R.; Hoelter, D.; Frey, H. *Macromolecules* **1998**, *31*, 3790-3801.

(13) Voit, B. *Journal of Polymer Science, Part A: Polymer Chemistry* **2000**, *38*, 2505-2525.

(14) Frechet, J. M. J. *Science (Washington, DC, United States)* **1994**, *263*, 1710-1715.

(15) Hobson, L. J. *Chemical Communications (Cambridge)* **1997**, 2067-2068.

(16) Rietveld, I. B.; Bedeaux, D. *Journal of Colloid and Interface Science* **2001**, *235*, 89-92.

(17) Tande, B. M.; Wagner, N. J.; Mackay, M. E.; Hawker, C. J.; Jeong, M. *Macromolecules* **2001**, *34*, 8580-8585.

(18) Jeong, M.; Mackay, M. E.; Vestberg, R.; Hawker, C. J. *Macromolecules* **2001**, *34*, 4927-4936.

(19) Drew, P. M.; Adolf, D. B. *Soft Matter* **2005**, *1*, 146-151.

(20) Cai, C.; Chen, Z. Y. *Macromolecules* **1998**, *31*, 6393-6396.

(21) Lepoittevin, B.; Matmour, R.; Francis, R.; Taton, D.; Gnanou, Y. *Macromolecules* **2005**, *38*, 3120-3128.

(22) Gauthier, M.; Li, W.; Tichagwa, L. *Polymer* **1997**, *38*, 6363-6370.

(23) Lee, C. C.; MacKay, J. A.; Frechet, J. M. J.; Szoka, F. C. *Nature Biotechnology* **2005**, *23*, 1517-1526.

(24) Tande, B. M.; Wagner, N. J.; Kim, Y. H. *Macromolecules* **2003**, *36*, 4619-4623.

(25) Lederer, A.; Voigt, D.; Appelhans, D.; Voit, B. *Polymer Bulletin (Heidelberg, Germany)* **2006**, *57*, 329-340.

(26) Gillies, E. R.; Frechet, J. M. J. *Drug Discovery Today* **2005**, *10*, 35-43.

(27) Portney, N. G.; Ozkan, M. *Analytical and Bioanalytical Chemistry* **2006**, *384*, 620-630.

(28) Dykes, G. M. *Journal of Chemical Technology & Biotechnology* **2001**, *76*, 903-918.

(29) Amama, P. B.; Maschmann, M. R.; Fisher, T. S.; Sands, T. D. *Journal of Physical Chemistry B* **2006**, *110*, 10636-10644.

(30) Wang, Y. A.; Li, J. J.; Chen, H.; Peng, X. *Journal of the American Chemical Society* **2002**, *124*, 2293-2298.

(31) Sano, M.; Kamino, A.; Shinkai, S. *Angewandte Chemie, International Edition* **2001**, *40*, 4661-4663.

(32) Geng, J.; Li, H.; Zhou, D.; Huck, W. T. S.; Johnson, B. F. G. *Polyhedron* **2006**, *25*, 585-590.

(33) Matyjaszewski, K. *ACS Symposium Series* **2000**, *768*, 2-26.

(34) Matyjaszewski, K.; Xia, J. *Chemical Reviews (Washington, D. C.)* **2001**, *101*, 2921-2990.

(35) Coessens, V.; Pintauer, T.; Matyjaszewski, K. *Progress in Polymer Science* **2001**, *26*, 337-377.

(36) Pintauer, T.; Matyjaszewski, K. *Coordination Chemistry Reviews* **2005**, *249*, 1155-1184.

(37) Matyjaszewski, K. *ACS Symposium Series* **1998**, *685*, 2-30.

(38) Patten, T. E.; Matyjaszewski, K. *Advanced Materials (Weinheim, Germany)* **1998**, *10*, 901-915.

(39) Wang, J.-L.; Grimaud, T.; Shipp, D. A.; Matyjaszewski, K. *Macromolecules* **1998**, *31*, 1527-1534.

(40) Patten, T. E.; Matyjaszewski, K. *Accounts of Chemical Research* **1999**, *32*, 895-903.

(41) Matyjaszewski, K. *Chemistry--A European Journal* **1999**, *5*, 3095-3102.

(42) Mark, J. E. *Polymer Data Handbook*; Oxford University Press: New York, **1999**, 859.

CHAPTER II

FUNCTIONAL MODIFICATION OF POLY(PROPYLENE IMINE) DENDRIMERS

Introduction

Diffusion of solute molecules is an important physical property of polymer solutions and gels. It is important to understand the effect of polymer concentration, size and shape of the diffusant, temperature, and molecular interaction within the polymer solutions or polymer gels. Study of diffusion behavior of molecules having various functional groups, such as, alcohol, amine, ammonium salt, amide, and carboxylate acid, in poly(vinyl alcohol) shows that molecular size and chemical interaction are very important in diffusion behavior.[1] However, most studies of polymer diffusion have been devoted to linear polymers.[2,3,4] Further understanding of the diffusion process should include narrow polydispersity of the linear polymers. Better control of molecular size and spherical shape make dendrimers an attractive choice to compare with all linear polymers. In addition, dendritic polymers are monodisperse.[5-12] These features make dendrimers useful as ideal diffusion molecules. For the self-diffusion of dendritic polymers, three different PPI dendrimers with hydrophilic triethylenoxy methyl ether

Scheme 1. Structures of PPI Dendrimers, G2, G4, and G5.

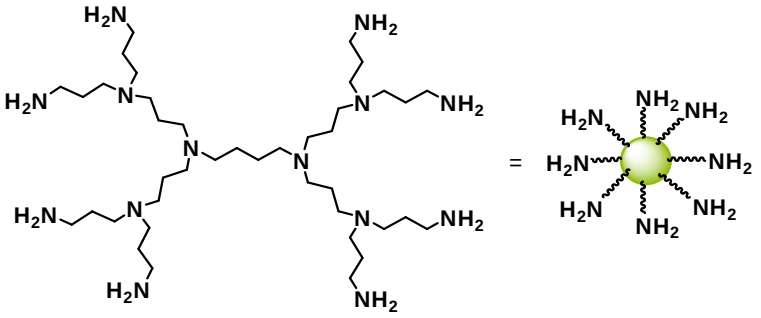

DAB-*dendri*-$(NH_2)_8$, G2

1

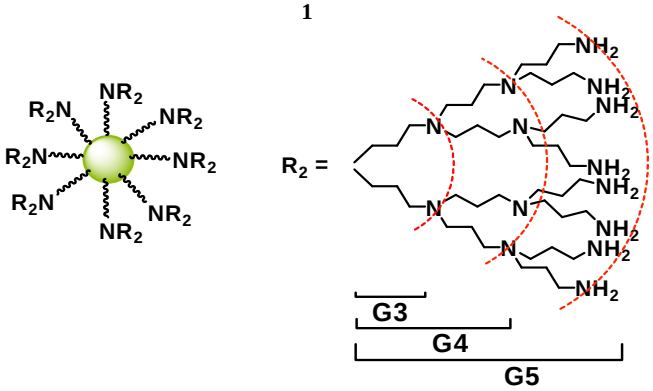

DAB-*dendri*-$(NH_2)_{32}$, G4 and DAB-*dendri*-$(NH_2)_{64}$, G5

2 **3**

(TEO) groups at chain ends were synthesized by a procedure, modified from Pan and Kreider, and characterized by ^{1}H NMR and ^{13}C NMR.[13,14] These PPI dendrimers were studied and compared with linear poly(ethylene glycol)s (PEGs). The diffusion study of the modified PPI dendrimers was accomplished by the Zhu group at the University of Montreal.[1]

The structures of PPI dendrimers have amine sites at all branch points and chain ends. Dendrimers change conformation to be more spherical with increasing molecular weight. The conformational change is significant between dendrimers **2** and **3** because the mass increases more than the volume of the sphere that encloses the molecule.[5-12]

Our group has synthesized PPI dendrimers quaternized at chain ends only, at chain ends and branch points, and at branch points only.[14] For these purposes the primary amine end groups of DAB-*dendr*-$(NH_2)_n$ (n = 8, 32 and 64) **1**, **2**, and **3** first were converted to tertiary amines using formic acid and formaldehyde. The synthesis of tertiary amine dendrimers with both hydrophilic and hydrophobic groups at every end and their conversion from poly(propylene imine) dendrimers DAB-*dendr*-$(NH_2)_n$ (n = 8, 32 and 64) **1**, **2**, and **3** to quaternary ammonium ion dendrimers have been studied. The method for methylation of dendrimers with formaldehyde in formic acid was proven by ^{13}C NMR to produce mixed secondary/ tertiary amines even with a large excess of reagents and long reaction time. A need for complete conversion of primary amines to tertiary amines has prompted us to investigate reductive ethylation of the primary and secondary amines.

Primary amine dendrimers coordinate with a Group I or II metal.[15-19] The methylation was also considered to prevent amine-metal ion coordination during a standard work-up. The product tertiary amine dendrimers have been completely extracted from aqueous sodium hydroxide solution. It is also desirable if the reductive methylation proceeds in one step without use of $LiAlH_4$ because Li^+ or Al^{3+}coordinates with dendrimer more strongly than Na^+ with dendrimers so that Li^+ and Al^{3+} can be difficult to remove from the dendrimers.

Reductive alkylation by $NaBH_4$-CH_3COOH has been reported for the conversion of a primary or secondary amine to a tertiary ethyl amine in one step. The reductive alkylation has been primarily developed by Gribble and colleagues, who noted that the

reaction mixture should be free of moisture and that sodium borohydride should be added into the amine-carboxylic acid mixture kept at approximately 50 ^{o}C.[20-26]

After the preliminary ethylation of dendrimers **1**, **2**, and **3** in $NaBH_4$-CH_3COOH, deuteroethyl PPI dendrimers were prepared in one step with sodium borodeuteride in acetic acid-d_4 at 50-55 ^{o}C under nitrogen atmosphere. The reaction of the PPI dendrimers **1**, **2**, and **3** with $NaBD_4$– CD_3COOD gave the desired tertiary amine in good yield. The synthesis of deuteroethyl PPI dendrimers is presented and discussed.

Dendrimers with deuterated ethyl tertiary amine chain ends were prepared to understand conformation of the dendrimers by neutron diffraction and chain motions in solid state by ^{2}H NMR. Deuterated ethylation of **2** and **3** was carried out for the structural analysis.

Results and Discussion

Amidation of PPI Dendrimers at Chain Ends. The purpose of PPI dendrimers having triethylenoxy methyl ether chain ends was to determine how molecular size affects diffusion in gels of aqueous poly(vinyl alcohol). Hydrophilic dendrimers modified at chain ends were prepared in two steps from PPI dendrimers **1**-**3**. Oxalyl chloride **5** was reacted with 2-[2-(2-methoxyethoxy)ethoxy]acetic acid **4** in toluene to give 2-[2-(2-methoxyethoxy)ethoxy]acetyl chloride **6**.[1,13,14,27] Oxalyl chloride was used instead of $SOCl_2$ because it leaves no sulfur-containing colored impurities. Reaction of the acid chloride **6** with **1**, **2**, and **3** gave the amide dendrimers **7**, **8**, and **9** as shown in Scheme 2.[1,13,14] *N,N*-Dimethylformamide (DMF) was used as the solvent and catalyzed

formation of the amide. The ^{1}H and ^{13}C NMR spectra of the three hydrophilic dendrimers **7-9** made by a slightly modified procedure here were the same as the spectra of those reported before.[13,14]

The NMR relaxation time experiments were performed by the Zhu group to study the motion of different parts of the dendrimer, such as core and terminal groups.[1] The proton NMR relaxation time (T_1 and T_2) experiments show that the mobility of both core and terminal groups in the dendrimers **1-3** decreases as the size of the dendrimers increases. The experiments also indicate that the chain ends are more mobile than the core groups of the protons for the dendrimers **1-3**.

Scheme 2. Amidation of PPI Dendrimers at Chain Ends.

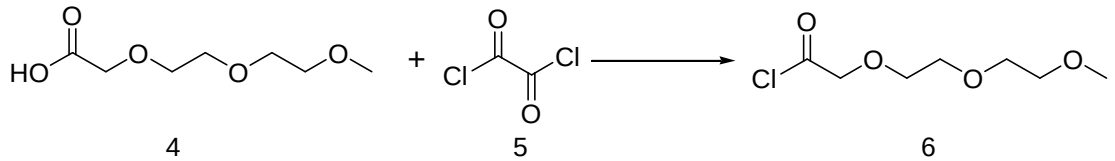

4 5 6

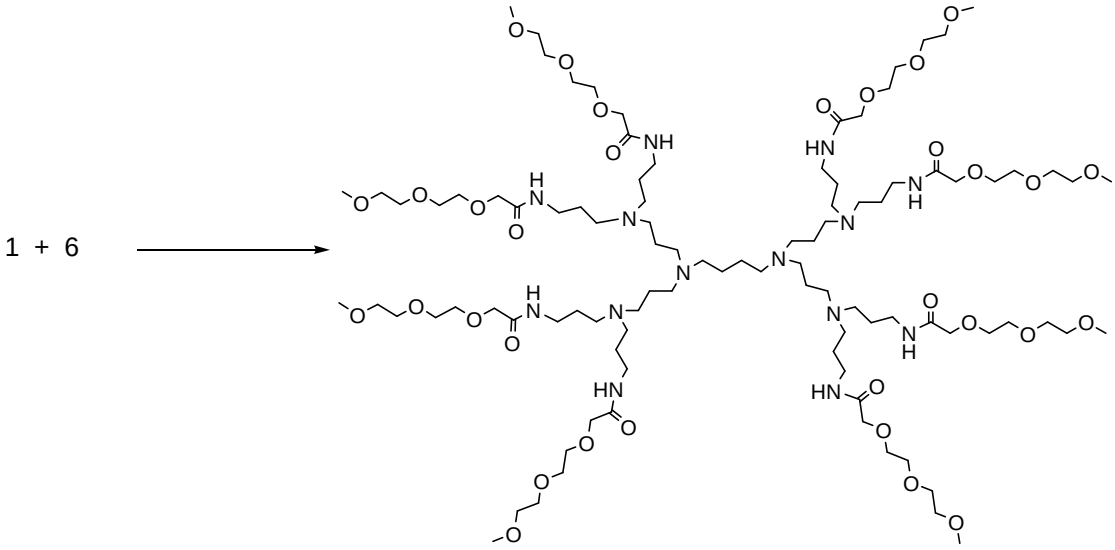

7

2 + 6 → 8

3 + 6 → 9

Reactions of PPI Dendrimers DAB-*dendri*-$(NH_2)_n$ (n = 8, 32, and 64) with $NaBH_4$-CH_3COOH. The purpose of ethylation of the chain ends of PPI dendrimers was to prepare deuterated dendrimers for study of their packing by neutron diffraction and for study of their chain motion by solid state ^2H NMR spectroscopy. In order to examine suitable reaction conditions for ethylation of the dendrimers using the $NaBH_4$-CH_3COOH system, the following were considered: reaction time, co-solvent, reaction scale, and type of sodium borohydride. Results of ethylation of the dendrimers in $NaBH_4$-CH_3COOH are as shown in Table 1.

Scheme 3. Ethylation of PPI Dendrimers in Glacial Acetic Acid and Sodium Borohydride.

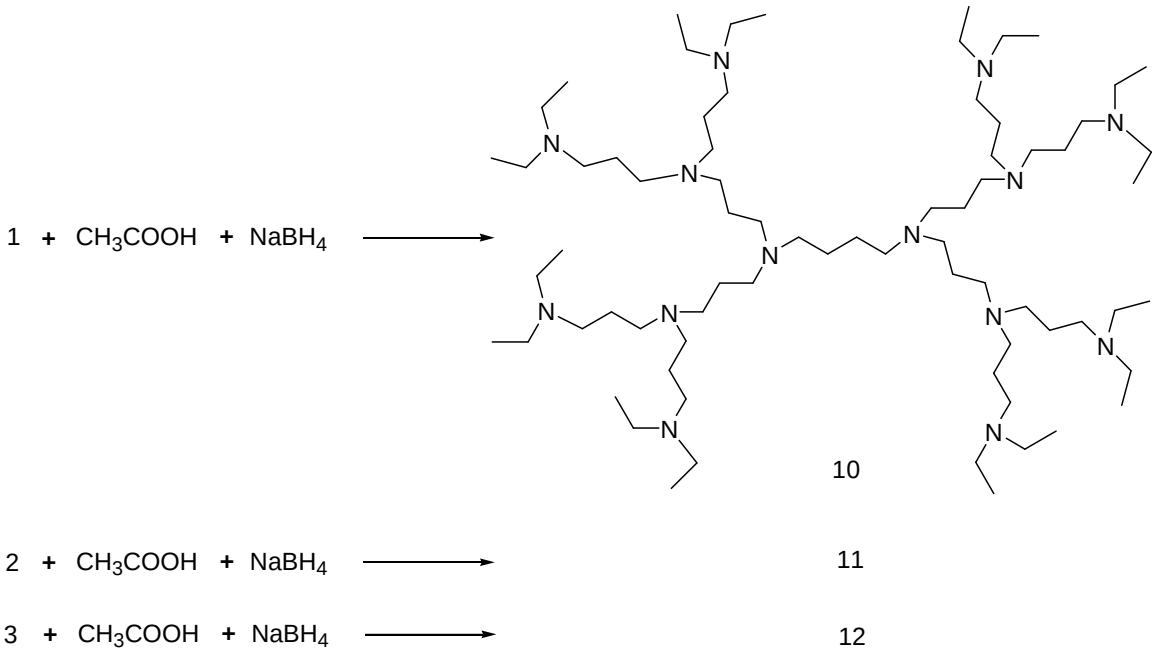

Table 1. Reaction Conditions for Ethylation of Amines in Glacial Acetic Acid and Sodium Borohydride.[a]

product	reaction time	cosolvent (mL)	dendrimer reactant (g)	type of $NaBH_4$ (g)	Yield[b] (%)
10	8.5 h	THF (10)	1.000	powder (3.760)	96
10	17.5 h	-	0.250	granule (0.977)	96
10	3 days	THF (10)	1.000	powder (3.760)	72
10	5 days	-	1.000	powder (3.760)	88
11	11.5 h	-	0.250	granule (0.828)	86[c]
11	5 days	-	1.000	powder (3.276)	86
12	11.5 h	-	0.250	granule (0.811)	97
12	5 days	-	1.000	powder (3.212)	96

[a] Reaction was performed at 55 ^{o}C. [b] Recovered product yields without trace of solvent peaks in NMR spectra. [c] Observed only mixed secondary/tertiary dendrimers.

Regardless of changes in reaction time, reaction scale, and type of sodium borohydride, there was no apparent difference in ethylation for any of the cases in terms of product recovered yield. The reaction of sodium borohydride with glacial acetic acid was somewhat vigorous. Giving off H_2 gas caused the reaction mixture to overflow out of the reaction flask in a short period of time. To avoid the potential hazard with a large reaction scale, different types of sodium borohydride were examined in an effort to slow down the reaction. Three types of sodium borohydride are commercially available; caplets, granules, and powder. Gribble and others used caplets and granules predominantly to prevent rapid evolution of H_2.[20,22] Two sodium borohydrides, granules and powder, were selected to investigate in our experiments. No significant difficulty in handling the reaction was found in either case under the same experimental conditions. However, only the powder is available for sodium borodeuteride.

Due to deuterium kinetic isotope effects, reduction with $NaBD_4$ was expected to take much longer than with $NaBH_4$. The dendrimers are stable up to 5 days in the $NaBH_4$-CH_3COOH system. The reaction of **2** with $NaBH_4$-CH_3COOH gave mixed secondary/tertiary dendrimers after 11.5 h and complete conversion to tertiary amines after 5 days. In some experiments, tetrahydrofuran (THF) was used as a cosolvent to decrease the viscosity of the solution and to increase the solubilty of the sodium borohydride powder. Comparison of the results with or without THF indicated there was no significant difference.

The mechanism of alkylation of amines has been proposed and supported by a few experiments.[21,22,25,26,28,29] Scheme 4 illustrates the possible mechanism of alkyation of an amine with sodium borohydride in carboxylic acid.

Scheme 4. Possible Reductive Deuteroethylation Mechanism

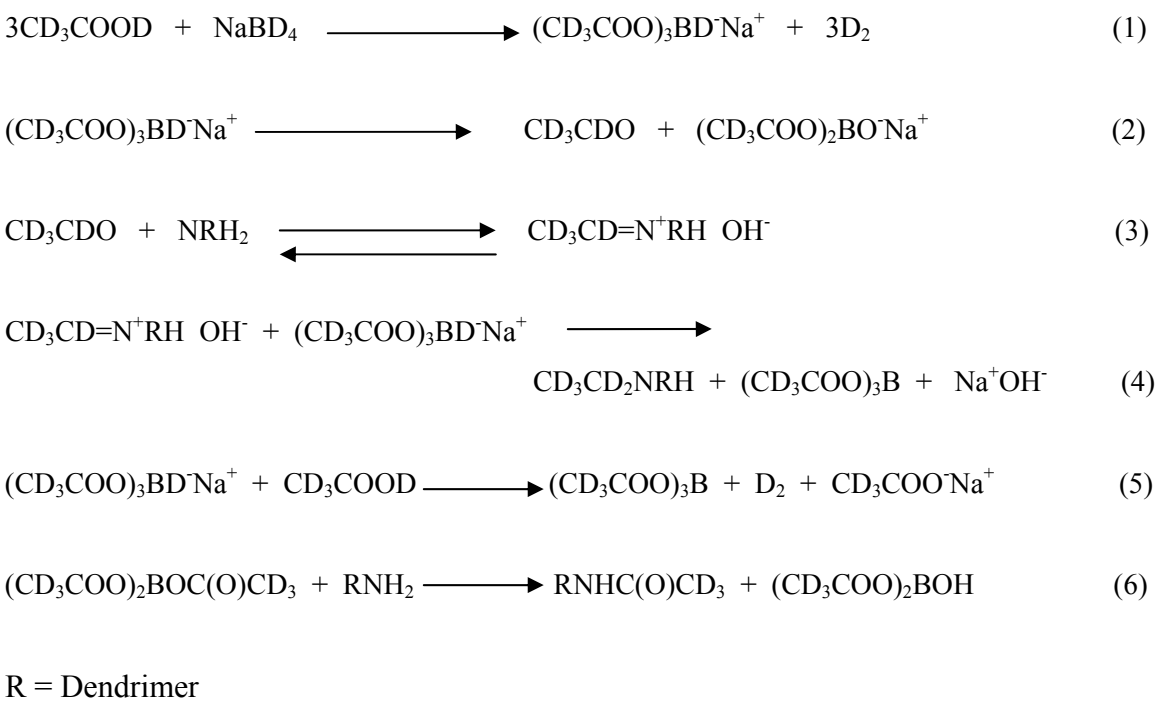

R = Dendrimer

The step (2) is considered the key stage for the reductive ethylation by self-reduction of trialkyloxyborohydride to free aldehyde which reacts with the amine in the next step (3).[26] From the above mechanism, successful reductive alkylation requires that steps (2) and (3) be much faster than steps (5) and (6).

Moisture must be kept out of reaction mixture. Acyloxyborohydrides decompose in the presence of moisture which prevents further ethylation of the amine.[22]

This reductive ethylation of dendrimers with CH_3COOH-$NaBH_4$ gave a higher yield of tertiary amine than the methylation with formaldehyde in formic acid. However, the reductive methylation of amines with HCOOH-$NaBH_4$ has been reported to be uncontrollable due to vigorous production of H_2.[20] As a result, few reactions have been

studied with HCOOH-$NaBH_4$. During preliminary experiments, we found no methylation of amines with HCOOH-$NaBH_4$ with aromatic or branched aliphatic amines. Repeating the methylation of HCOOH-$NaBH_4$ by the literature method was also unsuccessful.

Reactions of PPI Dendrimers DAB-*dendri*-$(NH_2)_n$ (n = 32 and 64) with $NaBD_4$-CD_3COOD. The reactions of PPI dendrimers DAB-*dendr*-$(NH_2)_n$ (n = 32 and 64) with $NaBD_4$-CD_3COOD were achieved in one step by the method of Gribble and coworkers as shown in Scheme 5.[20] The hydrophobic deuterated ethyl chains were introduced to give perethyl terminated dendrimers in 74-83 % yield with no trace of secondary amine peaks at 15.0 and 43.5 ppm in the ^{13}C NMR spectra. The deuterated dendrimers **13** and **14** have very clean proton NMR spectra and show the $NCH_2\boldsymbol{CH_2}CH_2N$ and $NCH_2\boldsymbol{CH_2CH_2}CH_2N$ peaks at 1.57 ppm and the $N\boldsymbol{CH_2}CH_2\boldsymbol{CH_2}N$ and $N\boldsymbol{CH_2}CH_2CH_2\boldsymbol{CH_2}N$ peaks at 2.40 ppm.

Scheme 5. Deuteroethyl PPI dendrimers

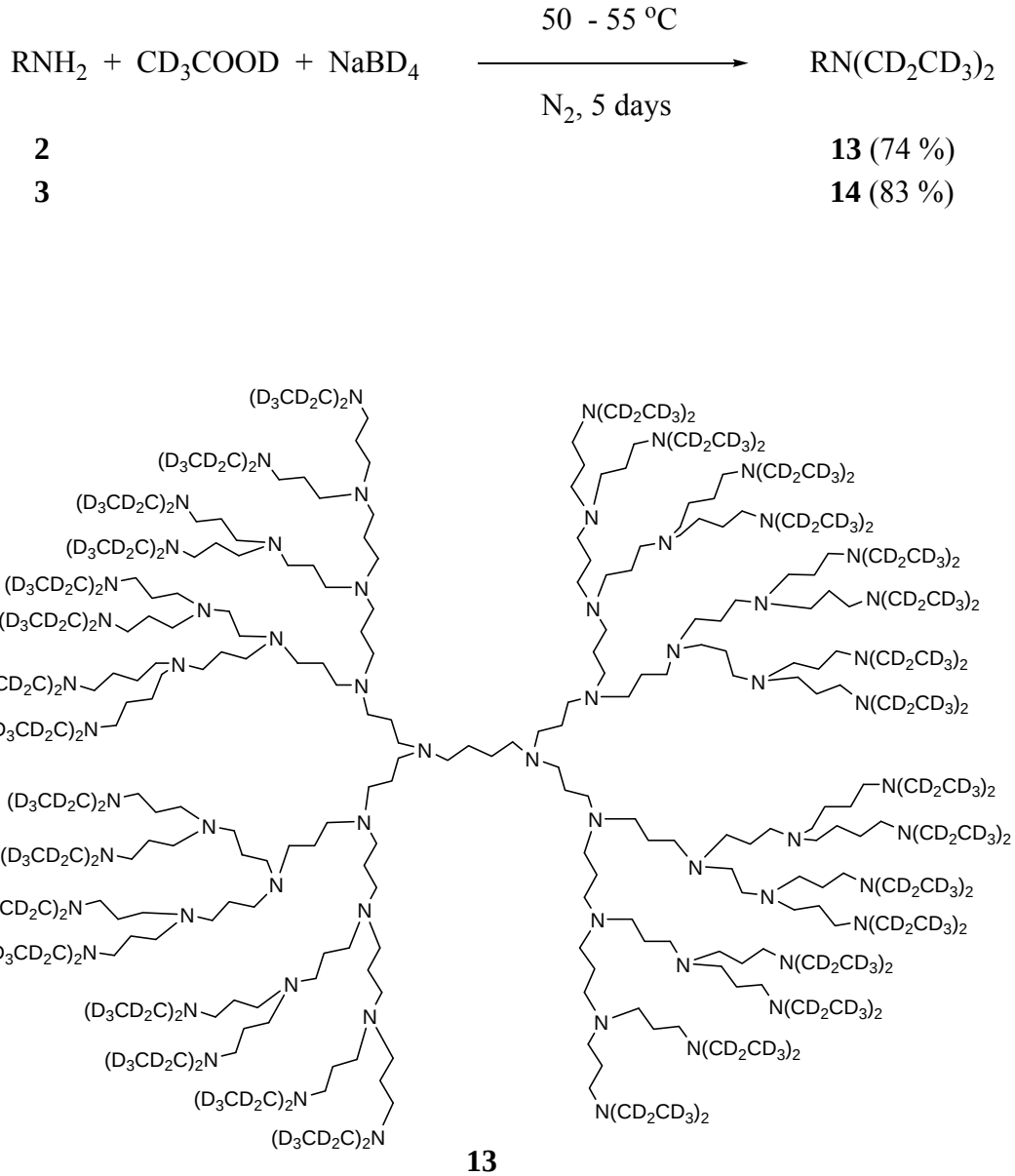

13

Conclusions

Oxalyl chloride was reacted with 2-[2-(2-methoxyethoxy)ethoxy]acetic acid in toluene, followed by PPI dendrimers **1-3** and TEA in DMF to give the hydrophilic amide dendrimers **7**, **8**, and **9**. All dendrimer chain ends were reacted and determined by ^{1}H NMR and ^{13}C NMR. The self-diffusion experiment of three hydrophilic amide dendrimers was performed by the Zhu group at Department de Chemie, Universite de Montreal in Canada.[1] The results show that the self-diffusion coefficients of the dendrimers decrease with increasing molecular size of the diffusant as poly(vinyl alcohol) (PVA) concentration increases and as temperature decreases. NMR relaxation time measurements indicate that the terminal protons are more mobile than the core protons for all generations of the dendrimers. The mobility for all protons is also slower as dendrimer generation gets larger.

Tertiary amine dendrimers with hydrophobic chains on every end were synthesized from poly(propylene imine) (PPI) dendrimers DAB-*dendr*-$(NH_2)_n$ (n = 32 and 64) with $NaBD_4$ in CD_3COOD (74-83 % yields). Complete conversion to tertiary amine dendrimers by reductive ethylation was accomplished in a one pot reaction and determined by ^{1}H NMR and ^{13}C NMR.

Experimental Section

Materials. PPI dendrimers DAB-*dendr*-$(NH_2)_n$ (n = 8, 32 and 64) and 2-[2-(2-methoxyethoxy)ethoxy]acetic acid were purchased from Aldrich (Milwaukee, WI). For the *N*-perdeuteroethylation**,** CD_3COOD (99.5 atom % D) was purchased from CDN

Isotopes and $NaBD_4$ (powder, 99 atom % D) was purchased from Cambridge Isotope Laboratories, Inc. For the *N*-ethylation, $NaBH_4$ (powder, 98 %) was purchased from Aldrich and $NaBH_4$ (granules, -10+40 mesh, 97 %) was purchased from Alfa Aesar. Triethylamine (TEA) was dried over anhydrous 3 Å molecular sieves and freshly distilled. All other chemicals were used as received.

2-[2-(2-Methoxyethoxy)ethoxy]acetyl Chloride.[1,13,14,27] A solution of 2-[2-(2-methoxyethoxy)ethoxy]acetic acid (5.34 g, 30.0 mmol) and oxalyl chloride (6.35 g, 50.0 mmol) in 3 mL of toluene was stirred for 4 h at 65 °C. The solvent and excess reagent were removed under reduced pressure, and the residue was dried at 40 °C under vacuum to give a light yellow oil (5.34 g, 90%) which was used without further purification.

Amidation of Poly(propylene imine) Dendrimers. 2-[2-(2 Methoxyethoxy)ethoxy]acetyl chloride (3.00 g, 15.3 mmol) was added to a solution of PPI dendrimer DAB-*dendr*-$(NH_2)_8$ (**1)** (1.00 g, 1.29 mmol), DMF (5.0 mL), and TEA (0.900 g, 8.89 mmol) at 0 °C. The solution was stirred under nitrogen at 70 °C for 24 h. Water (5 mL) was added to hydrolyze the excess acid chloride. The mixture was made basic to pH > 14 using 5 g (27 mmol) of tetramethylammonium hydroxide pentahydrate and was extracted with CH_2Cl_2 (4 times 10 mL). The combined dichloromethane solutions were dried over Na_2SO_4 and evaporated. The oily residue was dried at 40 °C under vacuum to give a light yellow oil of **7** (2.21 g, 83%). DAB-*dendr*-$(NH_2)_n$ (n = 32 and 64) (**2** and **3)** were also modified with triethylenoxy methyl ether end groups by the same procedure to yield compounds **8** and **9**. The ^1H and ^{13}C NMR spectra of dendrimers made by the current procedure were the same as the spectra of those reported earlier, which were prepared by a slightly different procedure.[13,14]

Procedure for the *N*-Ethylation of 1 in CH_3COOH-$NaBH_4$.[20] Glacial CH_3COOH (641 mmol, 36.7 mL) was added dropwise to the dendrimer **1** (1.29 mmol, 1.00 g, 1.00 mmol / NH_2) in a dry three-necked round-bottomed flask by a syringe with magnetic stirring under N_2 at 40-45 ^oC in an oil bath. The temperature was then raised to 50 ^oC. Sodium borohydride (96.4 mmol, 3.76 g) was added portionwise to the mixture over 1-2 h at 50-55 ^oC. The mixture was heated at 50-55 ^oC for 5 days under nitrogen, to give a brownish yellow solution. The mixture was cooled to room temperature and then to 0 ^oC in an ice bath. Deionized water (~100 mL) was added to the magnetically stirred mixture kept in the ice bath, followed by NaOH pellets to pH > 14. The basic mixture was extracted with dichloromethane (5 x 30 mL). The organic layers were combined and dried with anhydrous sodium sulfate overnight. The extract was concentrated to remove solvent and excess reagent under reduced pressure. The crude oily dark brown product **10** (1.52 g, 96.6 %) was dried under vacuum at 40 ^oC for 12 h. ^1H NMR (300 MHz, $CDCl_3$, δ):1.01(t, $NCH_2\boldsymbol{CH_3}$), 1.38(m, $NCH_2\boldsymbol{CH_2CH_2}CH_2N$), 1.58 (m, $NCH_2\boldsymbol{CH_2}CH_2N$), 2.40 (broad t, $N\boldsymbol{CH_2}CH_2\boldsymbol{CH_2}N$ and $N\boldsymbol{CH_2}CH_2CH_2\boldsymbol{CH_2}N$), 2.51 (q, $N\boldsymbol{CH_2}CH_3$); ^{13}C NMR (75.4 MHz, $CDCl_3$, δ): 11.62 ($NCH_2\boldsymbol{C}H_3$), 24.40 ($NCH_2\boldsymbol{C}H_2CH_2N$), 24.51 ($NCH_2\boldsymbol{C}H_2\boldsymbol{C}H_2CH_2N$), 25.51 ($NCH_2\boldsymbol{C}H_2CH_2N$-$(CH_2CH_3)_2$), 46.80 ($N\boldsymbol{C}H_2CH_3$), 51.05 ($N\boldsymbol{C}H_2CH_2CH_2N$-$(CH_2CH_3)_2$), 52.13 and 52.29 ($N\boldsymbol{C}H_2CH_2\boldsymbol{C}H_2N$ and $N\boldsymbol{C}H_2CH_2CH_2\boldsymbol{C}H_2N$).

Compound 11: By the previous *N*-ethylation procedure, **2** (0.285 mmol, 1.00 g), glacial CH_3COOH (565 mmol, 32 mL), and $NaBH_4$ (84.9 mmol, 3.28 g, powder, 98%) gave a brownish yellow thick liquid (1.29 g, 85.5%). ^1H NMR (300 MHz, $CDCl_3$, δ): 0.98 (t, $NCH_2\boldsymbol{CH_3}$ for tertiary amine), 1.07 (t, $NCH_2\boldsymbol{CH_3}$ for seccondary

amine), 1.56 (m, $NCH_2\boldsymbol{CH_2}CH_2N$), 2.38 (broad t, $N\boldsymbol{CH_2}CH_2\boldsymbol{CH_2}N$ and $N\boldsymbol{CH_2}CH_2CH_2\boldsymbol{CH_2}N$), 2.49 (q, $N\boldsymbol{CH_2}CH_3$ for tertiary amine), 2.60 (q, $N\boldsymbol{CH_2}CH_3$ for secondary amine); ^{13}C NMR (75.4 MHz, $CDCl_3$, δ): 12.17 ($NCH_2\boldsymbol{C}H_3$), 24.89 ($NCH_2\boldsymbol{C}H_2CH_2N$), 47.30 ($N\boldsymbol{C}H_2CH_3$), 51.52 and 52.60 ($N\boldsymbol{C}H_2CH_2\boldsymbol{C}H_2N$ and $N\boldsymbol{C}H_2CH_2CH_2\boldsymbol{C}H_2N$).

Compound 12: By the previous *N*-ethylation procedure, **3** (0.140 mmol, 1.00 g), glacial CH_3COOH (554 mmol, 32 mL), and $NaBH_4$ (83.2 mmol, 3.21 g, powder, 98%) gave a brownish yellow thick liquid (1.20 g, 96%). ^1H NMR (300 MHz, $CDCl_3$, δ): 0.98 (t, $NCH_2\boldsymbol{CH_3}$), 1.56 (m, $NCH_2\boldsymbol{CH_2}CH_2N$), 2.38 (broad t, $N\boldsymbol{CH_2}CH_2\boldsymbol{CH_2}N$ and $N\boldsymbol{CH_2}CH_2CH_2\boldsymbol{CH_2}N$), 2.48 (q, $N\boldsymbol{CH_2}CH_3$); ^{13}C NMR (75.4 MHz, $CDCl_3$, δ): 11.79 ($NCH_2\boldsymbol{C}H_3$), 24.49 ($NCH_2\boldsymbol{C}H_2CH_2N$), 46.88 ($N\boldsymbol{C}H_2CH_3$), 51.11 and 52.16 ($N\boldsymbol{C}H_2CH_2\boldsymbol{C}H_2N$ and $N\boldsymbol{C}H_2CH_2CH_2\boldsymbol{C}H_2N$).

Compound 13: Deuterated derivatives of the PPI dendrimers DAB-*dendri*-$(NH_2)_{32}$ **2** were prepared by the same procedure as described for the *N*-ethylation of **11**. The mixture of **2** (0.427 mmol, 1.50 g), CD_3COOD (848 mmol, 49 mL, 99.5%), and $NaBD_4$ (127 mmol, 5.40 g, powder, 99%) gave a brownish yellow thick liquid (1.75 g, 74%). ^1H NMR (300 MHz, $CDCl_3$, δ): 1.58 (m, $NCH_2\boldsymbol{CH_2}CH_2N$ and $NCH_2\boldsymbol{CH_2CH_2}CH_2N$), 2.40 (m, $N\boldsymbol{CH_2}CH_2\boldsymbol{CH_2}N$ and $N\boldsymbol{CH_2}CH_2CH_2\boldsymbol{CH_2}N$); ^{13}C NMR (75.4 MHz, $CDCl_3$, δ): 10.50 ($NCD_2\boldsymbol{C}D_3$), 24.50-25.10 ($NCH_2\boldsymbol{C}H_2CH_2N$), 46.00 ($N\boldsymbol{C}D_2CD_3$), 51.08 ($N\boldsymbol{C}H_2CH_2CH_2N$-$(CH_2CH_3)_2$), 52.19 and 52.51 ($N\boldsymbol{C}H_2CH_2\boldsymbol{C}H_2N$ and $N\boldsymbol{C}H_2CH_2CH_2\boldsymbol{C}H_2N$).

Compound 14: Deuterated derivatives of the PPI dendrimer DAB-*dendri*-$(NH_2)_{64}$ **3** were prepared by the same procedure as the *N*-ethylation of **12**. The mixture of **3**

(0.176 mmol, 1.26 g), CD_3COOD (697 mmol, 40 mL, 99.5%), and $NaBD_4$ (104 mmol, 4.40 g, powder, 99%) gave a brownish yellow thick liquid (1.68 g, 83%). ^1H NMR (300 MHz, $CDCl_3$, δ): 1.57 (m, $NCH_2\boldsymbol{CH_2}CH_2N$ and $NCH_2\boldsymbol{CH_2CH_2}CH_2N$), 2.41 (m, $N\boldsymbol{CH_2}CH_2\boldsymbol{CH_2}N$ and $N\boldsymbol{CH_2}CH_2CH_2\boldsymbol{CH_2}N$); ^{13}C NMR (75.4 MHz, $CDCl_3$, δ): 10.70 ($NCD_2\boldsymbol{C}D_3$), 24.10-25.10 ($NCH_2\boldsymbol{C}H_2CH_2N$), 46.00 ($N\boldsymbol{C}D_2CD_3$), 51.10 ($N\boldsymbol{C}H_2CH_2CH_2N$-$(CH_2CH_3)_2$), 52.21 and 52.57 ($N\boldsymbol{C}H_2CH_2\boldsymbol{C}H_2N$ and $N\boldsymbol{C}H_2CH_2CH_2\boldsymbol{C}H_2N$).

References

(1) Baille, W. E.; Malveau, C.; Zhu, X. X.; Kim, Y. H.; Ford, W. T. *Macromolecules* **2003**, *36*, 839-847.

(2) Masaro, L.; Zhu, X. X.; Macdonald, P. M. *Macromolecules* **1998**, *31*, 3880-3885.

(3) Masaro, L.; Zhu, X. X.; Macdonald, P. M. *Journal of Polymer Science, Part B: Polymer Physics* **1999**, *37*, 2396-2403.

(4) Masaro, L.; Zhu, X. X. *Macromolecules* **1999**, *32*, 5383-5390.

(5) Newkome, G. R.; Moorefield, C. N.; Vogtle, F. *Dendrimers,* 2nd Edition; Wiley: Chichester, United Kingdom, **2001**.

(6) Tomalia, D. A.; Durst, H. D. *Topics in Current Chemistry* **1993**, *165*, 193-313.

(7) van Genderen, M. H. P.; de Brabander-Van Den Berg, E. M. M.; Meijer, E. W. *Advances in Dendritic Macromolecules* **1999**, *4*, 61-105.

(8) Tomalia, D. A. *Materials Today (Oxford, United Kingdom)* **2005**, *8*, 34-46.

(9) Matthews, O. A.; Shipway, A. N.; Stoddart, J. F. *Progress in Polymer Science* **1998**, *23*, 1-56.

(10) Tomalia, D. A. *Progress in Polymer Science* **2005**, *30*, 294-324.

(11) Tomalia, D. A.; Frechet, J. M. *Progress in Polymer Science* **2005**, *30*, 217-219.

(12) Smith, D. K.; Hirst, A. R.; Love, C. S.; Hardy, J. G.; Brignell, S. V.; Huang, B. *Progress in Polymer Science* **2005**, *30*, 220-293.

(13) Pan, Y.; Ford, W. T. *Macromolecules* **2000**, *33*, 3731-3738.

(14) Kreider, J. L.; Ford, W. T. *Journal of Polymer Science, Part A: Polymer Chemistry* **2001**, *39*, 821-832.

(15) Ottaviani, M. F.; Bossmann, S.; Turro, N. J.; Tomalia, D. A. *Journal of the American Chemical Society* **1994**, *116*, 661-671.

(16) Jendrusch-Borkowski, B.; Awad, J.; Wasgestian, F. *Journal of Inclusion Phenomena and Macrocyclic Chemistry* **1999**, *35*, 355-359.

(17) Vassilev, K.; Kreider, J.; Miller, P. D.; Ford, W. T. *Reactive & Functional Polymers* **1999**, *41*, 205-212.

(18) Vassilev, K.; Ford, W. T. *Journal of Polymer Science, Part A: Polymer Chemistry* **1999**, *37*, 2727-2736.

(19) Velarde-Ortiz, R.; Larsen, G. *Chemistry of Materials* **2002**, *14*, 858-866.

(20) Gribble, G. W.; Jasinski, J. M.; Pellicone, J. T.; Panetta, J. A. *Synthesis* **1978**, 766-768.

(21) Gribble, G. W.; Lord, P. D.; Skotnicki, J.; Dietz, S. E.; Eaton, J. T.; Johnson, J. *Journal of the American Chemical Society* **1974**, *96*, 7812-7813.

(22) Marchini, P.; Liso, G.; Reho, A.; Liberatore, F.; Micheletti Moracci, F. *Journal of Organic Chemistry* **1975**, *40*, 3453-3456.

(23) Gribble, G. W.; Wright, S. W. *Heterocycles* **1982**, *19*, 229-233.

(24) Gribble, G. W.; Nutaitis, C. F. *Organic Preparations and Procedures International* **1985**, *17*, 317-384.

(25) Gribble, G. W. *Chemtech* **1996**, *26*, 26-31.

(26) Gribble, G. W. *Chemical Society Reviews* **1998**, *27*, 395-404.

(27) Adams, R.; Ulich, L. H. *Journal of the American Chemical Society* **1920**, *42*, 599-611.

(28) Pelter, A.; Levitt, T. E. *Tetrahedron* **1970**, *RCGJ*, 1899-1908.

(29) Pelter, A.; Levitt, T. E. *Tetrahedron* **1970**, *26*, 1545-1553.

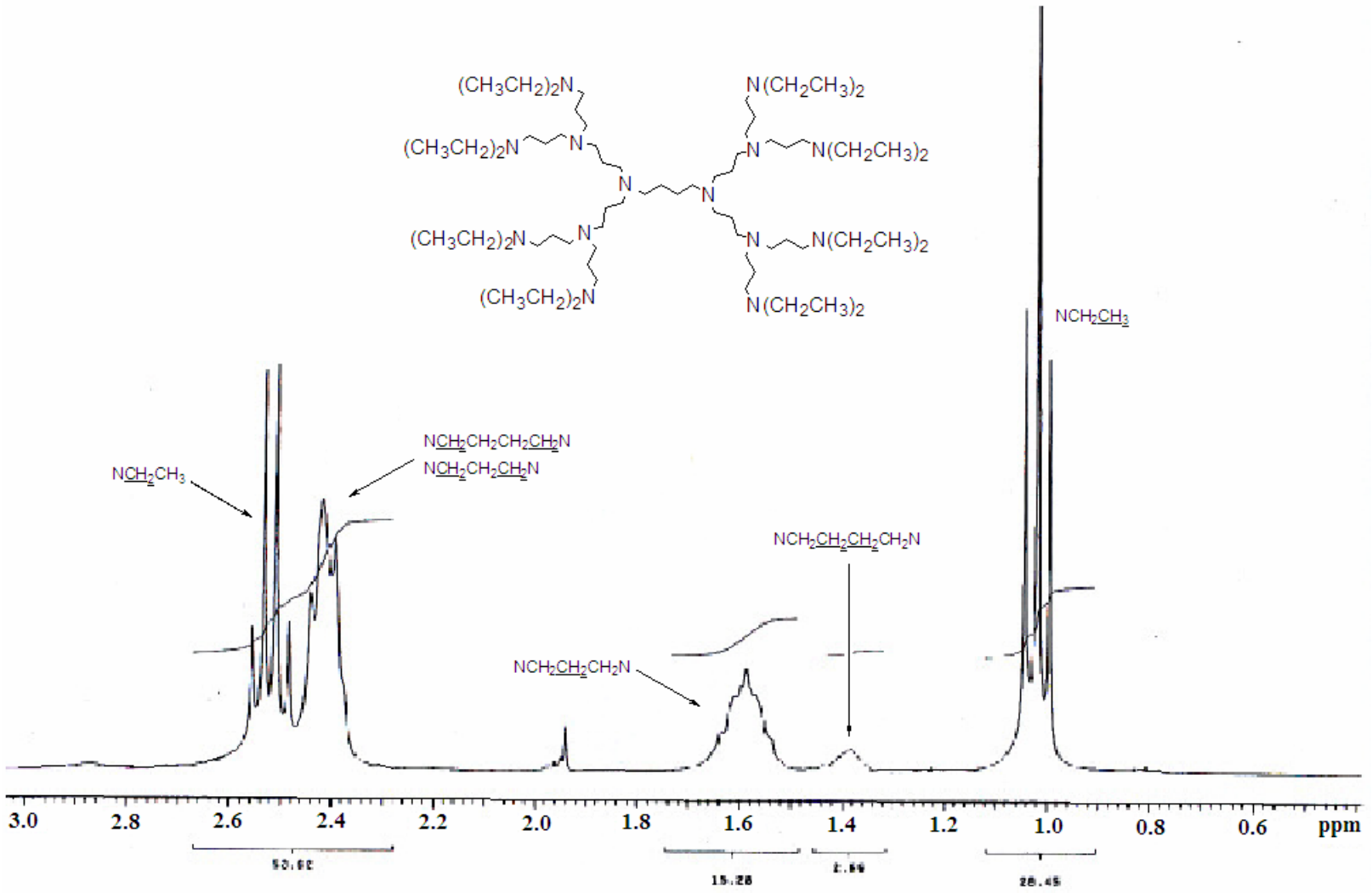

Figure 1. 300 MHz ^{1}H NMR spectrum of compound **10** in $CDCl_3$.

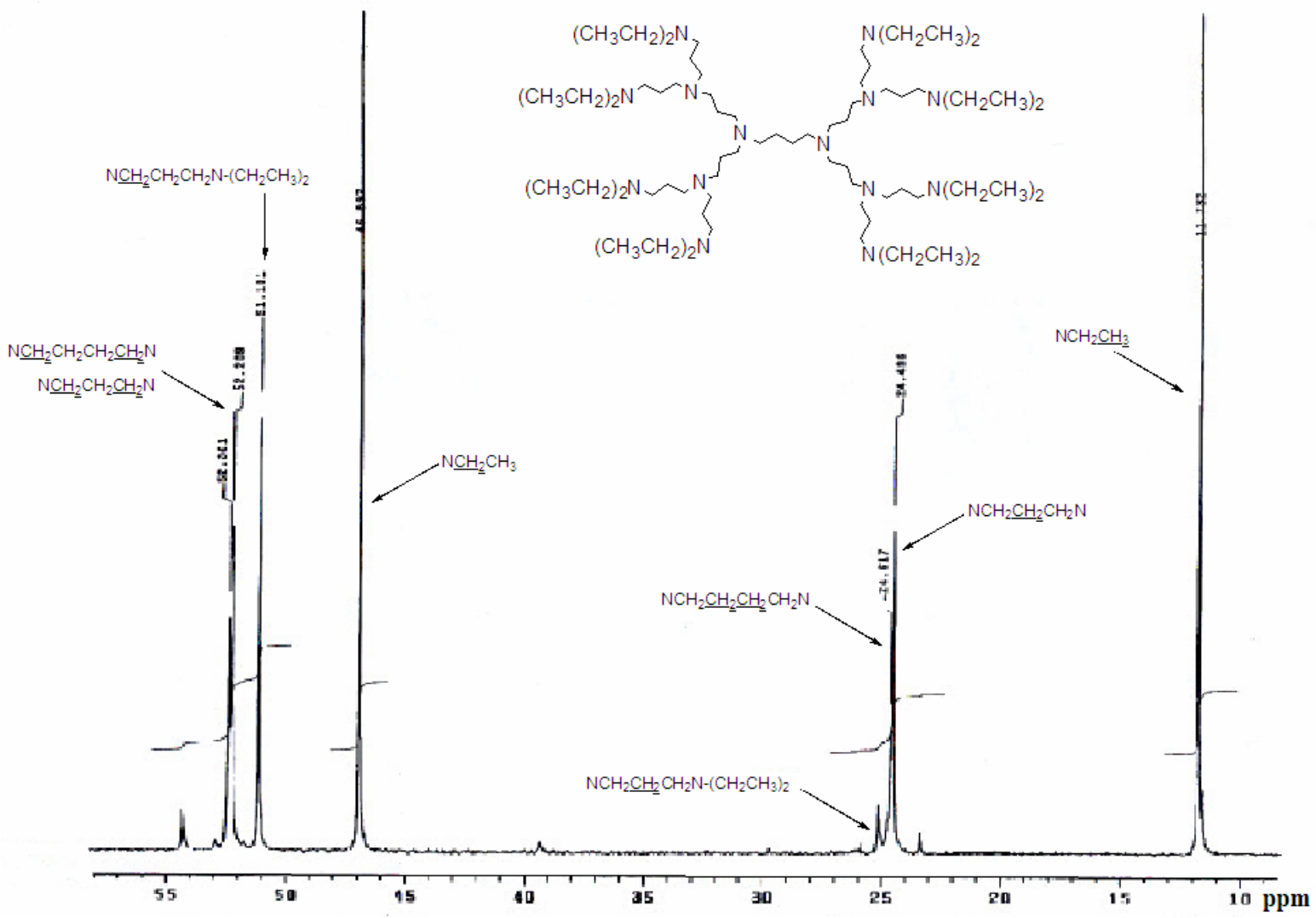

Figure 2. 75 MHz ^{13}C NMR spectrum of compound **10** in $CDCl_3$.

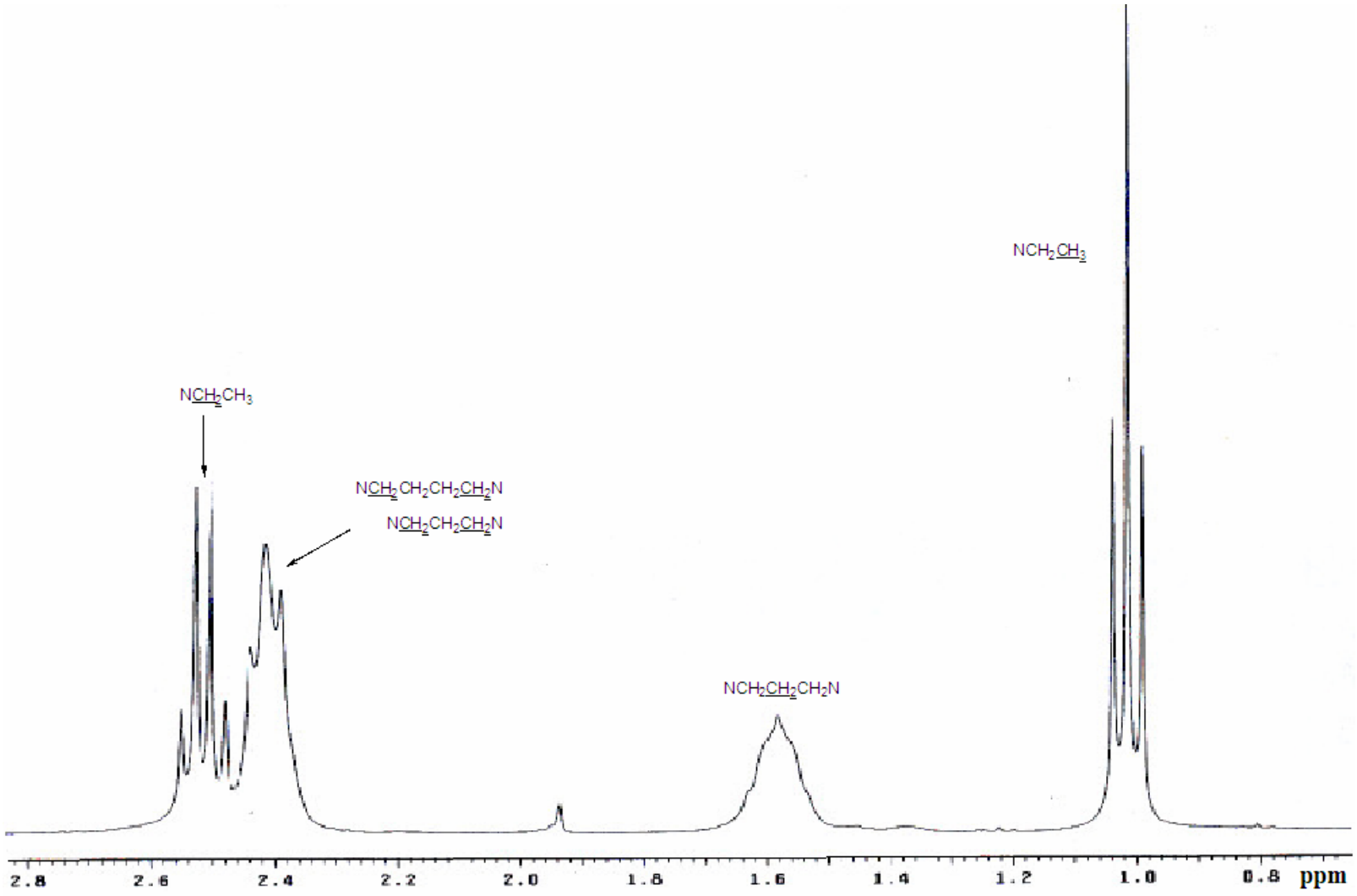

Figure 3. 300 MHz ^{1}H NMR spectrum of compound **11** in $CDCl_3$.

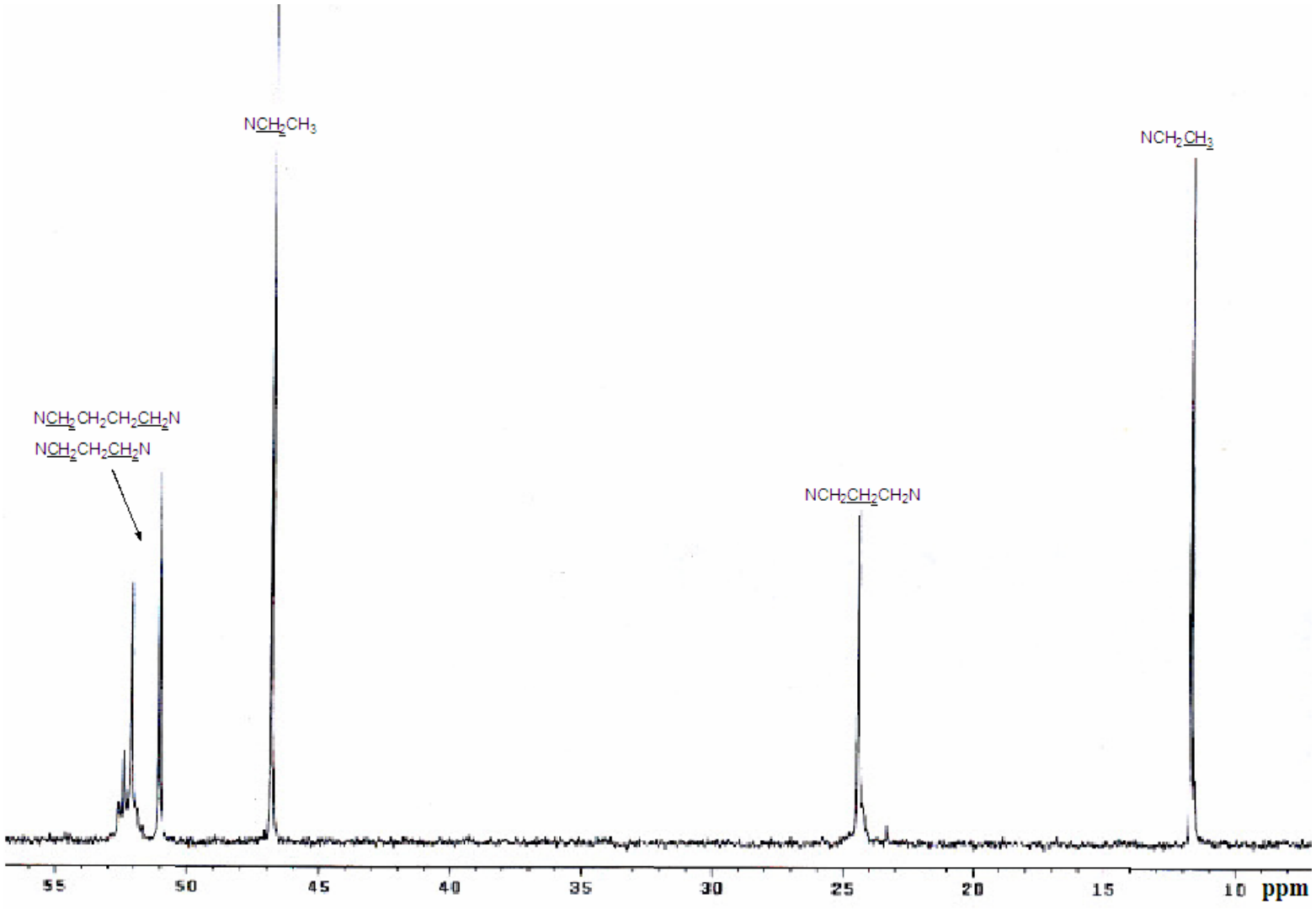

Figure 4. 75 MHz ^{13}C NMR spectrum of compound **11** in $CDCl_3$.

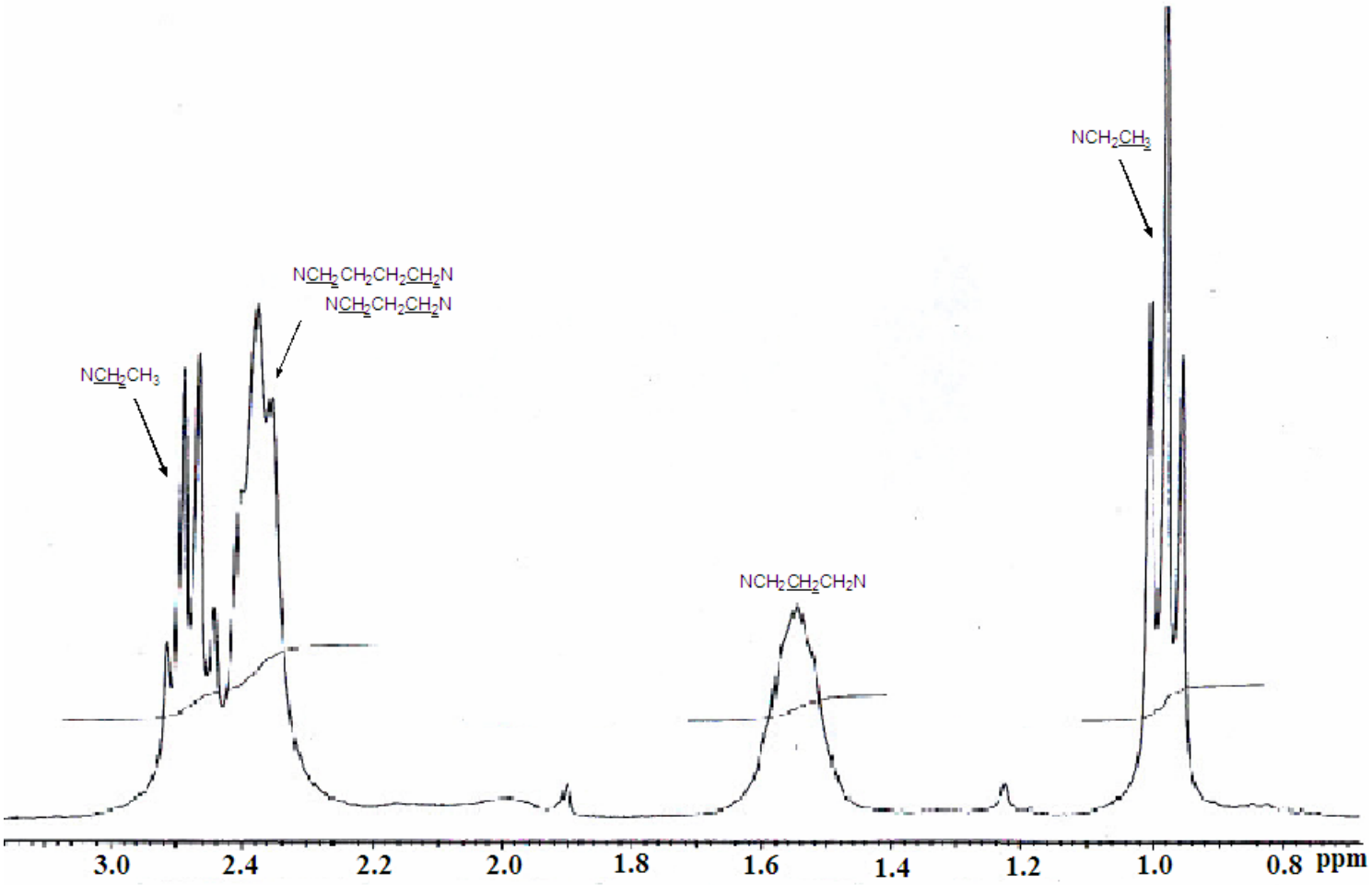

Figure 5. 300 MHz ^{1}H NMR spectrum of compound **12** in $CDCl_3$.

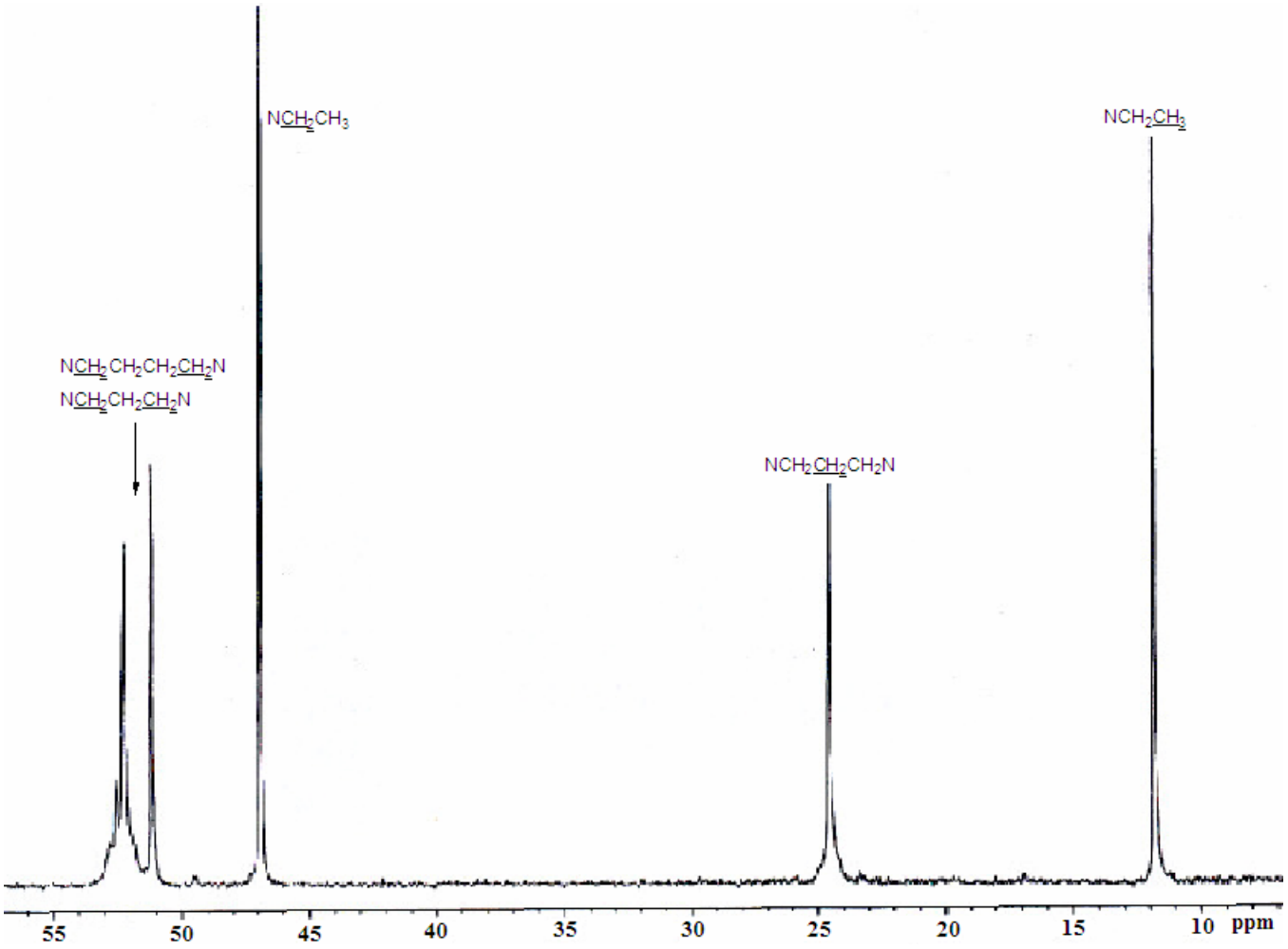

Figure 6. 75 MHz ^{13}C NMR spectrum of compound **12** in $CDCl_3$.

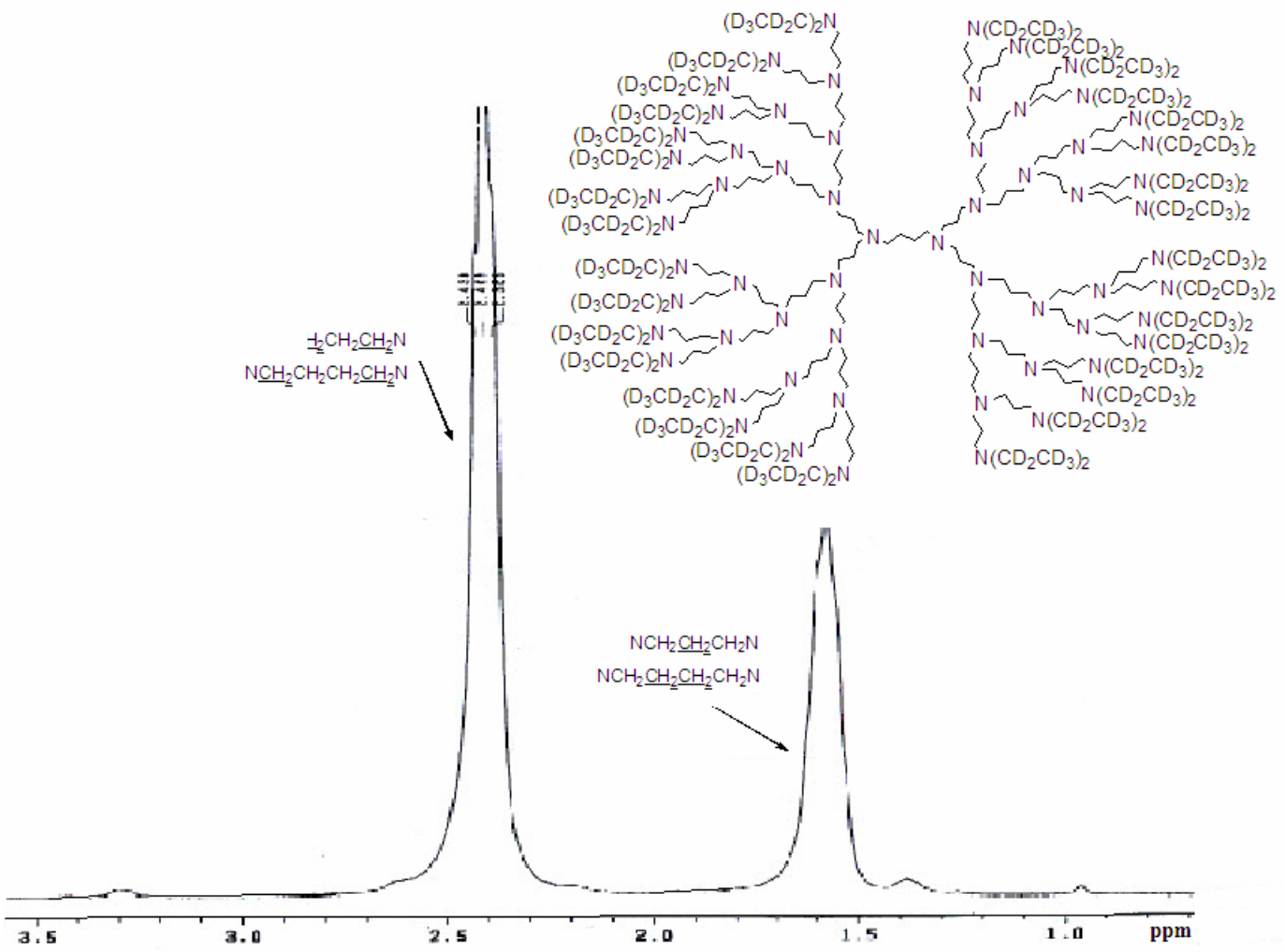

Figure 7. 300 MHz ^{1}H NMR spectrum of compound **13** in $CDCl_3$.

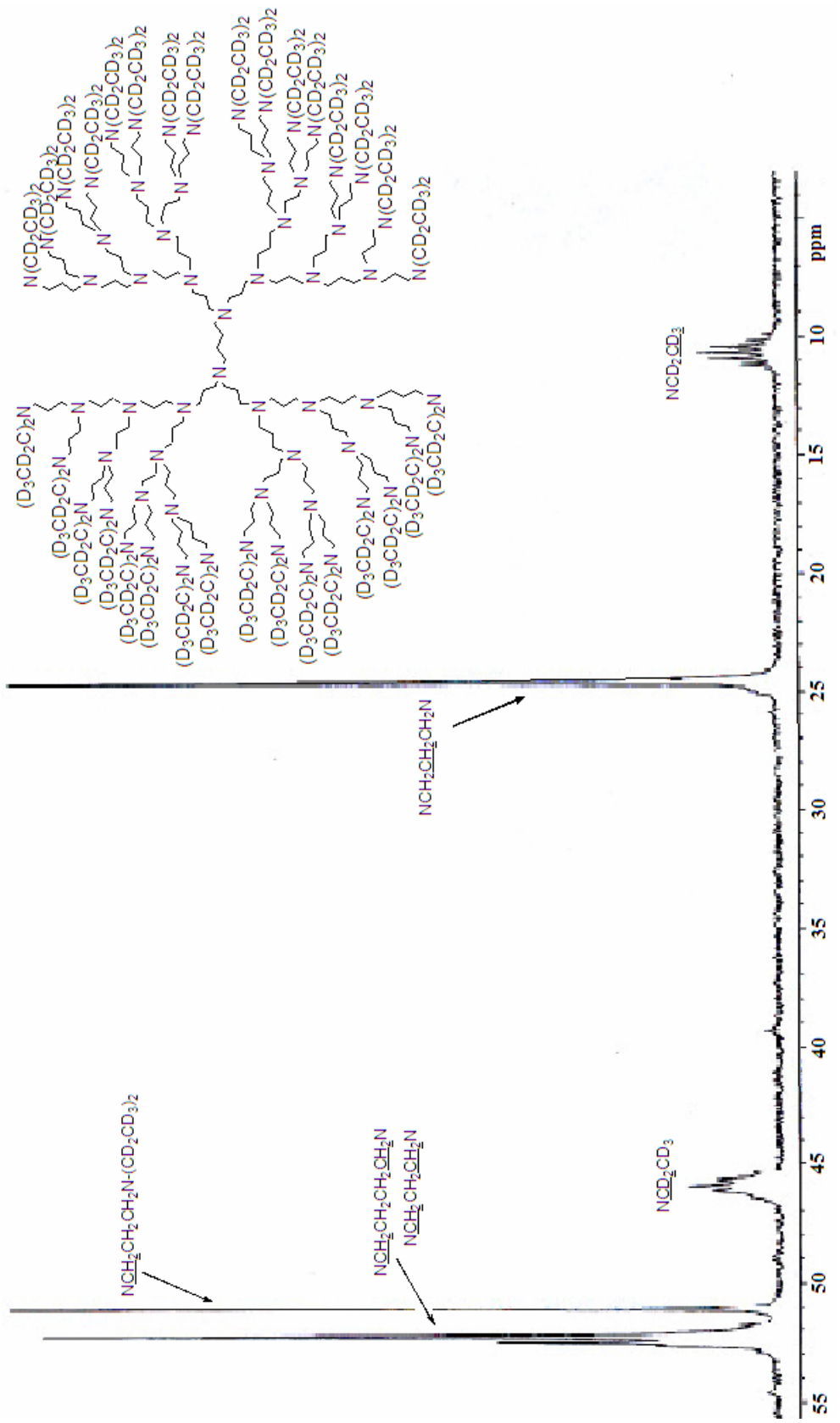

Figure 8. 75 MHz ^{13}C NMR spectrum of compound **13** in $CDCl_3$.

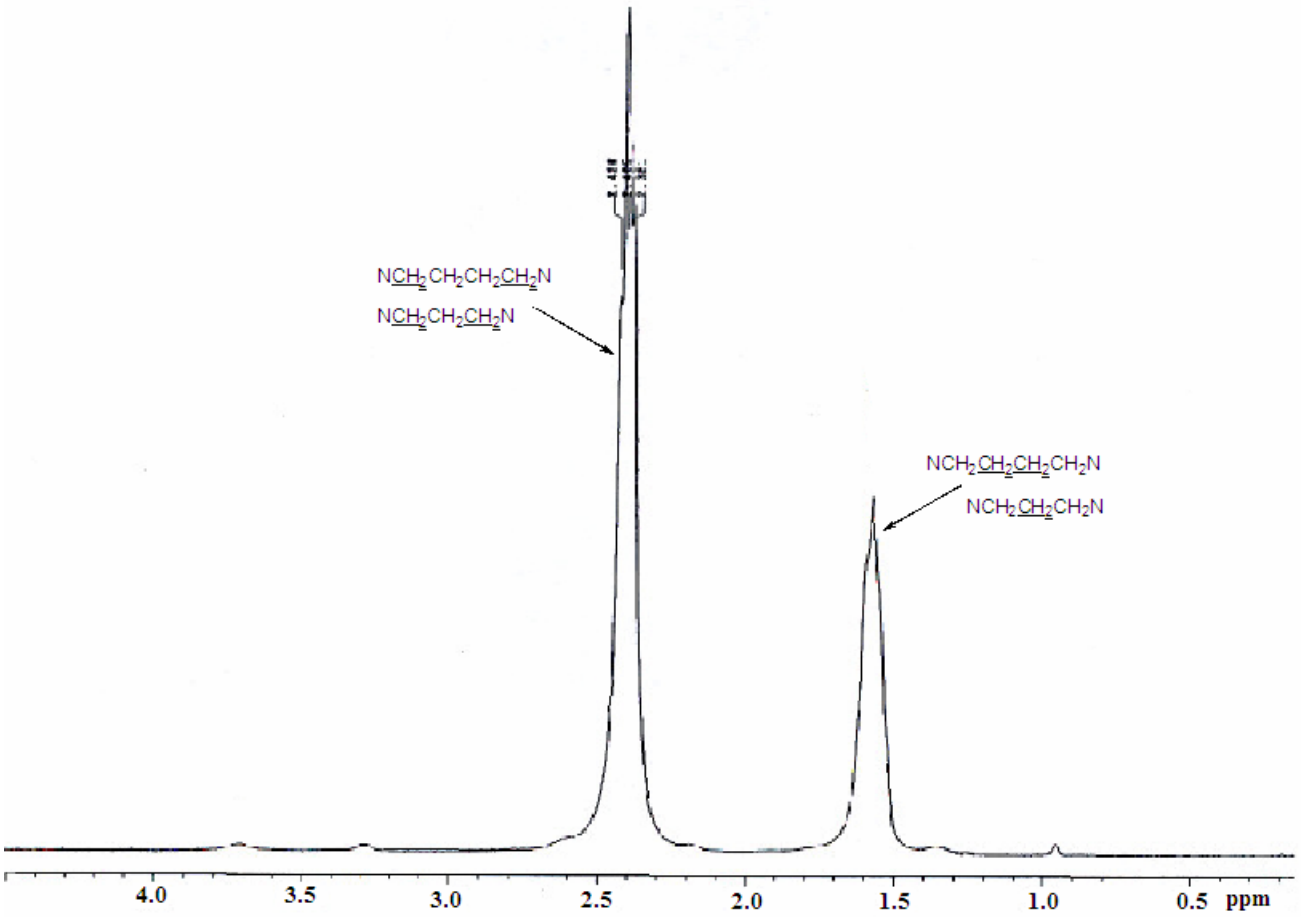

Figure 9. 300 MHz ^{1}H NMR spectrum of compound **14** in $CDCl_3$.

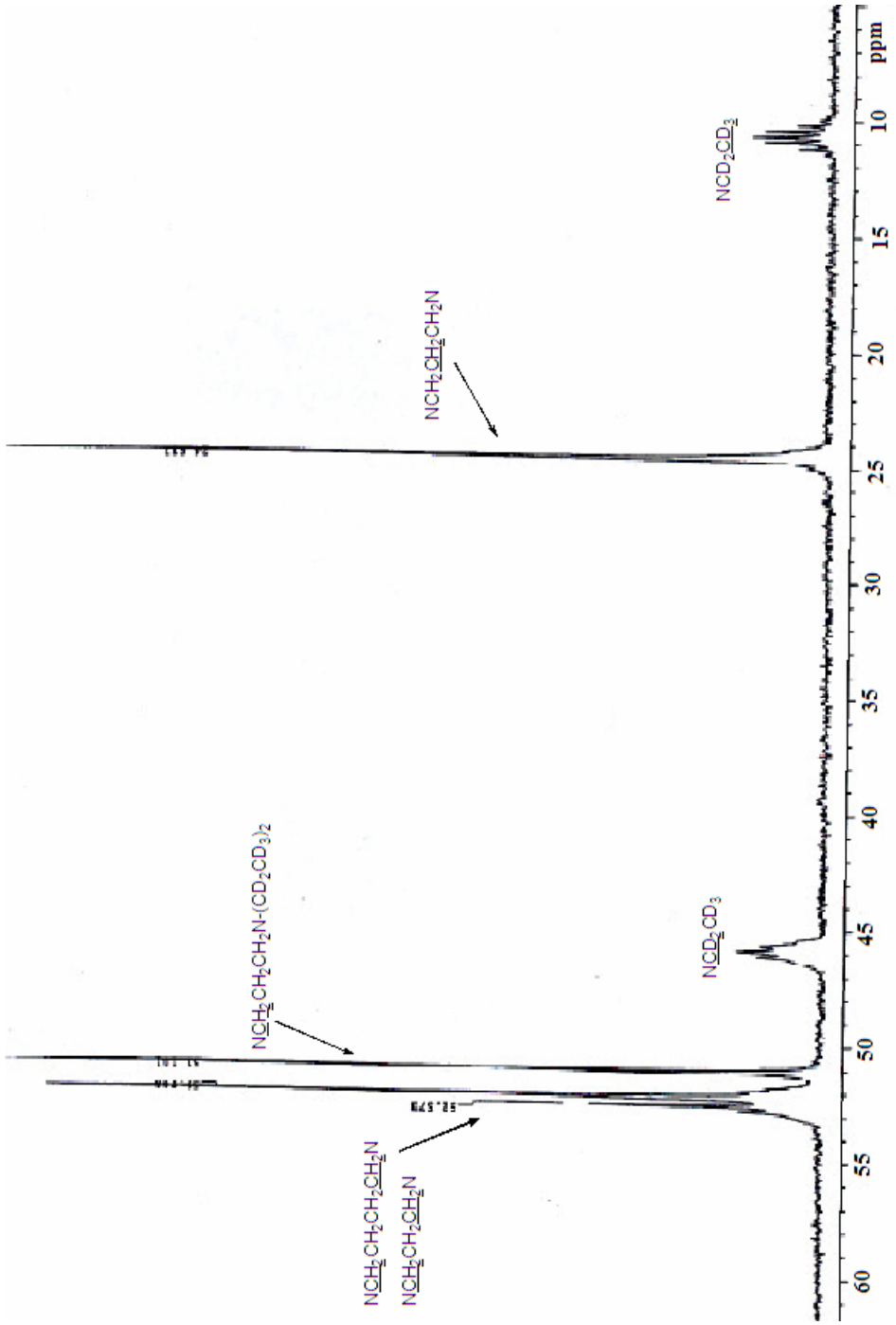

Figure 10. 75 MHz ^{13}C NMR spectrum of compound **14** in $CDCl_3$.

CHAPTER III

AMPHIPHILIC DENDRITIC BLOCK COPOLYMERS

Abstract

Atom transfer radical polymerization (ATRP) was applied to the synthesis of monodisperse branched polystyrene with chain lengths of 20-50 repeat units from dendrimer chain ends. The preparation of the monodisperse core based on the dendrimer with styrene at the chain ends allows for amphiphilic poly(styrene-*b*-acrylic acid) unimolecular micelles with a dendrimer core by ATRP.

For a branched polystyrene, a narrow polydispersity (PDI) = 1.15 with a diameter of ~15 nm was obtained with PPI DAB-*dendr*-$(NH_2)_{64}$ halogenated initiator in the presence of Cu(I)/(II)-*N,N,N′,N′,N″*-pentamethyldiethylenetriamine (PMDETA) in DMF-anisole. Block copolymerization of *t*-butylacrylate (*t*-BA) onto the polystyrene was performed in anisole mediated by a copper(I)/(II)-PMDETA catalyst. Molecular weight distributions (M_w/M_n) of the branched block copolymers were 1.2-1.6 with diameters of 17-28 nm. Removal of the ester group of P*t*BA to poly(acrylic acid)(PAA) in CH_2Cl_2/CF_3COOH at room temperature gave amphiphilic block copolymers.

Emulsion polymerization was applied to the synthesis of the polymer colloids. Polymerization of styrene in aqueous DMF dispersions of the amphiphilic poly(styrene-*b*-methacrylic acid) unimolecular micelles with a dendrimer core and sodium dodecyl sulfate (SDS) produced stable latexes at 80 ^{o}C. The polystyrene latexes had diameters of 45-55 nm with broad particle size distribution (PDI).

Introduction

Amphiphilic block copolymers can self-assemble into aggregates and micelles in solutions.[1,2] These properties make self-assembled block copolymers attractive for potential applications such as drug delivery, coatings, and colloid stabilization.[1,3] Amphiphilic macromolecules can form unimolecular micelles, which consist of a hydrophobic core surrounded by a shell of the solvated hydrophilic part of the block copolymer, stretched out from the core of the hydrophobic part of the molecule.[1]

Well-defined and narrow polydispersity amphiphilic block copolymers with controlled molecular weights can be synthesized by living radical polymerization.[1-4] Living radical polymerization is applicable to many vinyl monomers under mild reaction conditions in a wide range of reaction temperatures. The polymerization requires the absence of oxygen but is tolerant to water. Living radical polymerization has led to an increase in the type of amphiphilic polymers that are easily accessible. The polymerization involves the reversible activation and deactivation of growing radicals while a concentration of propagating radicals maintains low. The low radical concentration suppresses termination reactions. Therefore, it leads to the formation of

polymer with narrow polydispersity, with control of the molecular weight and chain end functionality.[4,5] Transition-metal mediated living radical polymerization, such as atom transfer radical polymerization (ATRP) and nitroxide-mediated radical polymerization, have been developed and used for the preparation of many different block copolymers.[1,4] For ATRP, many catalysts have been described with several transition metals, such as copper, iron, nickel, ruthenium, and palladium.[6,7] Most studies also have been carried out with copper(I)-based catalysts with a wide range of ligands, including multidentate alkylamines, substituted bipyridines, and pyridineimines.[1,6,7]

This research reports a new class of macroinitiators which provide an initiating group for ATRP and can allow us to synthesize the monodisperse branched polystyrene with chain lengths of 20-50 repeat units from dendrimer chain ends. Prior to synthesis of amphiphilic poly(styrene-*b*-methacrylic acid) unimolecular micelles with a dendrimer core, preparation of a dendrimer initiator is necessary for ATRP.

The selection criteria for each component of the polymerization mixture - transition metal, ligand, and solvent - are based on the optimization studies reported for styrene in bulk in the literature.[5-14] In particular, the use of the tridentate PMDETA in the copper mediated ATRP of styrene in DMF/anisole was chosen due to the faster polymerization rate for styrene than those using bipy as the ligand. The fast rate was not our goal because it might result in more coupling products. A slow rate at a lower temperature would be better. However, the copper-PMDETA catalyst system provided a fast initiation step for radical formation by abstracting the halide at the chain end and followed by the reversible exchange between a low concentration of growing radicals and dendritic halide initiators. The reversible process may result in a polymer chain that

grows slowly and gradually and prevents termination under our specific conditions. The fast rate observed using the copper-PMDETA catalyst system occurs because the coordination complexes between copper and aliphatic amines have lower redox potentials than the copper-bypy complex, resulting in higher rates of activation of the dormant halides.[15]

Dendrimers have highly branched structures. They offer control of molecular architecture, size and shape, and a multiplicity of chain ends that can be functionalized.[16]

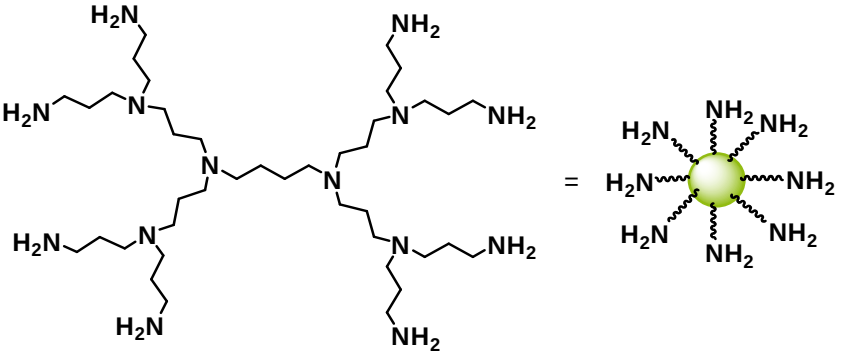

DAB-*dendri*-$(NH_2)_8$, G2
1

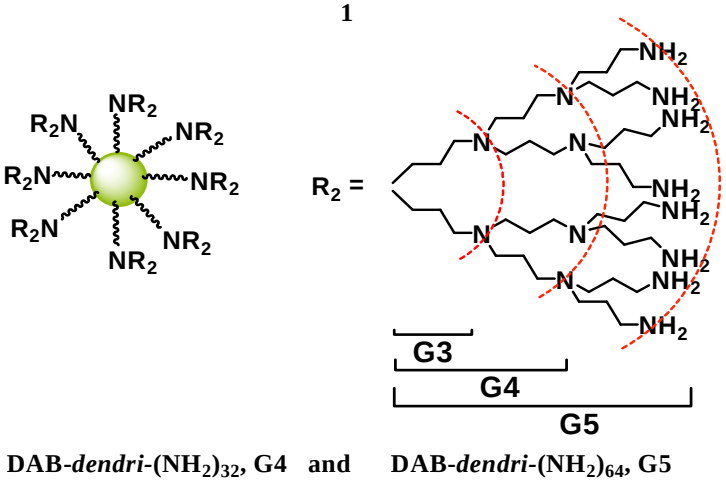

DAB-*dendri*-$(NH_2)_{32}$, G4 and DAB-*dendri*-$(NH_2)_{64}$, G5
2 **3**

The structures of PPI dendrimers have amine sites at all branch points and chain ends. The diameters of spherical dendrimers in general range from 3 nm to 10 nm. Growth of polymer chains by controlled methods from the end groups of a dendrimer would convert a monodisperse dendrimer to a larger molecule and maintain low polydispersity. The use of the copper-PMDETA catalyst system with the PPI dendritic initiators for ATRP may provide better control of chain functionalities, architectures, and compositions as well as the extension to new monomers. The goal of this research was synthesis of monodisperse polymer particles with about 10 nm to 100 nm size in diameter, which can be difficult by emulsion polymerization.

The method chosen was to synthesize and characterize the monodisperse branched polystyrene with chain lengths of 20-50 repeat units and poly(*t*-butyl methacrylate) with chain lengths of 100-500 repeat units from dendrimer chain ends of a 64-arm dendritic ATRP initiator, G_5(AmBr64).

Aggregation properties of amphiphilic monodisperse block copolymer dendrimers DAB-*dendr*-$(NH_2)_8$, as templates for styrene latexes will be discussed. In seed growth emulsion polymerization, an assembly of block copolymer PS_{52}-$PMAA_{26}$ on a dendrimer core as a template for small and monodisperse styrene latexes will be also discussed.

Results and Discussion

Reaction of PPI Dendrimer DAB-*dendr*-$(NH_2)_{64}$ with 2-Bromoisobutyryl Bromide. Syntheses of 64-arm dendritic ATRP initiators are outlined in Scheme 1. Initiators and dendrimer based initiators for the polymerization of styrene, *t*-butyl

methacrylate, and *t*-butyl acrylate used for this project are shown in Figure 1. Syntheses of initiators for controlled growth radical polymerization via ATRP were accomplished using modifications of reported procedures.[18,19]

Preliminary experiments with PPI Dendrimer DAB-*dendr*-$(NH_2)_8$ (**1)** show that the halogenated initiator can be synthesized by condensation of the 64 primary amine group at chain ends of dendrimer **1** with 2-bromoisobutyryl bromide (**5)** at room temperature. The dendritic initiator can also be used for polymerization of styrene in a mixed catalyst-cosolvent system (Cu(I)Cl/Cu(II)Cl_2)/PMDETA-DMF/anisole. The polystyrene can be then utilized for block copolymerization of *t*-BA with a mixed catalyst system, (Cu(I)Cl/Cu(II)Cl_2)/PMDETA, in anisole to produce amphiphilic block copolymers.

Scheme 1. Amphiphilic Block Copolymers

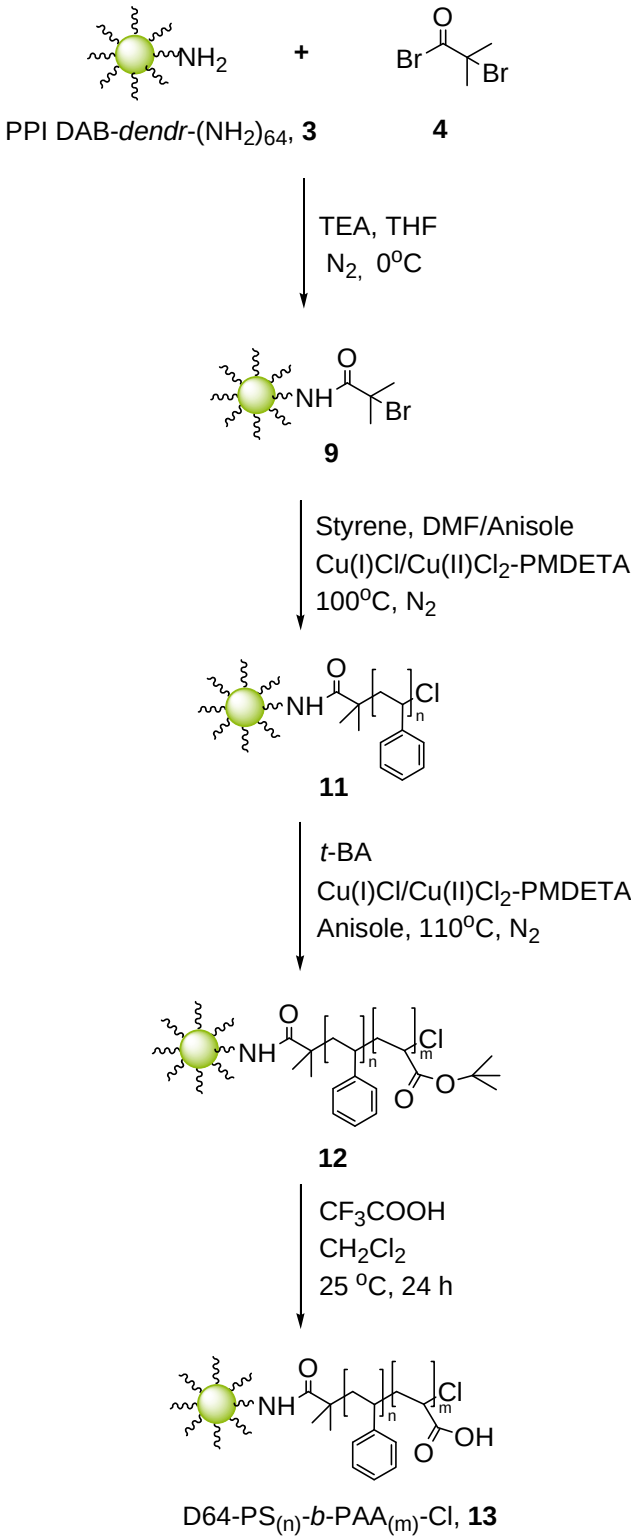

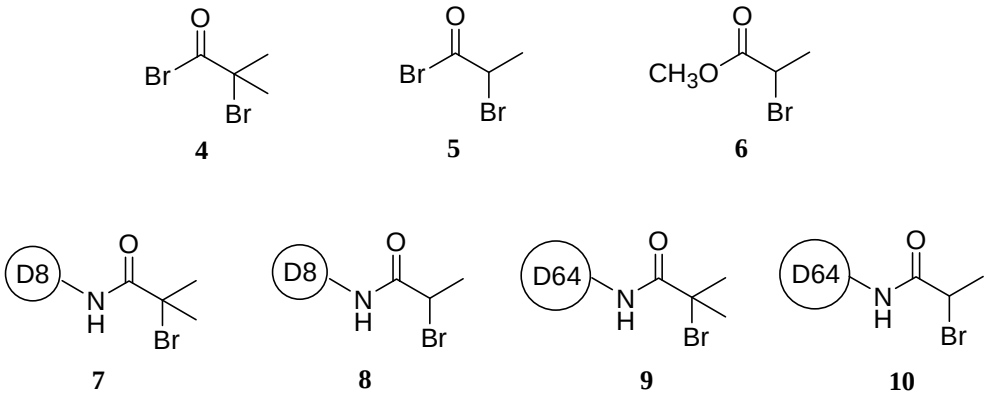

Figure 1. Initiators and dendrimer based initiators for the polymerization of styrene, *t*-butyl methacrylate, and *t*-butyl acrylate.

The 64-arm dendritic ATRP initiator **9** was prepared by condensation of the 64 primary amine groups on PPI DAB-*dendr*-$(NH_2)_{64}$ (**3**) with 2-bromoisobutyryl bromide (**4**) at 0 ^{o}C in 79 % recovery. Experimental conditions are summarized in Table 1.

The new peaks in the proton NMR spectrum that support the structure of **9** are the methyl group at 1.8 ppm, the amide NH at 7.9 ppm, the $NCH_2CH_2CH_2NHCO$ quartet at 3.3 ppm, and the $CHCH_3Br$ quartet at 4.5 ppm (Figure 2).

Table 1. **Synthesis of Dendritic Initiators with PPI DAB-*dendr*-$(NH_2)_{64}$.**

R-X[a]	Reaction Condition	Yield[d] (%)
4[b]	TEA, THF, 0°C, N_2	42-71
4[c]	TEA, THF, 0°C, N_2	79
5[b]	TEA, THF, 0°C-RT, ≥24h, N_2	~21
5[b]	TEA, THF, 0°C, N_2	5-40

[a] See Figure 1. [b] Molar ratio as of **3**:R-X:TEA = 1:1.1:1.1. [c] Molar ratio as of **3**:R-X:TEA = 1:1.5:1.5.
[d] Stable products observed after standing for over 7 days at room temperature and also after storing at -4 °C over one month.

For the synthesis of both the bromide PPI dendrimer initiators from **1** and **3**, no side reaction such as an elimination reaction of HBr was observed when the reaction time was less than one hour at 0 °C. However, when the reaction time was greater than one hour, peaks at 4-5 ppm were observed in the ^{1}H NMR spectrum. The peaks are presumably from the vinyl group of the elimination product at the end of chains in the tertiary carbon. Increase in the reaction temperature from 0 °C to room temperature apparently caused an elimination reaction in the product to give methacrylamide end groups. Heating and/or long standing at room temperature may also cause the elimination reaction. The condensation of PPI dendrimer DAB-*dendr*-$(NH_2)_{64}$ (**3**), as well as DAB-*dendr*-$(NH_2)_8$ (**1**) with 2-bromoisobutyryl bromide (**4**) and 2-bromopropionyl bromide (**5**), was achieved in moderate yield by the modified methods of Haddleton and Matyjaszewski.[18-21] This was the first attempt to use PPI dendrimers DAB-*dendr*-$(NH_2)_8$ (**1**) and DAB-*dendr*-$(NH_2)_{64}$ (**3**) for ATRP initiators, based on a literature search.

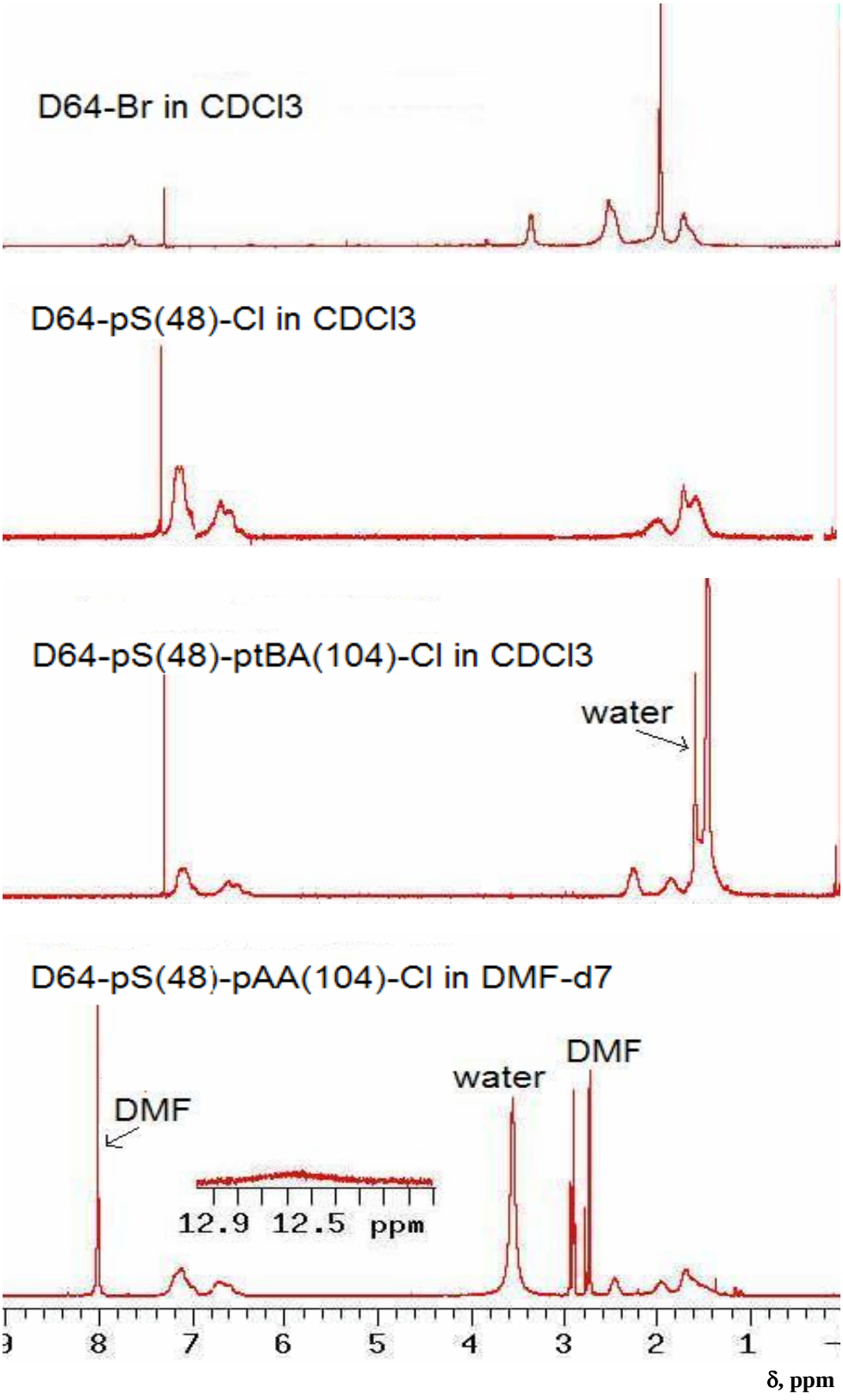

Figure 2. ^{1}H NMR spectra of the PPI dendritic initiator and the corresponding block copolymers.

Regardless of the success of the synthesis of the halogenated ATRP initiator with the PPI dendrimer DAB-*dendr*-$(NH_2)_8$ (**1**), improvement on isolating the product was needed. The initiator **10** was obtained in very low recovery (5-40 %). Combined with proper multiple solvent extractions and with more hydrophobic methyl groups to the dendritic initiator, the yield of initiator **9** was improved to 40-80 %. Two factors were important for recovery of the ATRP initiator. Firstly, the triethylamine hydrochloride side-product from the condensation reaction, was less soluble in THF. However, the modified step was to dissolve the salt in methylene chloride and wash with 5 % aqueous NaOH (pH $\geq$ 14) to remove the salt from the dendritic bromide initiator by multiple extractions. The modified step gave a 3-fold improvement on the recovery of the dendrimer initiator, in particular, for the bromide dendrimer **9**. Secondly, the bromide initiators, for example, 2-bromopropionyl bromide (**5**) and 2-bromoisobutyryl bromide (**4**), also have an effect on the recovery of the product in the case of the dendrimer **3** (Scheme 2). Specifically, the recovery yields of **7** and **9** were better than that of **8** and **10** (Figure 1). The dendritic initiators **8** and **10** seem more hydrophilic than **7** and **9** because of having one less hydrophobic methyl group. The initiators **8** and **10** tend to remain in the aqueous phase more than organic phase. The improvement of the recovery of the product is very important for further synthesis of block copolymers by ATRP. However, for the dendrimer **1** the two bromide initiators (**4** and **5**) did not have a great effect on the recovery of the product compared to the dendrimer **3**.

Polymerization of Styrene and *t*-BMA from the Dendritic Initiators. Polymerization of styrene was studied under various conditions. The best conditions for narrow molecular weight distribution involved the use of **9**/Cu(I)Cl-Cu(II)Cl_2/PMDETA as the dendritic initiator/catalyst/ligand at 100 ^oC in DMF-anisole (Scheme 1).

The monomer conversion was determined by integration of the vinyl resonance (5 - 6 ppm) relative to either the combined values for the aromatic resonance from polystyrene (6 –7.2 ppm) or the methoxy resonance from anisole (3.82 ppm) in the ^1H NMR spectra (Figure 3). As the reaction progressed, the area of the vinyl resonance at 5 - 6 ppm decreased with respect to the methoxy resonance from anisole as an internal standard at 3.82 ppm. The monomer conversion for polymerization of styrene was reproducible. The polymerization in Cu(I)/(II)-PMDETA system led to narrow polydispersity (PDI = 1.1-1.5) (Table 2) and better control of the molecular weight distribution and polydispersity in DMF/anisole as co-solvent system.

Preliminary experiments for the polymerization of styrene with dendrimer initiators are reported in Table 2. The dendritic initiator **1** was used mainly to explore and optimize the conditions. ATRP of styrene with the PPI dendrimer initiator **9** was found to be reproducible at 100 ^oC (Scheme 1).

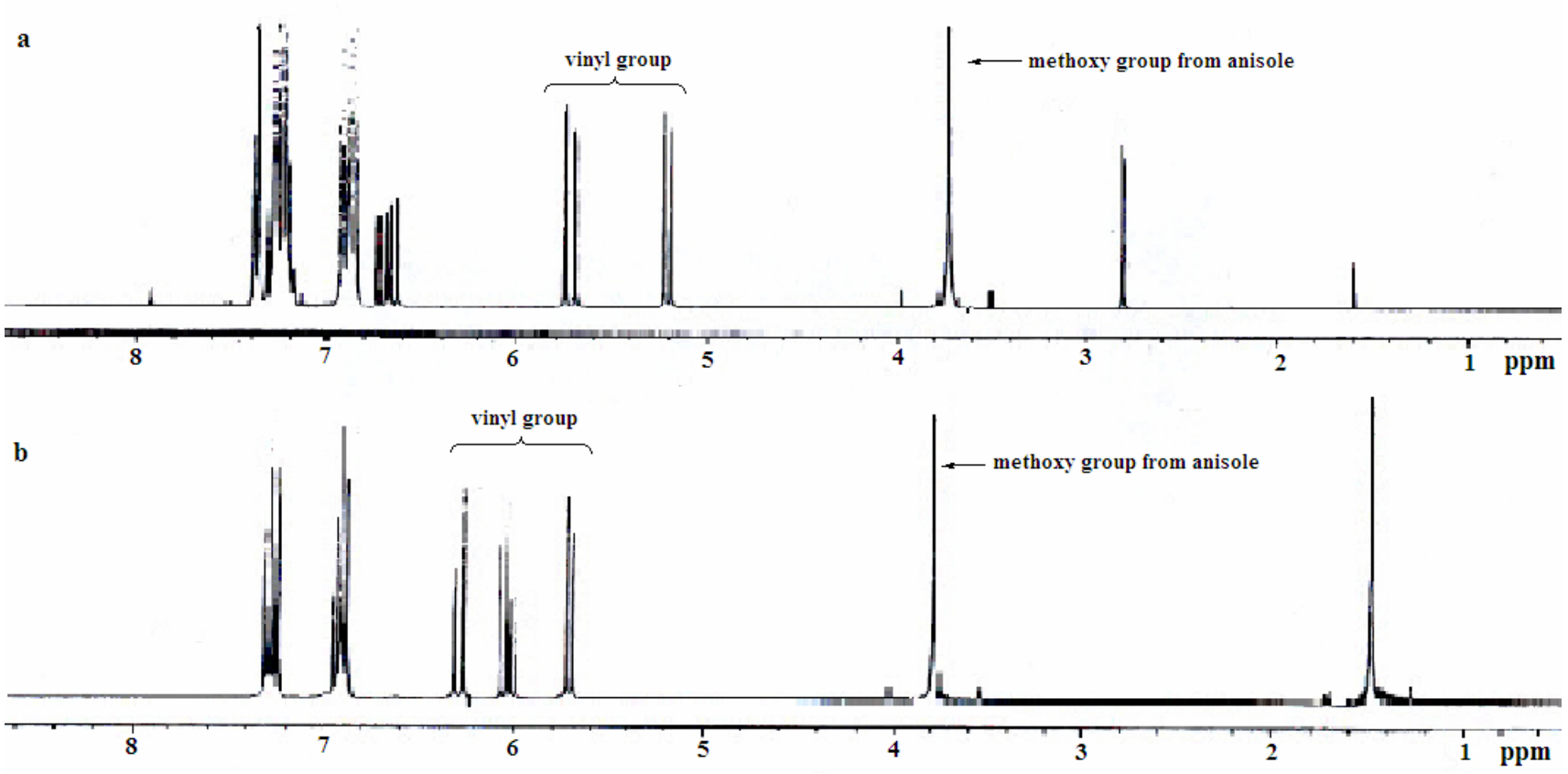

Figure 3. ^{1}H NMR spectra of determination of monomer conversion by integration of the vinyl resonances (6 - 5 ppm) relative to the methoxy resonance from anisole (3.82 ppm) for (a) dendrimer polystyrene **11** and by integration of the vinyl resonances (6.5 - 5.5 ppm) relative to the methoxy resonance from anisole (3.82 ppm) for (b) dendrimer block copolymer **12a**.

Table 2. Poly(styrene-*b*-*tert*-butyl methacrylate) Block Copolymers Using Poly(propylene imine) Initiators.

sample	macro-initiaor[a]	condition	$\overline{DP}$[b]	$M_{n,calc}$[c]	GPC		DLS (nm)[e]		comment[f]
					$M_{n,GPC}$[d]	PDI	major particle size	minor particle size	
2093	8	St/Cu(I)Br DMF 110 °C/380 min	37	32600	111400	1.31	(17-28)	(540) (1060) (3920)	Gel formed
3054	7	St/Cu(I)Cl DMF 110 °C/360 min	60	20100	41300	1.16	(12-29)	(57) (440) (500)	Gel formed
3066	6 & 9	St/Cu(I)Cl DMF 100 °C/105 min	41	18160[g] 4440[g]	6000	1.14	3.7	408	Thick syrup
3070	9	St/Cu(I)Cl DMF 100 °C/240 min	15	113800	10700	1.18	(697)		Gel formed
3077[h]	4			1965			2.3		
3079	3077	St/Cu(I)Cl DMF/toluene 100 °C/260 min	52	44900	24800	1.21	(14.9)[i] (16.2)[j]	(58)[i] (452)[i] (5300)[i] (53)[j] (299)[j]	Thick syrup
3081	3077	St Cu(I)Cl/Cu(II)Cl DMF/anisole 100 °C/32h	52	44900	37000	1.13	11.3 (11.4)	28 (25) (476)	No Gel formed
3083[l]	3081	*t*-BMA Cu(I)Cl/Cu(II)Cl anisole 90 °C/90 min	164	231500	150800	1.88	9.8 (12.1)	22 (903)	No Gel formed
3085[k]	3081	*t*-BMA Cu(I)Cl/Cu(II)Cl anisole 90 °C/110 min	68	122290	64300	1.31	16.1 (20.3)	(697)	No Gel formed
3089[k]	3081	*t*-BMA Cu(I)Cl/Cu(II)Cl anisole 90 °C/80 min	34	83610	67200	1.40	14.6		No Gel formed
3093[l]	3079	*t*-BMA Cu(I)Cl/Cu(II)Cl anisole 80 °C/190 min	26	74510	28100	1.25	24.6	198	No Gel formed

[a]See Figure 1. [b]Calculated from ^{1}H NMR measurement of monomer consumed and eight polymer chains per dendrimer. [c]Calculated from the monomer conversion and $[I]_o$. [d]Calibrated against linear PS standards. [e]Numbers in parenthesis obtained without filtration, THF used as solvent, and size (nm) reported in diameter. [f]Observed during the polymerization. [g]Obtained two types of polymers by mixing two different types of initiators with molar ratio of **6**:**9**:M:PMDETA:Cu(I)Cl = 10:1:500:11:11. [h]Dendrimer inititator used for polymerization of styrene to obtain 3079 and 3081. [i]Toluene used. [j]THF used. [k]Molar ratio : I:M:PMDETA:Cu(I)Cl = 1:578:6.4:6.4. [l]Molar ratio : I:M:PMDETA:Cu(I)Cl = 1:90:1:1.

The polymerization of styrene with dendritic initiators by ATRP could not be conducted in bulk because of insolubility of the dendritic initiators in either monomer (styrene) or ligand (PMDETA), or any common solvent, such as, dioxane. The initiators and catalyst did somehow dissolve in the mixture of styrene-PMDETA at room temperature and produced a small amount of a dark green jelly. This jelly may be either swollen initiator or a copper(II) containing species. As a result, it could cause the polymerization to be irreproducible depending on the amount of the jelly substance formed. Inhomogeneous conditions could also cause the uncontrollable polymerization of styrene with the dendritic initiator during the polymerization. The polymerization of styrene was accomplished at 100 ^{o}C while the copolymerization of *t*BMA was done at 110 ^{o}C. For the solvent, DMF was chosen because the dendritic initiator was soluble in DMF. However, there might cause a problem. DMF tends to be trapped inside the dendrimer core so that the possible problem arises for the macro-dendrimer initiator in the removal of DMF along with the catalyst. On the other hand, DMF dissolves the dendrimer initiator for homogeneous ATRP of styrene. Regardless of the above possible problems, DMF was found to be good for the case of styrene as it produced a controllable and reproducible rate of polymerization. DMF is miscible with methanol. It allowed purifying the polymer from DMF by precipitating the polymer into methanol. The previously mentioned conditions found in the preliminary experiment with dendrimer **1** provided a controllable polymerization of the PPI dendrimer **3** by ATRP in a copper(I) mediated catalyst system.

Complete removal of copper catalyst is another problem for the PPI dendritic block copolymers onto **1** and **3** compared to a small molecule such as methyl 2-

bromopropionate (**6**). The PPI dendrimer is well-known to be capable of complexing with Co, Fe, Ni, Cu, etc. The dendritic copolymers were therefore liable to be contaminated with a small amount of copper catalyst that was evident from the light green or bluish color. On the contrary, polystyrene made from methyl 2-bromopropionate (**6**) as an initiator was a white solid powder that indicated no copper catalyst contamination. Moreover, the copper contaminant on the dendritic block copolymer might also have an effect on the further ATRP polymerization of the second block.

Samples **3079** and **3081** were polymerized with styrene at 100 ^{o}C as summarized in Table 2. Sample **3079** was a thick syrup in DMF/toluene. Sample **3081** formed no gel in DMF/anisole. The difference between the two final physical states could be due to a combination of catalyst system, solubility of polymer formed in the reaction medium, and formation of inter- or intramolecular covalent coupling product. DMF dissolved dendrimer initiators, and both anisole and toluene dissolved polystyrene. The DMF/anisole system formed no gel so that polymerization was homogeneous. However, DMF/toluene system did not improve control of the polymerization of styrene. Cuprous chloride and cupric chloride were used as catalysts with the ligand PMDETA. The cuprous chloride/cupric chloride system was observed to be more controllable than cuprous bromide/cupric bromide system in ATRP.

In order to obtain block copolymers with no residue of polystyrenes, one approach was to try to prevent the formation of covalent coupling product. Covalent coupling product might be promoted by increasing the viscosity of the solution during polymerization. A way to reduce viscosity of the solution is to use a better solvent for the

block copolymer so that chains graft onto the dendrimer core and diffuse into the reaction medium. The dilution would decrease the viscosity of the solution. It leads to maintaining a homogeneous solution and also reduces the formation of a coupling product during polymerization. As a result, polymerization could be well controllable.

The experiments in Table 2 show convenient conditions for ATRP. Sample **3079** produced the resulting thick syrupy solution when solvent was used half of the amount of monomer. However, samples **3081**, **3083**, **3085**, and **3089** formed no gel in the reaction medium when solvent was used in equal or 2-fold of the amount of monomer. Decreasing the viscosity of solution helped prevent gel formation during the polymerization in these four cases. GPCs of the polymers in Figure 4 showed that the block copolymers **3081**, **3083**, **3085**, and **3089** contained the precursor **3081** as a shoulder peak in the range of 14.2-14.3 min retention time as shown in Figure 4b, 4c, 4d, and 4e. It indicates that some of the polystyrene chains did not continue to grow P*t*BMA blocks.

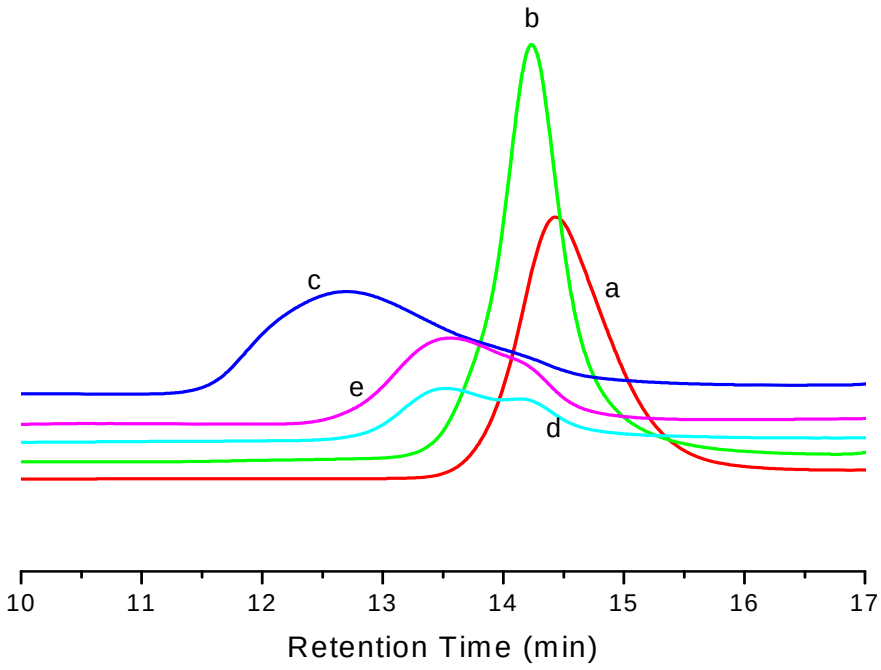

Figure 4. GPC traces determined by RI detector of (a) D8-pS_{52}-Cl (**3079**), (b) D8-pS_{52}-Cl (**3081**), (c) D8-pS_{52}-p*t*BMA_{164}-Cl (**3083**), (d) D8-pS_{52}-p*t*BMA_{68}-Cl (**3085**), and (e) D8-pS_{52}-p*t*BMA_{34}-Cl (**3089**) (see Table 2).

In order to decrease the viscosity of solution and continue chain growth at the same time, the amount of solvent used was 8 times of the amount of monomer. Figure 5 shows the GPC results for the styrene homopolymer and the block copolymer from dendrimer **1**. Figure 5b shows that the block copolymer **3093** does not contain any large amount of polystyrene **3079** because the trace has no shoulder of the starting polystyrene on it.

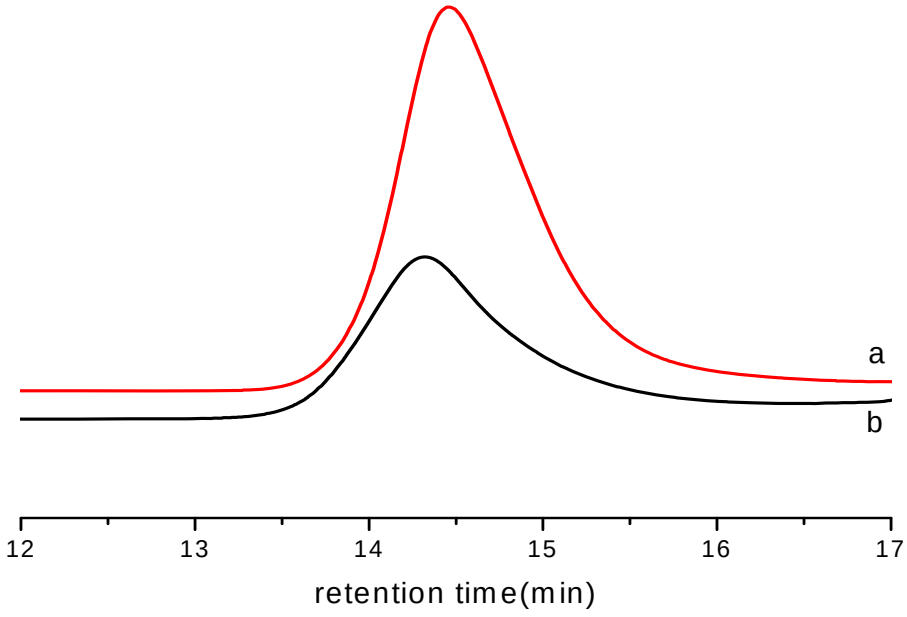

Figure 5. GPC traces measured by RI detector of (a) D8-pS_{52}-Cl (**3079**) and (b) D8-pS_{52}-p*t*BMA_{26}-Cl (**3093**).

Polymerization of styrene and *t*-BA from the dendrimer 3. For the dendrimer **3** the dilute conditions that gave the best results for the dendrimer **1** were used. Table 3 reports the conditions used for ATRP polymerization onto a dendrimer **3** core.

Table 3. Block copolymerization with dendritic initiator 9.

product	[M]/[I]/[Cu(I)]/[L]	monomer	time (h)	conv (%) by NMR	assumed polymer structure
11[a]	200/1/1[c]/1	St	40	24	D64-(pS_{48}-Cl)$_{64}$
12a[b]	800/1/1[c]/1	*t*BA	102	13	D64-(pS_{48}-p*t*BA_{104}-Cl)$_{64}$
12b[b]	1600/1/1[d]/1	*t*BA	48	13	D64-(pS_{48}-p*t*BA_{215}-Cl)$_{64}$
12c[b]	3200/1/1[d]/1	*t*BA	76.5	14	D64-(pS_{48}-p*t*BA_{445}-Cl)$_{64}$

[a]100 °C for polystyrene. [b]110 °C for P*t*BA. [c]Cu(II)/Cu(I) = 0.2. [d]Cu(II)/Cu(I) = 0.1.

The GPCs in Figures 6 and 7 show the use of two different detectors, RI and viscometry, for block copolymers with the dendrimer **3**. No shoulders on the chromatograms indicated that the dilution was indeed useful to eliminate the residue of polystyrene for block copolymerization in ATRP of the dendrimer **3**. Residual amine groups present in the samples were pretreated with phenyl isocyanate in THF solution prior to running the sample through the GPC columns. This allows for clear solutions to provide accurate GPC analyses detected both from viscometry/universial calibration

(univ cal) and light scattering without some of the rest sample adsorbed in the GPC column. Molecular weights shown in the GPC analyses between RI detector and viscometry/ univ cal (or light scattering) detector(s) are largely different for the polymer **11** in Table 4. The discrepancy of molecular weights might result from the residue of the free amine group in the sample adsorbed in the GPC column. GPC analysis using the RI detector did not require with the derivatization with phenyl isocyanate. Molecular weights from the RI detector gave much smaller values than calculated and viscometry-univ cal/light scattering values. The viscometry-univ cal/light scattering molecular weights were closer to calculated values.

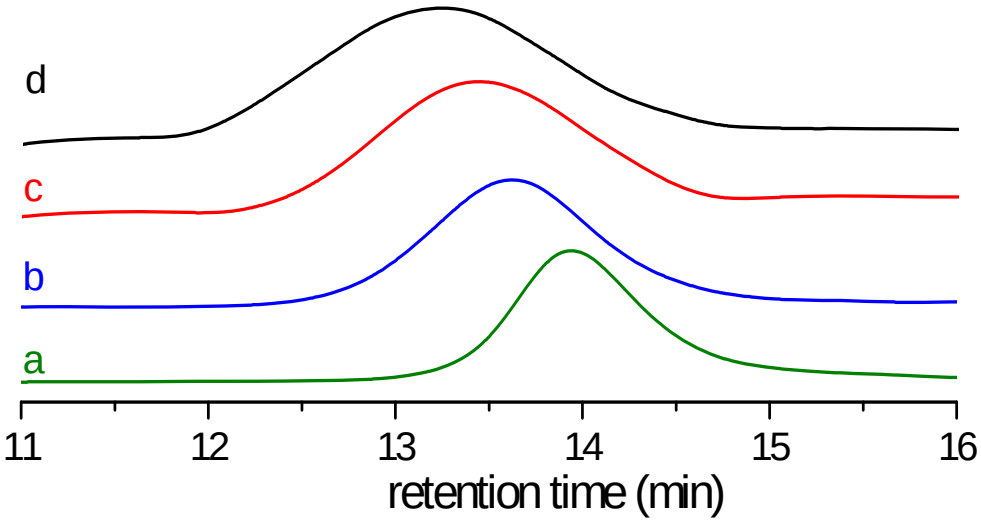

Figure 6 . GPC traces measured by RI detector of (a) D64-Polystyrene$_{48}$-Cl (**11**), (b) D64-Poly(styrene$_{48}$–*b*-*tert*-butyl acrylate$_{104}$)-Cl (**12a**), (c) D64-Poly(styrene$_{48}$–*b*-*tert*-butyl acrylate$_{215}$)-Cl (**12b**), and (d) D64-Poly(styrene$_{48}$–*b*-*tert*-butyl acrylate$_{445}$)-Cl (**12c**).

Table 4. GPC of Polymers with ATRP of Generation 5 PPI Dendrimer Initiator 3[a].

		RI[c]		viscometry/Universial Calibration					light scattering			PS equivalent		
product	$M_{n,calc}$[b]	M_n	PDI	M_n	M_w	M_z	PDI	$[\eta]$ dL/g	dn/dc	M_w	D (nm)	P_n	P_w	P_z
11	337000	66300	1.15	82200	112000	149000	1.36	0.309	0.130	132000	15.4	60500	86400	111000
12a	1190000	97500	1.28	131000	168000	201500	1.28	0.499	0.100	188000	17.0	91500	140000	193000
12b	2090000	116000	1.42	155000	206000	262000	1.33	0.649	0.080	218000	21.5	100000	192000	384000
12c	3980000	141000	1.60	194000	297000	420000	1.53	0.851	0.062	292000	27.6	142000	270000	416000

[a]GPC results obtained from THF solution. [b]$M_{n,calc}$ =[M]/[I] where [M] is the concentration of monomer consumed from NMR analysis of the reaction mixture.
[c]Results from OSU. All other results are from T. H. Mourey, Eastman Kodak Co.

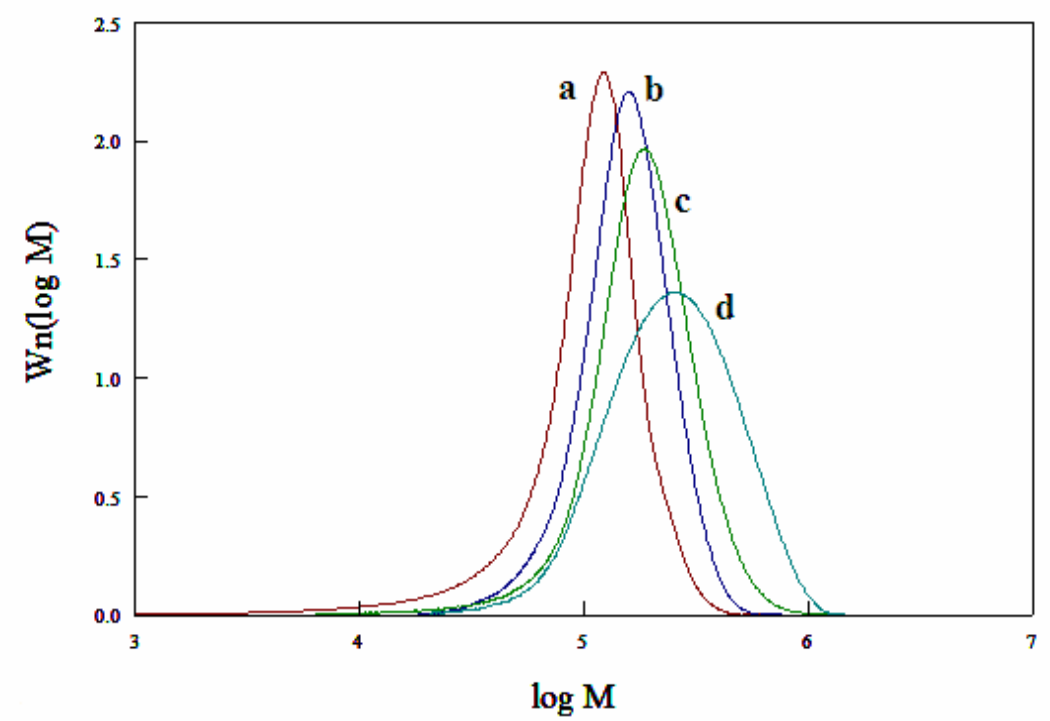

Figure 7. GPC traces measured by viscometry detector of (a) D64-Polystyrene$_{48}$-Cl (**11**), (b) D64-Poly(styrene$_{48}$–*b*-*tert*-butyl acrylate$_{104}$)-Cl (**12a**), (c) D64-Poly(styrene$_{48}$–*b*-*tert*-butyl acrylate$_{215}$)-Cl (**12b**), and (d) D64-Poly(styrene$_{48}$–*b*-*tert*-butyl acrylate$_{445}$)-Cl (**12c**). [From Thomas H. Mourey, Imaging Materials and Media Research and Development, Eastman Kodak Company Research Laboratories].

Polymerization of *t*-BA was mediated by Cu(I)Cl-Cu(II)Cl$_2$/PMDETA using the macroinitiator (**11**) at 110 ^{o}C in anisole (Scheme 1). Table 4 summarizes the results. The monomer conversion was determined by ^{1}H NMR with integration of the vinyl resonance (5 - 6 ppm) relative to the methoxy resonance from anisole (3.82 ppm) (Figure 3). The monomer conversion for block copolymerization of *t*-BA and the rates of polymerization were reproducible. The molar ratio as of I:M:PMDETA:Cu(I)/Cu(II) = 1:800-3200:1:1

was used for better control of its molecular weight distribution and polydispersity. The amount of monomer was 8 to 32-times the normal amount of monomer used for block copolymerization to reduce the rate of termination of polymer radicals relative to the rate of propagation. The reaction in the presence of Cu(I)Cl/Cu(II)Cl_2/PMDETA led to block copolymers of polydispersity (PDI = 1.28-1.60 by RI detector and 1.36-1.53 by viscometry) with diameter of ranging from 17 to 28 nm (Table 4).

In general, a slow rate of polymerization with dendrimer initiator **9** was observed for ATRP of *t*-BA at 110 ^{o}C (Table 3: **12a**, **12b**, and **12c**) in anisole due to the dilute polymerization conditions. The GPC traces in Figure 6 provide that block copolymers **12a**, **12b**, and **12c** grew as the molecular weights of each were increased. These GPC results indicate that block copolymerization provides controllability for ATRP of *t*-BA at 110 ^{o}C.

The GPC data in Table 4 indicates that the molecular weights of the branched polymers are less than the molecular weights calculated on the basis of 64 growing chains. Absolute molecular weights measured by viscometry and universal calibration (M_n) and by light scattering (M_w) are much less than molecular weights calculated by assuming $M_{n,calc}$ = [M]/[I] where [M] = concentration of monomer consumed and [I] = initiator concentration. Therefore, the number of active growing chains per dendrimer was much less than the assumed number of 64. This could happen because of termination of chains located close in space on the dendritic molecule, because steric crowding of the initiator sites by growing chains prevented growth from many of the initiator groups, or because of some unknown reaction that converted initiator sites to inactive chain ends. The unknown could be associated with intermolecular radical-radical coupling as well as

intramolecular coupling at high molecular weights due to the possible elimination product at the end of chains as seen for the case of **1** in Table 2. The potential for cross-linking is possible to occur during polymerization as a result of radical coupling of the growing polymer chain ends. GPC for molecular weight from linear polystyrene standard are not accurate for highly branched polystyrenes. The measured absolute molecular weights are larger than those calculated for linear polystyrene (PS) and linear poly(methyl methachrylate) (PMMA) standards. Molecular weights increase as the calculated of DP_n (degree of polymerization) of P*t*BA increases. For example, $M_{n,RI}$, $M_{n,vis}$, and $M_{n,LS}$ are much smaller than $M_{n,calc}$ calculated assuming a 64-branch star due to the compact nature of spherical dendrimer/PS composite (Table 4). The star molecule has a small number of branches because of many less active initiator sites on the dendrimer. However, ATRP controlled the growth of PS and P*t*BA blocks as shown by systematic increase of molecular weights from increasing amounts of *t*BA monomers.

Although GPC calibrated by linear polymer standards is not accurate for molecular weight, peak width in GPC is reliable for determining polydispersity (PDI). The PDI values of polymers **12a**, **12b**, and **12c** measured by both RI and viscometry detectors are consistent in the range of 1.2-1.6. This indicates that ATRP was controllable for the growth of the chain ends on to a dendritic core.

Poly(styrene-*b*-acrylic acid) (13). Conversion of the P*t*BA blocks to poly(acrylic acid)(PAA) blocks with CF_3COOH in CH_2Cl_2 for 24 h at 25 ^oC was performed. A 25-fold molar excess of CF_3COOH was used with respect to the *t*-butyl groups in the blocks. As shown in Figure 2 for sample **13a**, the disappearance of the

characteristic strong peak at 1.56 ppm corresponding to the methyl protons of the *t*-butyl group demonstrates the complete conversion of P*t*BA blocks to PAA blocks. DMF-d_7 was used as the NMR solvent because PAA dissolved well in DMF-d_7 enabling identification of the carboxylic acid group in PAA at 12.5 ppm. Otherwise $CDCl_3$ was the common NMR solvent for both PS and P*t*BA (Figure 2).

Dynamic Light Scattering Measurements of Initial Reaction Mixtures. A mixture of amphiphilic block copolymer dendrimer in DMF and water was stirred at room temperature for 30 min. The solution was transferred to a glass cuvette, and the average diameter of the scattering particles was measured by DLS to be > 80 nm in most cases at pH > 8. DMF-water was effective as a co-solvent for styrene latexes with low polydispersity at above pH 8. THF-water was ineffective due to aggregates of the amphiphilic dendritic block copolymer at either low or high pH. The data of DLS are reported in Table 5.

Table 5. Dynamic Light Scattering (DLS) of PS-PAA Block Copolymers.

polymer	DLS (diameter, nm)			
	DMF	Water/DMF(20/1)		
		pH 10	pH 7	pH 4
13a	16	48 / 738	294	104
13b	17	355	25 / 406	140
13c	22	28 / 347 / 617	37 / 356 / 740	92

The diameters of particles were measured by DLS. Each individual particle was observed for samples **13a**, **13b,** and **13c** in DMF. However, multiple diameters in samples **13a**, **13b,** and **13c** were found in water/DMF. The DLS shows each particle aggregates in different sizes at pH 7 and pH 10 although aggregates in size at pH 4 are uniform. At pH 4 individual particles might aggregate at once and then not change. At pH > 7 individual particles might aggregate and then break them out into the smaller clustered particles due to more exposure of the free carboxylate form of PAA.

Latex Synthesis. In spite of the advantage associated with small particle size, the presence of large amounts of surfactant in the latex is highly undesirable for adhesive and coating applications.[27] The small and mobile surfactant molecules might migrate toward the surface layer of the coating material and can degrade the film properties. One approach to eliminate such a surfactant migration problem is to exploit the surfactant-free method, in which the carboxyl groups derived from acid monomers, such as, methacrylic acid (MAA) or acrylic acid (AA), are responsible for stabilization of the latex particles. In the report here, the amphiphilic dendritic PS-*b*-PMAA **3100** was investigated as a seed for semi-continuous emulsion polymerization of styrene (see Table 6 and Experimental section). The ability of self-assembly in amphiphilic block copolymers can be utilized to control aggregates and form micelles in aqueous solution for surfactant-free emulsion polymerization.[28,29] Here, one problem is that the dendritic block copolymer was not soluble in water at any range of pH. The block copolymer was shown by DLS measurements to be aggregated at pH > 8. It may indicate that the interaction of PMAA segments is caused by assembling them at the dendrimer surface. With aid of DMF as

co-solvent, **3100** was able to dissolve in aqueous solution because both polystyrene and polymethacrylic acid blocks are soluble in DMF.[30] When the diameter of the dendritic block copolymer in aqueous-DMF solution at various pHs was measured by DLS, the dendritic block copolymers were found to self-aggregate in the pH range of 8-13. It is possible that the PMAA segment formed a more hydrophobic and compact coil conformation at pH > 8. The ability of PMAA is well documented to exhibit a pH-dependent conformational transition in aqueous solution from compact coil to random coil and simultaneously shows a drastic change in hydrophobicity of the segment by varying the pH. PAA is also known to behave in a very different manner.[31-34] The inability of a random coil of PAA to aggregate in acidic media can be explained by the absence of α-methyl groups in the polymeric chains.[32] Therefore, if such PAA segments can be introduced to the dendrimer core next to a PS segment, stable colloidal particles can form in aqueous solution. The amphiphilic block copolymers are known to be efficient when optimal composition has short blocks of PS(~10) and long blocks of PAA(>50).[35] An increase in the hydrophilic block length has been also reported to result in the formation of smaller particle sizes.[36] The higher repulsion favors a decrease in the radius of curvature and contributes to the formation of smaller sizes from copolymers with longer PAA block length.[31] However, block copolymers with shorter PAA block length self-assemble into larger sizes.

Table 6. Particle Sizes by TEM and DLS for Polystyrene Latexes.

Product sample	ingredients	DLS diameter (nm)	TEM[a] diameter (nm) (avg.)
4014	D8-pS_{52}-*b*-$pMAA_{26}$-Cl (**3100**)[b] (10 mg) styrene (1.5 mL) KPS (45 mg) water/DMF(27.5 mL/1 mL)	179	152
4025	D8-pS_{52}-*b*-$pMAA_{26}$-Cl (**3100**)[b] (5 mg) styrene (0.5 mL) KPS (45 mg) water/DMF(27.5 mL/1 mL) SDS (50-100 mg)	45-55	-
4080	(D64-pS_{48}-*b*-pAA_{104}-Cl (**13a**) (20 mg) styrene (1 mL) KPS (30 mg) water/DMF(27.5 mL/1 mL)	293	104[c]
4081	D64-pS_{48}-*b*-pAA_{104}-Cl (**13a**) (50 mg) styrene (0.5 mL) KPS (30 mg) water/DMF(27.5 mL/1 mL) SDS (50 mg)	40-60	-

[a]See Figure 8. [b]Sample 3100 is described in Experimental section. [c]Sample was stained with uranyl acetate.

Latex particles were prepared by emulsion polymerization of styrene in the presence of sodium dodecyl sulfate (SDS) or without SDS anionic surfactant and amphiphilic PS-*b*-PMAA **3100** with potassium persulfate (KPS) initiator in DMF-water at 80 ^{o}C. The polymerization was accomplished by the semicontinuous method. The polymerization produced relatively monodisperse latexes with average diameters between

120 and 180 nm when no SDS was used (Figure 8a and Table 6). The particle size distribution (PSD) was broad with diameters of 45-55 nm when SDS was used.

The pH of the polymerization medium was around 9 for full ionization of the carboxylic acid unit. The pH was adjusted by addition of $NaHCO_3$ aqueous solution during the polymerization to reach monodisperse and nano-sized particles. The diameter of styrene latex was measured as 313 nm by DLS when the polymerization medium was tested as acid, such as pH 4-6, during the polymerization. The diameter was larger than that from the basic medium for polymerization. The optimal pH should be about 9 for full dissociation of carboxylic acid unit in the seed-growth emulsion polymerization of styrene with the dendrimer.

Emulsion polymerization of styrene with D64-pS_{48}-*b*-pAA_{104}-Cl (**13a)** was also accomplished in the presence of SDS or in the absence of SDS anionic surfactant and with KPS initiator in DMF-water at 80 ^{o}C. Transmission electron microscope (TEM) images of polystyrene latex particles prepared with **13a** (Figure 8b) show similar results to those of **3100**. In the presence of SDS, polystyrene latex particles are around ~40-60 nm in diameter but over 100 nm in diameter in the absence of SDS.

The TEM image of sample **13a** in Figure 8b shows both individual and clustered spherical particles. The diameters from DLS were much larger than those from TEM. The discrepancy was expected because DLS measures a hydrodynamic size and counts a cluster as one particle.

(a)

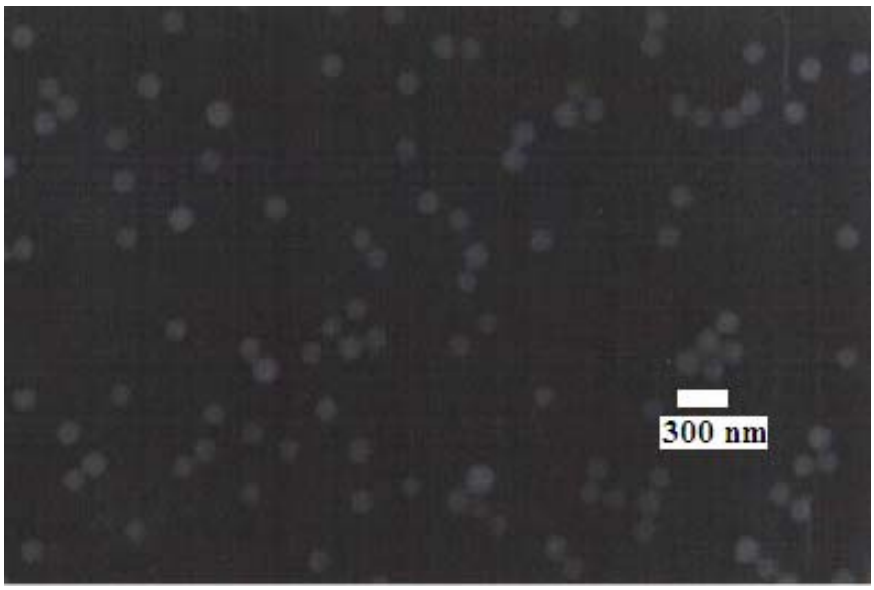

(b)

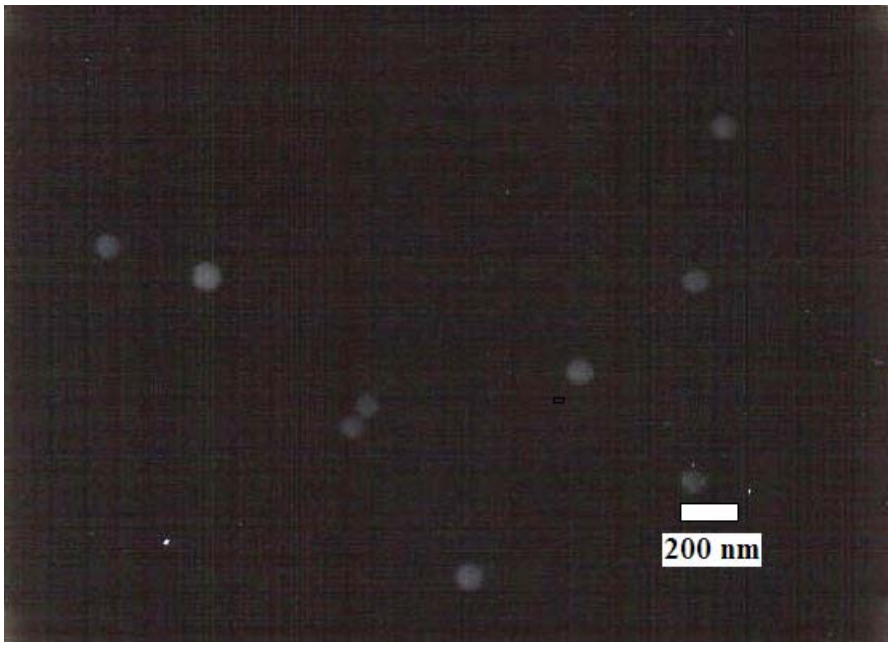

Figure 8. Transmission electron microscope (TEM) images of polystyrene latex particles. (a) Polystyrene latex from **3100**; Diameter: 152 nm. (b) Polystyrene latex **13a**; Diameter: 104 nm; The TEM sample was stained with uranyl acetate. (See Table 6).

Dendritic latex synthesis seems to agree with the analysis of D64-pS-*b*-p*t*BA-Cl by GPC. If the dendrimer had been fully substituted with halides at the chain ends and subsequently polymerized fully at chain ends followed by deprotection of ester groups, the fully negatively charged chain ends of polystyrene latex should be expected to disperse into the basic aqueous solution at pH 10-11. Without aggregation, the polystyrene latex particles would be less than 50 nm in diameter in the absence of SDS. However, the latex was in fact more than 100 nm in diameter in the absence of SDS. The larger size of the latex indicates that the latex formed aggregates due to not fully negatively charged chain ends of the D64-pS-b-pAA-Cl.

The amounts of dendrimer template and styrene had little affect on the particle sizes. However, the presence of SDS reduced the average diameter to approximately 50 nm with broad particle size distribution (PSD). More than 100 nm and narrower particle size distribution was obtained in the absence of SDS.

Emulsion polymerization provided broader particle size distribution (PSD) but smaller diameters of individual clusters in the presence of SDS regardless of the lengths of the PMAA (~26) and PAA (~104) blocks at the PS blocks (~50). In the absence of SDS, the emulsion polymerization showed the opposite results with the same polymers, i.e. narrow PSD and large aggregates.

Conclusions

The end groups of the poly(propylene imine) (PPI) dendrimer were converted to 2-bromoisobutyramides to initiate atom transfer radical polymerization (ATRP), and blocks of polystyrene (PS) and poly(*tert*-butyl acrylate) (P*t*BA) were grown by ATRP. The P*t*BA blocks were converted to poly(acrylic acid) (PAA) to give branched amphiphilic PS-PAA block copolymers.

The measured molecular weights of the PS-*b*-P*t*BA from PPI DAB-*dendr*-$(NH_2)_{64}$ are larger than those calculated for linear PS and linear PMMA standards. The measured molecular weights are much less than the molecular weights calculated assuming a 64-branch star. Molecular weights increase as the calculated of DP_n of P*t*BA increases.

The branched amphiphilic polymers are stars with small numbers of branches resulting from growth at a small number of initiator sites per dendrimer. The amphiphilic polymers are controlled by ATRP for the growth of PS and P*t*BA blocks. However, the number of active initiator sites on the dendrimer is very much smaller than expected assuming a 64-branch star.

Branched aggregates of the PS-P*t*BA and of the PS-PAA detected by dynamic light scattering (DLS) and transmission electron microscope (TEM) images of polystyrene latex particles in water-DMF mixtures show that the materials have aggregation characteristics of amphiphilic PS-PAA block copolymers.

Experimental Section

Materials. PPI DAB-*dendr*-$(NH_2)_n$ (n = 8 and 64), 2-bromoisobutyryl bromide, 2-bromopropionyl bromide, and *N,N,N',N''*-pentamethyldiethylenetriamine (PMDETA) (99%), were purchased from Aldrich (Milwaukee, WI) and used as received. Anisole (99%), THF (99.9%), and DMF (99.8%) were purchased from Acros and used as received. Triethylamine (TEA) was dried over anhydrous 3 Å molecular sieves and freshly distilled.

Copper(I) chloride (99.995+ %) was used as received from Aldrich. Copper(II) chloride (dihydrate) was purchased from EM Science. Copper(I) bromide (2 g, 98 %) was stirred over glacial acetic acid under N_2 at room temperature for 12 h. The deep blue-green mixture was filtered under N_2 and washed with ethyl alcohol and anhydrous diethyl ether until the color of the filtrate changed from blue-green to yellow. The purified copper(I) bromide (pale yellow) was dried via vacuum either at room temperature for 12 h or at 60 ^oC for 6 h and stored in the dark at room temperature. Diethyl ether tended to give a gray tint to the copper(I) bromide.

Styrene, *tert*-butyl methacrylate (*t*-BMA), and *tert*-butyl acrylate (*t*-BA) were purified by passage through a column of activated basic alumina (~150 mesh, 58 Å) to remove inhibitor and moisture. Sodium dodecyl sulfate (SDS), potassium persulfate (KPS, 99+ %), and sodium bicarbonate were purchased from Aldrich (Milwaukee, WI) and used as received unless otherwise stated. Water was purified using a Barnstead water purification system.

Characterization. Conversion was determined using ^1H NMR by measuring residual monomer relative to either a newly formed polymer or solvent as an internal

standard. The M_n and M_w/M_n of the polymer samples were measured with a Agilent series 1100 chromatograph using a THF as eluent (1 mL/min) at 40 ^oC using differential refractive index detection. Polymer Laboratories gel permeation chromatography (GPC) columns (2 PLgel 10μm mixed B 7.5 mm ID) were used. Samples and polystyrene standards were filtered through a Whatman polypropylene filter (0.2 μm) prior to injection. Amounts and concentrations of samples used for GPC analysis were 10 μL for injection and 5 mg of a sample in 1 mL of THF for sample preparation. Molecular weights of polystyrene and poly(*t*-butyl acrylate) were calibrated against polystyrene standards in the range of 1,800,000-500 g/mol.

Second GPC analyses were performed at Eastman Kodak Co. on solutions of the polymers in DMF containing 0.01 M lithium nitrate using two PSS Gram Linear 8 x 300 mm columns. The column set was calibrated with narrow molecular weight distribution poly(methyl methacrylate) standards and polystyrene standards. The instrument was equipped with differential refractometer and differential viscometer detectors. Concerning residual amine groups present in the samples, phenyl isocyanate (2 drops) was added to 10 mL of a 2 mg/mL THF solution of the polymer and warmed for 1 h. This derivatization treatment gives clear solutions for all polymers and permits reproducible chromatography in THF as shown in Table 4.

Particle sizes by dynamic light scattering (DLS) were measured by back-scattered light at 25 ^oC using a Malvern High Performance Particle Sizer (HPPS) 3.3 version instrument equipped with a He-Ne laser (633 nm). The samples were filtered with a Whatman polypropylene filter (0.2 μm).

The transmission electron microscopy (TEM) images were obtained at 80 keV with a JEOL JEM 100 CX II instrument. The emulsion was diluted with the ratio of 1:15 in water to give a stock solution of each sample. A suspension preparation technique was used to deposit the particles on a Formvar-coated copper grid. A drop of the stock solution was deposited onto the grid and blotted with a small piece of filter paper to dry.

Dendritic Macroinitiator 7.[18-21] A solution of **1** (0.262 g, 0.339 mmol) and TEA (0.302 g, 0.339 mmol/1 NH_2) in anhydrous DMF (3 mL) was placed in a 25-mL, two-necked, round-bottomed flask under nitrogen at 0 ^oC in an ice/water bath. With magnetic stirring, 2-bromoisobutyryl bromide (**4**) (0.685 g, 0.339 mmol/1 NH_2) was added dropwise by a syringe over 5 min and stirred for another 5 min at 0 ^oC. A 1.1-fold molar excess of TEA and the bromide **4** (with respect to the NH_2 groups at the end of chains) was used. The reaction mixture became a red-yellow suspension during the addition of the bromide. DI (deionized) water (1 mL) was added, and 5% aqueous NaOH (10 mL) was then added to pH 12. The basic aqueous solution was extracted with methylene chloride (3 x 10 mL). The organic layer was combined and dried over anhydrous K_2CO_3 for 3 h. The K_2CO_3 was filtered off. Solvent and excess reagents were then removed at room temperature by rotary evaporation. Residual DMF and TEA were removed by vacuum distillation with toluene at room temperature. The crude product was dried under vacuum at room temperature for 12 h. Initiator **7** (0.506 g, 76.0 %) was used for polymerization of styrene without further purification. ^1H NMR (300 MHz, $CDCl_3$, δ): 1.3 (br, $NCH_2CH_2CH_2CH_2N$), 1.4-1.9 (br, $NCH_2CH_2CH_2N$ and $NCH_2CH_2CH_2NHC{=}O$), 1.8 (d, CH_3), 2.5 (t and br, $NCH_2CH_2CH_2CH_2N$, $NCH_2CH_2CH_2N$, and

NC*H*$_2$CH$_2$CH$_2$NHC=O), 3.3 (q, NCH$_2$CH$_2$C*H*$_2$NHC=O), 4.5 (q, C*H*CH$_3$Br), 7.9 (t, N*H*C=O).

Dendritic Macroinitiator 9. [18-21] A solution of **3** (0.277 g, 0.0386 mmol) and TEA (0.375 g, 1.5 mol TEA/mol NH_2) in anhydrous THF (20 mL) was placed in a 50-mL, two-necked, round-bottomed flask under nitrogen at 0 ^oC in an ice/water bath. With magnetic stirring, 2-bromoisobutyryl bromide (**4**) (0.853 g, 1.5 mol/mol NH_2) was added dropwise by a syringe over 5 min and stirred for another 5 min at 0 ^oC. A 1.5-fold molar excess of TEA and the bromide **4** (with respect to the NH_2 groups at the end of chains) was used. Aqueous NaOH (5%, 10 mL) was then added to pH 14. The basic aqueous solution was extracted with methylene chlroride (3 x 20 mL). The combined organic layers were dried over anhydrous K_2CO_3. The solution was filtered, and the solvent and excess reagents were removed under vacuum. The crude product was dried under vacuum at room temperature for 24 h. Initiator **9** (0.457 g, 80%) was used for polymerization of styrene without further purification. ^{1}H NMR (300 MHz, $CDCl_3$, δ): 1.3 (br, NCH$_2$C*H*$_2$C*H*$_2$CH$_2$N), 1.4-1.9 (br, NCH$_2$C*H*$_2$CH$_2$N and NCH$_2$C*H*$_2$CH$_2$NHC=O), 1.8 (d, C*H*$_3$), 2.5 (t and br, NC*H*$_2$CH$_2$CH$_2$C*H*$_2$N, NC*H*$_2$CH$_2$C*H*$_2$N, and NC*H*$_2$CH$_2$CH$_2$NHC=O), 3.3 (q, NCH$_2$CH$_2$C*H*$_2$NHC=O), 4.5 (q, C*H*CH$_3$Br), 7.9 (t, N*H*C=O).

Polymerization of Styrene onto Dendritic Initiator 7.[11,21,37] Initiator **7** (0.168 g, 0.0855 mmol), PMDETA (0.119 g, 0.687 mmol) and styrene (7.12 g, 0.0684 mol) in DMF (0.14 mL) and anisole (7.84 mL) were placed in a 25-mL Schlenk flask equipped with a stopper and a tube with a stopcock covered with septum for withdrawal of samples and a nitrogen inlet and outlet. Three freeze-pump-thaw cycles were performed. All

glassware was oven-dried and purged with nitrogen before polymerization. To the dry flask with degassed dendritic initiator **7**, PMDETA, and styrene in DMF/anisole were added CuCl (0.068 g, 0.687 mmol) and $CuCl_2$ (0.007 g, 10 wt % of CuCl) at -70 ^oC under a nitrogen atmosphere. CuCl and $CuCl_2$ were added as solids under the nitrogen atmosphere. The flask was evacuated and flushed with dry nitrogen three times to remove oxygen. The initial mixture was a green suspension which became a homogeneous solution with stirring at room temperature for 30 min. The flask was immersed in a thermostated oil bath at 100 ^oC. For determination of polymerization with desirable monomer conversion, an 0.1 mL aliquot of the solution was taken every hour until the desired monomer conversion was measured by ^1H NMR. Catalyst residues were removed by passing the samples through a short column of activated basic alumina with $CDCl_3$ (1 mL) prior to NMR analysis. The eluate was collected directly into the NMR tube for monomer conversion. After 32 h, the remaining reaction mixture was cooled at 0 ^oC in an ice bath to stop the polymerization, diluted with CH_2Cl_2 (5 mL) and passed through basic alumina, and the alumina was washed with methylene chloride (5 x 1 mL). The filtrate was concentrated under reduced pressure by rotary evaporation. The residue was precipitated into methanol and filtered to give a green-white powder. The polymer (2.990 g, 77.9 %) was dried at room temperature for 12 h under vacuum.

Block Copolymer 3093. A solution of PMDETA (0.0418 g, 0.241 mmol), *t*-BMA (3.08 g, 0.0217 mol), and **3079** (1.355 g, 0.0302 mmol) in anisole (28 mL) were placed in a 25-mL, two-necked, round-bottomed flask and deoxygenated by three freeze-pump-thaw cycles under a nitrogen atmosphere. The flask was evacuated and flushed with dry nitrogen three times to remove oxygen. Then CuCl (0.024 g, 0.242 mmol) and

$CuCl_2$ (0.002 g, 10 wt % of CuCl) were added to the flask at -70 ^oC under N_2. The reaction mixture was stirred for 20 min until it turned into a green-blue homogeneous solution. The flask was placed into a thermostated oil bath at 80 ^oC. For determination of the degree of polymerization with targeted ~10 % monomer conversion, a 0.1 mL aliquot of the solution was taken every 30 min until the desired monomer conversion was measured by ^1H NMR. Catalyst residues were removed by passage of the solution through a short column of activated basic alumina with $CDCl_3$ (1 mL) prior to NMR analysis. After 195 min, the remaining reaction mixture was passed through basic alumina, and the alumina was washed with methylene chloride (5 x 1 mL). The filtrate was concentrated under reduced pressure by rotary evaporation. The residue was precipitated into methanol and microfiltered to give an off-white solid. The polymer **3093** (0.716 g) was dried under vacuum at room temperature for 9 h.

Polymerization of Styrene onto Dendritic Initiator 9. [11,21,27] All glassware was oven-dried and purged with nitrogen. Initiator **9** (0.442 g, 0.0265 mmol), PMDETA (0.293 g, 1.691 mmol) and styrene (35.3 g, 0.339 mol) in DMF (4.8 mL, 10 wt % of total reagents) and anisole (78.0 mL) were placed in a 250-mL Schlenk flask. Three freeze-pump-thaw cycles were performed. To the flask was added CuCl (0.168 g, 1.697 mmol) and $CuCl_2$ (0.034 g, 20 wt % of CuCl) at -70 ^oC under a nitrogen atmosphere. The flask was evacuated, refilled with nitrogen three times to remove oxygen, and held at 100 ^oC. For determination of the degree of polymerization, a 0.1 mL aliquot of the solution was taken for NMR analysis every hour until the desired monomer conversion was reached. The reaction mixture was cooled at 0 ^oC in an ice bath, diluted with CH_2Cl_2 (10 mL), and passed through basic alumina, and the alumina was washed with methylene chloride (10

mL). The polymer **11** (7.705 g, 80 %) was precipitated into methanol, filtered, and dried under vacuum at room temperature for 12 h.

Polymerization of *t*-Butyl Methacrylate. A solution of PMDETA (0.0686 g, 0.00769 mmol per end group with a 6.4-fold molar excess), *t*-BMA (5.06 g, 0.0356 mol), and **11** (0.346 g, 0.00769 mmol) in anisole (10 mL) were placed in a 25-mL, two-necked, round-bottomed flask and deoxygenated by three freeze-pump-thaw cycles under a nitrogen atmosphere. The flask was evacuated and flushed with dry nitrogen three times to remove oxygen. CuCl (0.039 g, 0.394 mmol) and $CuCl_2$ (0.004 g, 10 wt % of CuCl) were added to the flask at -70 ^{o}C under N_2. The reaction mixture was stirred for 20 min until it turned into a green-blue homogeneous solution. The flask was placed in a thermostated oil bath at 90 ^{o}C. For determination of the degree of polymerization with targeted ~10 % monomer conversion, a 0.1 mL aliquot of the solution was taken every 30 min until the desired monomer conversion was measured by ^{1}H NMR. Catalyst residues were removed by passage of the solution through a short column of activated basic alumina with $CDCl_3$ (1 mL) prior to NMR analysis. After 110 min, the remaining reaction mixture was passed through basic alumina, and the alumina was washed with methylene chloride (5 x 1 mL). The filtrate was concentrated under reduced pressure by rotary evaporation. The residue was precipitated into methanol and filtered to give a green-white solid. The polymer (0.637 g, 67.8 %) was dried under vacuum at room temperature for 12 h.

Conversion of the Poly(*t*-butyl methacrylate) Blocks to Poly(methacrylic acid).[38] In a 100-mL, round-bottomed flask, the block copolymer **3093** (0.860 g, 0.0115 mmol) was dissolved in methylene chloride (40 mL) and a 25-fold molar excess of TFA

(6.84 g, 0.0599 mol) was added slowly with magnetic stirring at room temperature. The mixture was stirred at room temperature for 24 h. The solvent and CF_3COOH were removed by rotary evaporation. The residue was diluted with THF (5 mL) and precipitated into hexane (~150 mL) to give an off white solid. The product **3100** (0.577 g, 80 %) was filtered and dried under vacuum at room temperature for 10 h. Characterization was accomplished using proton NMR in pyridine-d_5.

Polymer 12a. The polymerization was carried out in a 100-mL Schlenk flask. The reagents, PMDETA (0.0393 g, 0.227 mmol), *t*-BA (23.3 g, 0.183 mol), and **11** (1.184 g, 0.00355 mmol) in anisole (53.2 mL) were placed in the flask and deoxygenated by three freeze-pump-thaw cycles. CuCl (0.023 g, 0.232 mmol) and $CuCl_2$ (0.004 g, 20 wt % of CuCl) were added to the flask at -70 ^oC under N_2. The reaction mixture was immersed in a thermostated oil bath at 110 ^oC for 102 h. The remaining reaction mixture was cooled to 0 ^oC and then room temperature and diluted with methylene chloride, the reaction mixture was passed through basic alumina, and the alumina was washed with methylene chloride, followed by micro-filtration (0.2 μm filter). The filtrate was concentrated under reduced pressure by rotary evaporation. The residue was precipitated into methanol and filtered to give a white solid. The polymer **12a** (1.986 g) was isolated by precipitation into methanol, filtered, and dried under vacuum at room temperature for 12 h.

Polymer 12b. The polymerization was carried out in a 100-mL Schlenk flask. The reagents, PMDETA (0.0358 g, 0.207 mmol), *t*-BA (42.3 g, 0.333 mol), and **11** (1.076 g, 0.00322 mmol) in anisole (49.0 mL) were placed in the flask and deoxygenated by three freeze-pump-thaw cycles. CuCl (0.020 g, 0.202 mmol) and $CuCl_2$ (0.002 g, 10 wt

% of CuCl) were added to the flask at -70 ^{o}C under N_2. The reaction mixture was immersed in a thermostated oil bath at 110 ^{o}C for 48 h. The polymer **12b** (2.120 g) was isolated by precipitation into methanol, filtered, and dried under vacuum at room temperature for 12 h.

Polymer 12c. The polymerization was carried out in a-100 mL Schlenk flask. The reagents were used for this polymerization: PMDETA (0.0343 g, 0.198 mmol), *t*-BA (81.2 g, 0.638 mol), **11** (0.516 g, 0.0634 mmol) in anisole (46.5 mL), CuCl (0.010 g, 0.101 mmol), and $CuCl_2$ (0.001 g, 10 wt % of CuCl). The polymerization was performed at 110 ^{o}C for 67.5 h. The polymer **12c** (4.745 g) was isolated by precipitation into methanol, filtered, and dried under vacuum at room temperature for 12 h.

Conversion of the Poly(*t*-butyl acrylate) Blocks to Poly(acrylic acid).[38] In a 25-mL, round-bottomed flask, the block copolymer **12** (0.111 g, 0.000189 mmol) was dissolved in methylene chloride (15 mL) and a 25-fold molar excess of TFA (1.79 g, 0.0157 mole) was added slowly with stirring at room temperature. The mixture was stirred at room temperature for 24 h. The solvent and CF_3COOH were removed by rotary evaporation. The residue was diluted with methylene chloride (3 mL) and precipitated into hexane (~50 mL) to give an off-white solid. The product **13** (0.086 g, >99 %) was filtered and dried under vacuum at room temperature for 12 h. Characterization was accomplished using proton NMR in DMF-d_7.

Emulsion Polymerization.[39,40] To a 100-mL, three-necked, round-bottomed flask equipped with a condenser and a nitrogen inlet and outlet, D8-PS_{52}-$PMAA_{26}$-Cl (**3100**) (10 mg) in DMF (3 mL) and water (28 mL) were mixed at room temperature. The pH of the emulsion was measured with a pH meter. With magnetic stirring, SDS (50.0 mg) was

added, and 5 min later, styrene (1.0 mL) was added. Polymerization was achieved under a nitrogen atmosphere until the polymerization was completed. After 1.5 h, aqueous KPS stock solution (2.0 mL, 1.50 g of KPS in 100.0 mL of water) and aqueous $NaHCO_3$ (0.5 mL, 1.00 g of $NaHCO_3$ in 40.0 mL of water) were added. The mixture was stirred at room temperature for 0.5 h and was then placed in a thermostated oil bath at 80 ^oC. The polymerization was complete after 2 - 3 h. The emulsion was filtered off through cotton to remove some of aggregates. The pH of the emulsion was measured at room temperature.

References

(1) Narrainen, A. P.; Pascual, S.; Haddleton, D. M. *J. Polym. Sci.: Part A: Polym. Chem.* **2002**, *40*, 439.

(2) Feng, X.-S.; Pan, C.-Y.; Wang, *J. Macromol. Chem. Phys*. **2001**, *202*, 3403.

(3) Angot, S.; Taton, D.; Gnanou, Y. *Macromolecules*, **2000**, *33*, 5418.

(4) Tunca, U.; Karliga, B.; Ertekin, S.; Ugur, A. L.; Sirkecioglu, O.; Hizal, G. *Polymer*, **2001**, *42*, 8489.

(5) Patten, T. E.; Matyjaszewski, K. *Adv. Mater.* **1998**, *10*, 901.

(6) Teodorescu, M; Gaynor, S.C.; Matyjaszewski, K. *Macromolecules*, **2000**, *33*, 2335.

(7) Kickelbick, G.; Matyjaszewski, K. *Macromol. Rapid Commun*. **1999**, *20*, 341.

(8) Ziegler, M.; Matyjaszewski, K. *Macromolecules*, **2001**, *34*, 415.

(9) Xia, J.; Matyjaszewski, K. *Macromolecules*, **1999**, *32*, 2434.

(10) Perrier, S.; Berthier, D.; Willoughby, I.; Batt-Coutrot, D.; Haddleton, D. M. *Macromolecules*, **2002**, *35*, 2941.

(11) Haddleton, D. M.; Crossman, M. C.; Dna, B. H.; Duncalf, D. J.; Heming, A. M.; Kukulj, D.; Shooter, A. J. *Macromolecules*, **1999**, *32*, 2110.

(12) Liu, M.; Frechet, J. M. J. *Polym. Bull*. **1999**, *43*, 379.

(13) Tsarevsky, N. V.; Sarbu, T.; Gobelt, B.; M.; Matyjaszewski, K. *Macromolecules*, **2002**, *35*, 6142.

(14) Coessens, V.; Pintauer, T.; Matyjaszewski, K. *Prog. Polym. Sci*. **2001**, *26*, 337.

(15) Xia, J.; Matyjaszewski, K. *Macromolecules*, **1997**, *30*, 7697.

(16) Matthews, O. A.; Shipway, A. N.; Stoddart, J. F. *Prog. Polym. Sci*. **1998**, *23*, 1.

(17) Bosman, A. W.; Jansen, H. M.; Meijer, E. W. *Chem. Rev*. **1999**, *99*, 1665.

(18) Matyjaszewski, K.; Miller, P. J.; Pyun, J.; Kickelbick, G.; Diamanti, S. *Macromolecules* **1999**, *32*, 6526.

(19) Ohno, K.; Wong, B.; Haddleton, D. M. *J. Polym. Sci. Part A: Polym. Chem.* **2001**, *39*, 2206.

(20) Heise, A.; Diamanti, S.; Hedrick, J. L.; Frank, C. W.; Miller, R. D. *Macromolecules*, **2001**, *34,* 3798.

(21) Borner, H.; Beers, K.; Matyjaszewski, K.; Sheiko, S. S.; Moller, M. *Macromolecules*, **2001**, *34*, 4375.

(22) Ottaviani, M. F.; Bossmann, S.; Turro, N. J.; Tomalia, D. A. *J. Am. Chem. Soc.* **1994**, *116*, 661.

(23) Jendrusch-Borkowski, B.; Awad, J.; Wasgestian, F. *Journal of Inclusion Phenomena and Macrocyclic Chemistry* **1999**, *35*, 355.

(24) Vassilev, K.; Kreider, J.; Miller, P. D.; Ford, W. T. *Reactive & Functional Polymers* **1999**, *41*, 205.

(25) Vassilev, K.; Ford, W. T. *J. Polym. Sci.: Part A: Polym. Chem.* **1999**, *37*, 2727.

(26) Velarde-Ortiz, R.; Larsen, G. *Chem.Mater.* **2002**, *14*, 858.

(27) Chern, C.-S.; Lin, C.-H. *Polymer International* **1997**, *42*, 409.

(28) Narrainen, A. P.; Pascual, S.; Haddleton, D. M. *J. Polym. Sci.: Part A: Polym. Chem.* **2002**, *40*, 439.

(29) Feng, X.-S.; Pan, C.-Y.; Wang, *J. Macromol. Chem. Phys*. 2001, *202*, 3403.

(30) Choucair, A.; Lavigueur, C.; Eisenberg, A. *Langmuir*, **2004**, *20*, 3894.

(31) Niwa, M.; Higashizaki, T.; Higashi, N. *Tetrahedron* **2003**, *59*, 4011.

(32) Kazakov, S.; Muronetz, V. I.; Dainiak, M. B.; Izumrudov, V. A.; Galaev, I. Y.; Mattiasson, B. *Macromol. Biosci*. **2001**, *1*, 157.

(33) Olea, A. F.; Thomas, J. K. *Macromolecules* **1989***, 22,* 1165.

(34) Chu, D. Y.; Thomas, J. K. *J. Phys. Chem*. **1985**, *89*, 4065.

(35) Burguiere, C.; Pascual, S.; Bui, C.; Vairon, J.-P.; Charleux, B.; Davis, K. A.; Matyjaszewski, K.; Betremieux, I. *Macromolecules* **2001**, *34*, 4439.

(36) Liu, T.; Schuch, H.; Gerst, M.; Chu, B. *Macromolecules* **1999**, *32*, 6031.

(37) Schon, F.; Hartenstein, M.; Muller, A. H. E. *Macromolecules*, **2001**, *34*, 5394.

(38) Haddleton, D. M.; Perrier, S.; Bon, S.A.F. *Macromolecules*, **2000**, *33*, 8246

(39) Xu, Z.; Ford, W. T. *Macromolecules* **2002**, *35*, 7662.

(40) Xu, Z.; Ford, W. T. *J. Polym. Sci. Part A: Polym. Chem.* **2003**, *41*, 597.

CHAPTER IV

MORPHOLOGY STUDY OF AMPHIPHILIC BLOCK COPOLYMERS BY AFM

Abstract

Several morphologies of spherical and worm-like aggregates were prepared from (polypropylene imine) PPI dendritic block copolymers of polystyrene-*b*-poly(acrylic acid) (PS-*b*-PAA) in dilute solution. Aggregation was induced by the addition of polymer/DMF solutions to water. The morphology of the aggregates changed from spheres to worm-like and then back to spheres as water content increased to less than 75 % at a concentration of 0.2 (w/v) % block copolymer in DMF. Regardless of the different length of the PAA block with the fixed PS block length, all the aggregates showed the morphology reversibility by AFM images as water content was increased in DMF/water mixture.

Introduction

Amphiphilic block copolymers are well known to form either micelles or aggregates when dissolved in selective solvents, for example, a solvent where only one of the blocks is soluble.[1] Over the past few decades, amphiphilic block copolymers have

attracted various applications. Their ability to self-assemble and form stable micelles at very low polymer concentrations has led to a valuable area of polymer synthesis for effective surfactants,[2] drug carriers in drug delivery systems,[2-6] and templates in nanotechnologies.[3]

Amphiphilic block copolymers have either a linear or a branched topology. Block copolymers based on polystyrene (PS) and polyacrylic acid (PAA) are one variety of amphiphilic system that self-assembles in water.

The micelles can be formed when only one block of the polymer is soluble. In water, the micelles are formed from hydrophilic-hydrophobic diblock copolymer chains, where the core is formed by the hydrophobic block and the corona (or shell) by the hydrophilic block. By contrast, aggregates that have a hydrophilic core and a hydrophobic corona are formed in organic solvents. These are called reverse micelles (Scheme 1).[7,8]

Scheme 1. Different Types of Micelles

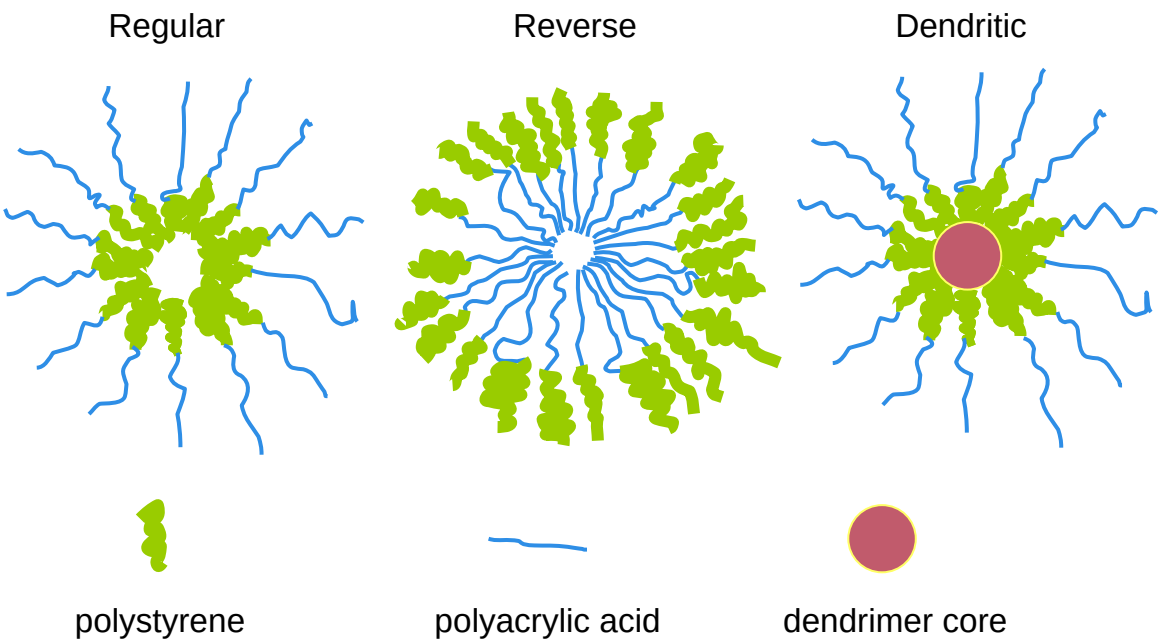

In regular micelles the micellar size and the aggregation number are independent of the polymer concentration and may change as a function of the block copolymer compositions. Most of these micelles are known to be spherical. However, they are reported to have other morphologies, such as cylinders, rods, worms, vesicles, hollow spheres, or even branched tubules, depending on the sample preparation, the temperature, the volume fraction, and the concentration.[7,8]

In most spherical block copolymer micelles, the corona blocks are much longer than the core blocks. The spherical micelles are mostly formed because the repulsive interactions among the corona chains are strong due to the relatively high density of

corona chains on the core surface. The corona chains in a good solvent extend away from a spherical core.[7-12]

Corona chain repulsion can balance the core interfacial tension effect, preventing an increase in the aggregation number and in the core size. The interfacial tension between the core and corona interface is minimized not only by an increase of the intercorona chain repulsion but also by an increase in the chain stretching of the micelle core.[7-12]

The strength of polymer-solvent interaction influences the morphology of aggregates.[7,12] The PS-solvent interaction affects the degree of stretching of the PS chains, while the PAA-solvent interaction is related to the repulsion among the corona chains. The solvent nature and composition determine the type of the copolymer-solvent interactions and affect the degree of swelling of the hydrophobic PS block, as well as the degree of ionization of PAA chains. With the solubility parameters of THF (δ = 18.6 $MPa^{1/2}$), DMF (δ = 24.8 $MPa^{1/2}$), and polystyrene (δ = 16.6-20.2 $MPa^{1/2}$), the degree of swelling of the PS chains is expected to be greater in THF than in DMF. On the other hand, to increase the strength of the PAA-solvent interaction, polar solvent should be considered. The dielectric constant of DMF (ϵ = 38.2) is higher than that of THF (ϵ = 7.5). Therefore, the strength of solvation of PAA by DMF should be stronger than that between PAA and THF. All these factors should be considered to understand the effect of the solvent on the morphology of the dendritic block copolymers.[7,12]

In general, aggregates are prepared from polystyrene-*b*-poly(acrylic acid) (PS-*b*-PAA) by addition of water to a solution of the polymer in a common solvent, such as DMF, for both PS and PAA blocks. Subsequently, the PS blocks start to associate to

form the micelles. In the early stage of micellization, the PS cores of the aggregates are generally highly swollen by DMF. The amount of the common solvent, DMF, in the PS gradually decreases due to transfer of DMF from the micelle to the water phase. Next, the concentration of linear polymers decreases and the solvent for the PS blocks is replaced. As a result, micelle core reduces the mobility of the chains. The structures of the aggregates become kinetically locked at some point in the water content range in the late stage of micellization.[7,8,12,13]

Thermodynamics and kinetics of micellization are important for the formation of the aggregates. When water content of the solvent mixture is relatively low, the morphology of the aggregates is mainly controlled by the thermodynamics. The thermodynamics of the micellization involves a force balance relating the repulsive interactions of the corona chains, the interfacial energy of the core/shell region, and the deformation of the PS blocks in the core.[10,14]

Kinetic aspects become very important with increasing water content. Two possible mechanisms such as chain insertion/expulsion (Scheme 2a) and micellar merger/splitting (Scheme 2b) have been suggested for the morphological transitions for the chain exchange of linear block copolymers between spherical micelles.[10,14-16]

Scheme 2. Possible Mechanisms for the Morphological Transition from Spheres to Rods.[14]

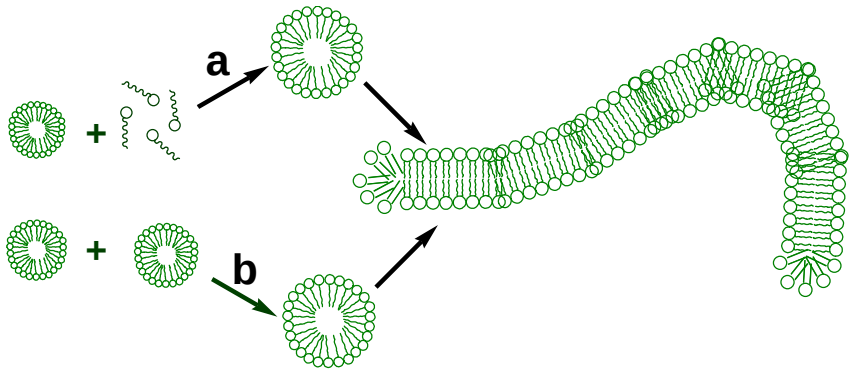

The first mechanism (Scheme 2a) involves a continuous insertion of single linear polymer chains into spherical micelles. The chain insertion increases the aggregation number as well as core dimension. Eventually the micelles change the structure from spheres to rod-like when the core diameter of the spherical micelles has reached some critical value.[10,14-16] Another possible mechanism (Scheme 2b) involves adhesive collisions of small spherical micelles which increase the aggregation number and form larger spherical micelles. Again, at some point, the morphology changes to rod-like. For both mechanisms, once the morphological transition occurs, further chain insertion or adhesive micelle collisions leads to an increase in the length of rod-like micelles.[10,14]

The kinetics of growth of aggregates via the insertion mechanism (Scheme 2a) depend on the polymer concentration as well as the mobility of the chains in and out of the micelles. Both the polymer concentration and the solvent content in the core decrease as the water content in the solvent mixture increases. The mobility of polymer chains seems to decrease significantly as the water content increases. Therefore, when the water

content is relatively low, the kinetics via the insertion mechanism (Scheme 2a) can be very fast because of the relatively high polymer concentration and the high mobility of the chains due to high solvent content in the core. At higher water contents, because of the lower polymer concentration and less chain mobility when there is low solvent content in the core, the kinetics of the insertion mechanism can become very slow.[10,14-16]

The kinetics of conversion of spherical micelles to rodlike micelles via the adhesive collision mechanism (Scheme 2b) depends on not only the mobility of chains for the structural rearrangement but also on the rate of adhesive collisions. Even if the chain mobility for the structural rearrangement of the micelles is reasonably high, it is possible that the efficiency of adhesive collision of the micelles is low. The low efficiency is a result of the strong interactions between the PAA and the solvent molecules, the partial ionization of the PAA blocks, and the resulting strong repulsion among the particles. Therefore, it can be expected that the efficiency of the adhesive collisions could be increased by reducing the charge density of the PAA and the repulsion between particles.[10,14] These transitions of rods to spheres depend mainly on the mobility of the chains to achieve a structure fission but do not involve the effective collision problem (Scheme 2).

The purpose of this research project is to study how the structures of dendritic block copolymers in selective solvents affect their micellar organization. In this study, atomic force microscopy (AFM) was used to characterize the evolution of the geometrical parameters, for example, the size and shape, of the micelles in the solid-state by AFM by evaporating the solvent. The effect of composition of the block copolymers on the morphology was also investigated.

In this chapter, the detailed study of the effect of the common solvent on the morphology of the diblock copolymers of polystyrene-*b*-poly(acrylic acid) on a dendrimer core is reported. In particular, the relationship between the degree of micellization and the nature of the common solvent, as well as the dependence of the aggregate structure on the compositions of the common solvent mixtures, are reported.

Results and Discussion

The formation of aggregates was studied as a function of water content for 0.2 (w/v) % solutions of PS_{48}-*b*-PAA_{104}-Cl (**12a**), PS_{48}-*b*-PAA_{215}-Cl (**12b**), and PS_{48}-*b*-PAA_{445}-Cl (**12c)** on a dendrimer core in DMF, prepared with the solution at pH 10 adjusted by the addition of ca. 0.1 M NaOH (pH ~13). DMF is a good solvent for both PS and PAA blocks but water is good only for the PAA blocks. The morphogenic effect of the solvent on the aggregates of polystyrene-*b*-poly(*t*-butyl acrylate) (D64-PS-*b*-P*t*BA-Cl) and polystyrene-*b*-poly(acrylic acid) (D64-PS-*b*-PAA-Cl) diblock copolymers on a dendrimer core was also studied by AFM.

AFM samples were prepared by spin coating the solutions of the polymers onto freshly cleaved mica. AFM images were acquired by operating in tapping mode with a silicon cantilever under ambient conditions.

Morphogenic Effects of Solvent on D64-pS-b-pAA-Cl Aggregates. The formation of aggregates is controlled by three factors. The three factors are the stretching or deformation of the hydrophobic chains in the aggregates core, the surface tension between the core and the solvent outside of the core, and the intercorona-chain interactions.

DMF and THF are well known good solvents for the PS blocks of PS-*b*-P*t*BA and PS-*b*-PAA copolymers. As for these specific dendritic PS-*b*-P*t*BA-Cl and PS-*b*-PAA-Cl copolymers, DMF is good for PAA blocks but THF is poor for PAA blocks. For the morphology of the aggregates of the dendritic PS-*b*-P*t*BA-Cl, DMF and THF were chosen as the common solvents.

Table 1 reports the relationship between the morphology of dendritic PS-Cl and PS-*b*-P*t*BA-Cl aggregates and the nature of the common solvent for the different PAA compositions. Spherical morphology was prevalent by the dendritic PS-P*t*BA polymers in both THF and DMF as shown in Table 1, regardless of PAA content increasing.

Table 1. Aggregate Morphologies of 0.2 (w/v) % of D64-PS-Cl and D64-PS-*b*-P*t*BA-Cl in THF and DMF.

polymer	structure	PS content (mol %)	PAA content (mol %)	THF/DMF
11	D64-PS_{48}-Cl	100	0	sphere
12a	D64-PS_{48}-*b*-P*t*BA_{104}-Cl	31.6	68.4	sphere
12b	D64-PS_{48}-*b*-P*t*BA_{215}-Cl	18.3	81.7	sphere
12c	D64-PS_{48}-*b*-P*t*BA_{445}-Cl	9.7	90.3	sphere

Dendritic PS-Cl. Spherical morphologies were obtained in both THF and DMF. Isolated aggregates with a spherical shape and monodisperse sizes were observed at a concentration of 0.2 (w/v) % block copolymer in THF (Figure 1).

However, the AFM image from DMF (not shown here) has very dense and circular surface aggregates with polydisperse sizes. Aggregates on local formation look to be formed multiple layers on the mica, which might be indicative of the non-uniform aggregation. As increasing in the polymer concentration, for example, 0.01 (w/v) %, 0.05 (w/v) %, and 0.2 (w/v) % in DMF, the aggregation number increases. For the moment that it takes to add DMF to water, the dendrimer molecules may flow and aggregate by a diffusion limited coalescence mechanism.[17] In contrast to DMF solutions, THF may evaporate too fast for the dendrimer aggregates to coalesce during spin coating.

Aggregates of the PS were investigated by dynamic light scattering. In pure DMF average sphere diameters of ~15 nm were measured for the intended D64-PS-PAA (0.1 mg/mL) material. A small amount of high molecular weight materials appeared as aggregates in the 60-400 nm range. Those aggregates could be bimodal or trimodal distributions which were observed with a peak in the intensity vs. diameter graphs.

(a)

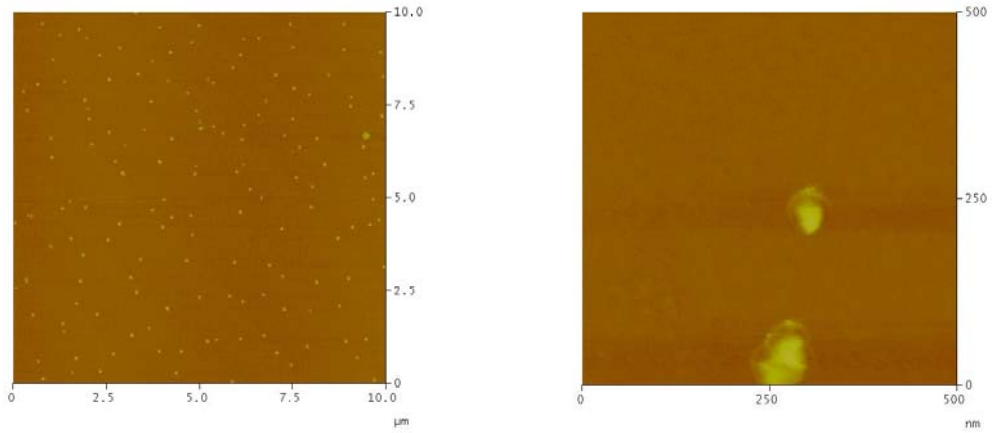

(b)

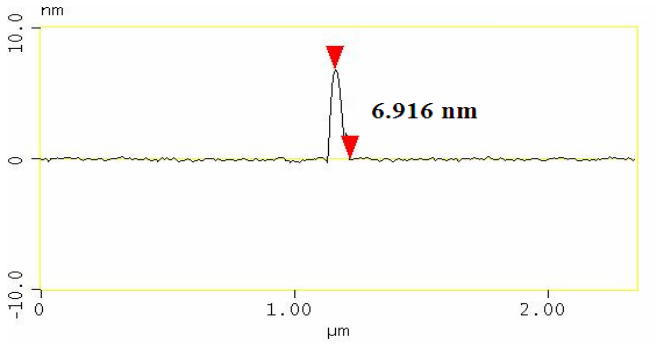

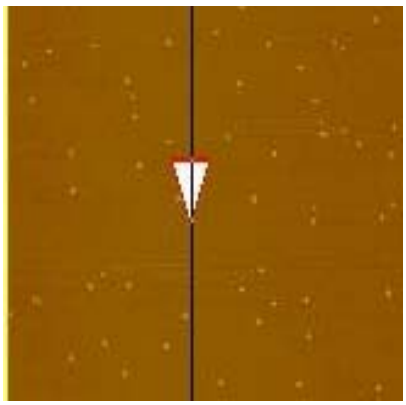

Figure 1. (a) AFM images of aggregates made by spin coating of the block copolymer (0.2 w/v) % in pS_{48}-Cl (**11**) in THF; (b) Section analysis.

Dendritic PS-*b*-P*t*BA-Cl. For all of the PS-*b*-P*t*BA-Cl block copolymers, isolated spherical aggregates with polydisperse sizes were observed at a concentration of 0.2 (w/v) % block copolymer in THF (Figures 2, 3, and 4). The increase in electrostatic repulsion may explain the formation of smaller aggregates in THF.

Regardless of the P*t*BA content, the aggregates prepared from THF showed only circular images. Like dendritic PS-Cl, the aggregates prepared from all the PS-*b*-P*t*BA-Cl block copolymers have the same elliptical streaked images from a 0.2 (w/v) % block copolymer in DMF (Figures 2, 3, and 4).

During the sample preparation for both dendritic PS-Cl and PS-*b*-P*t*BA-Cl, the PS chains are swollen with either DMF or THF. Over time during evaporation the solvent will remain either in the PS chains or in the PAA chains longer. THF has higher vapor pressure and lower viscosity than DMF. Due to slower evaporation, DMF may allow aggregates to spread out and move around on the mica surface. The aggregates end up densely packed into streaked aggregates in DMF. On the other hand in THF, aggregates may shrink and create more isolated spherical aggregates forming craters (Figure 3a and c) or disks (Figure 4a).

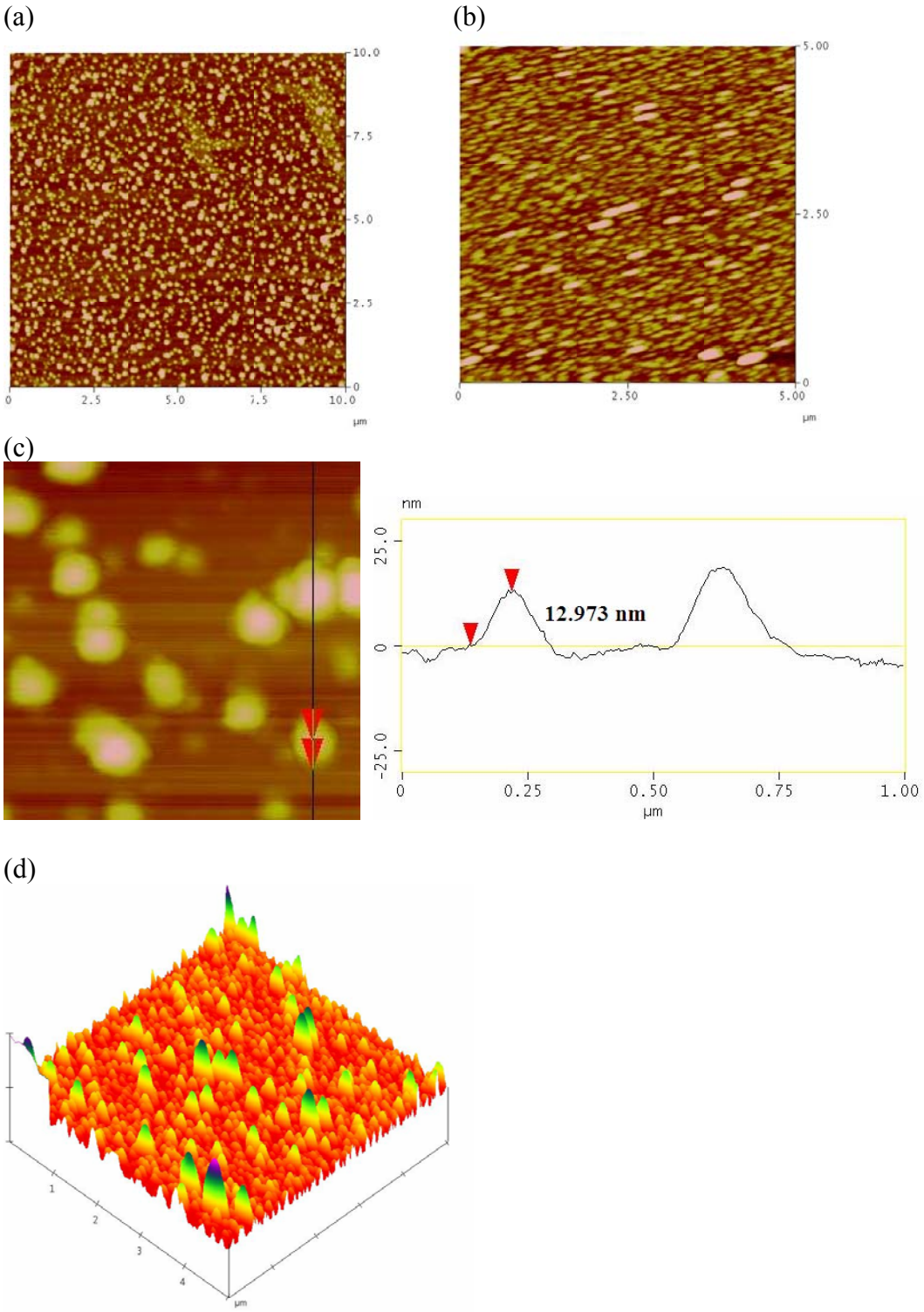

Figure 2. AFM images (height) of aggregates made by dissolution of the block copolymer (0.2 w/v %): (a) pS_{48}-*b*-p*t*BA_{104}-Cl (**12a**) in THF, (b) **12a** in DMF, (c) section analysis of **12a** in THF, (d) surface view of **12a** in DMF.

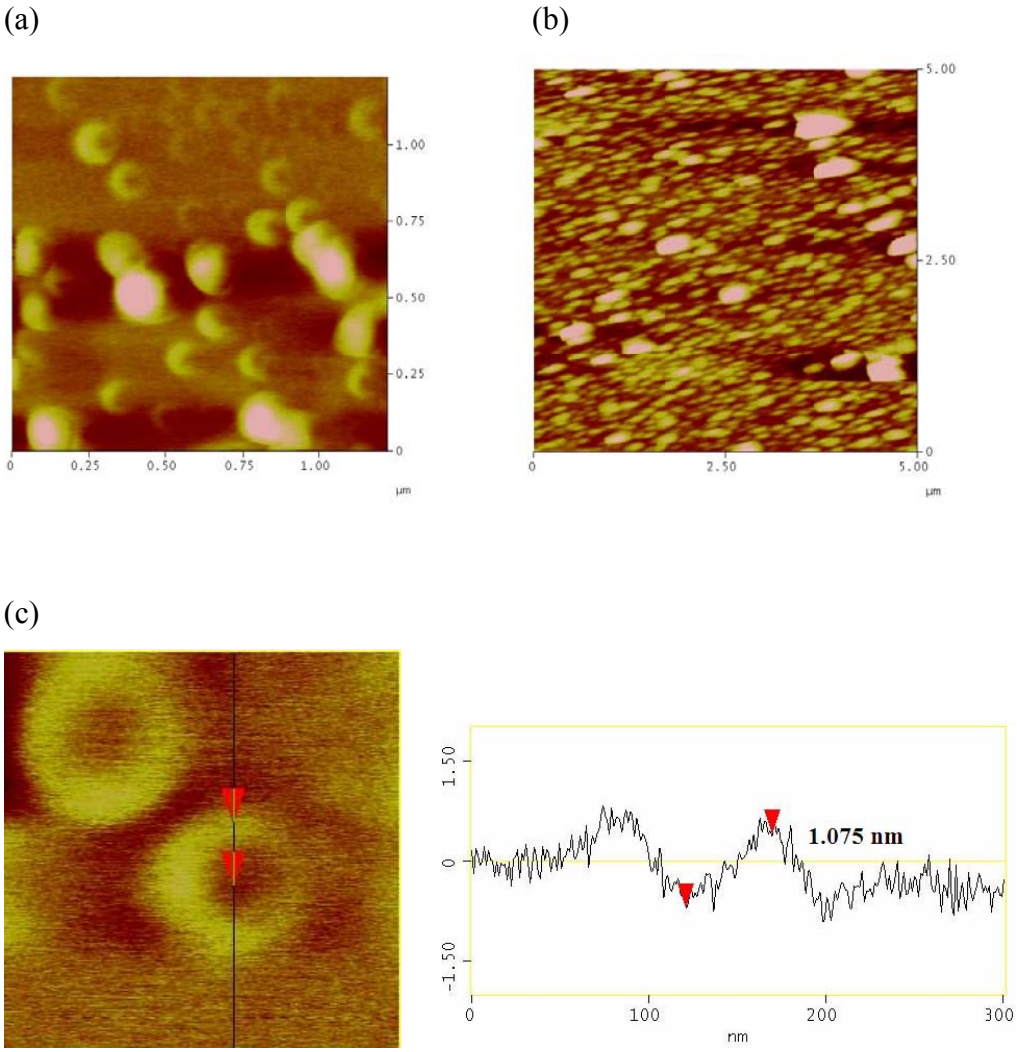

Figure 3. AFM height images of aggregates made by dissolution of the block copolymer (0.2 v/w %): (a) pS_{48}-*b*-p*t*BA_{215}-Cl (**12b**) in THF, (b) **12b** in DMF, (c) section analysis of **12b** in THF.

(a) (b)

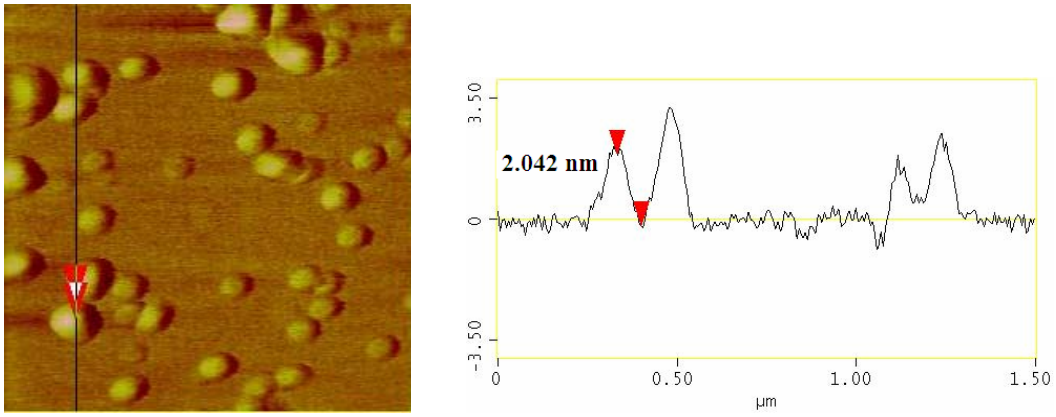

Figure 4. (a) AFM height image of aggregates made by dissolution of the block copolymer pS_{48}-*b*-p*t*BA_{445}-Cl (**12c**) (0.2 v/w %) in THF and (b) section analysis of **12c** in THF.

Aggregation of the Copolymers in DMF/Water Mixtures. Since water is a good solvent only for the PAA chains, the PS blocks start to aggregate when water is added. The interactions between the hydrophobic PS chain and the solvent mixture become less favorable and cause the aggregate to become less mobile when water is added to the block copolymer dissolved in DMF. The PAA chains are deprotonated and negatively charged in aqueous NaOH solution. As a result, there is stronger electrostatic repulsion among its chains. In the presence of electrostatic repulsion among the hydrophilic chains, higher water concentrations result in the aggregation of the chains and the formation of stable aggregates.

Dendritic PS-*b*-PAA-Cl. Since DMF is the only common solvent for both blocks of the dendritic PS-*b*-PAA-Cl polymers, DMF/water mixtures were prepared to explore the influence of water content on the aggregate morphology. An increase of water into the DMF solution makes the solvent poor for the PS blocks. In particular, the chain mobility of the PS is influenced by the water content that plays an important role in the course of micellization. Table 2 reports the spheres and worm-like shapes that were obtained in DMF/water mixtures over the range of PAA block lengths studied.

Table 2. Images of D64-PS-*b*-PAA-Cl, Polymers Spin-coated from a 0.2 (w/v) % DMF/Water Mixture at pH 10

polymer	DMF/Water mixture				
	2 % DMF	10 % DMF	25% DMF	50 % DMF	100 % DMF
D64-PS_{48}-*b*-PAA_{104}-Cl	-	-	sphere	worm-like	worm-like
D64-PS_{48}-*b*-PAA_{215}-Cl	sphere	sphere	worm-like	sphere	sphere
D64-PS_{48}-*b*-PAA_{445}-Cl	-	-	sphere	worm-like	sphere

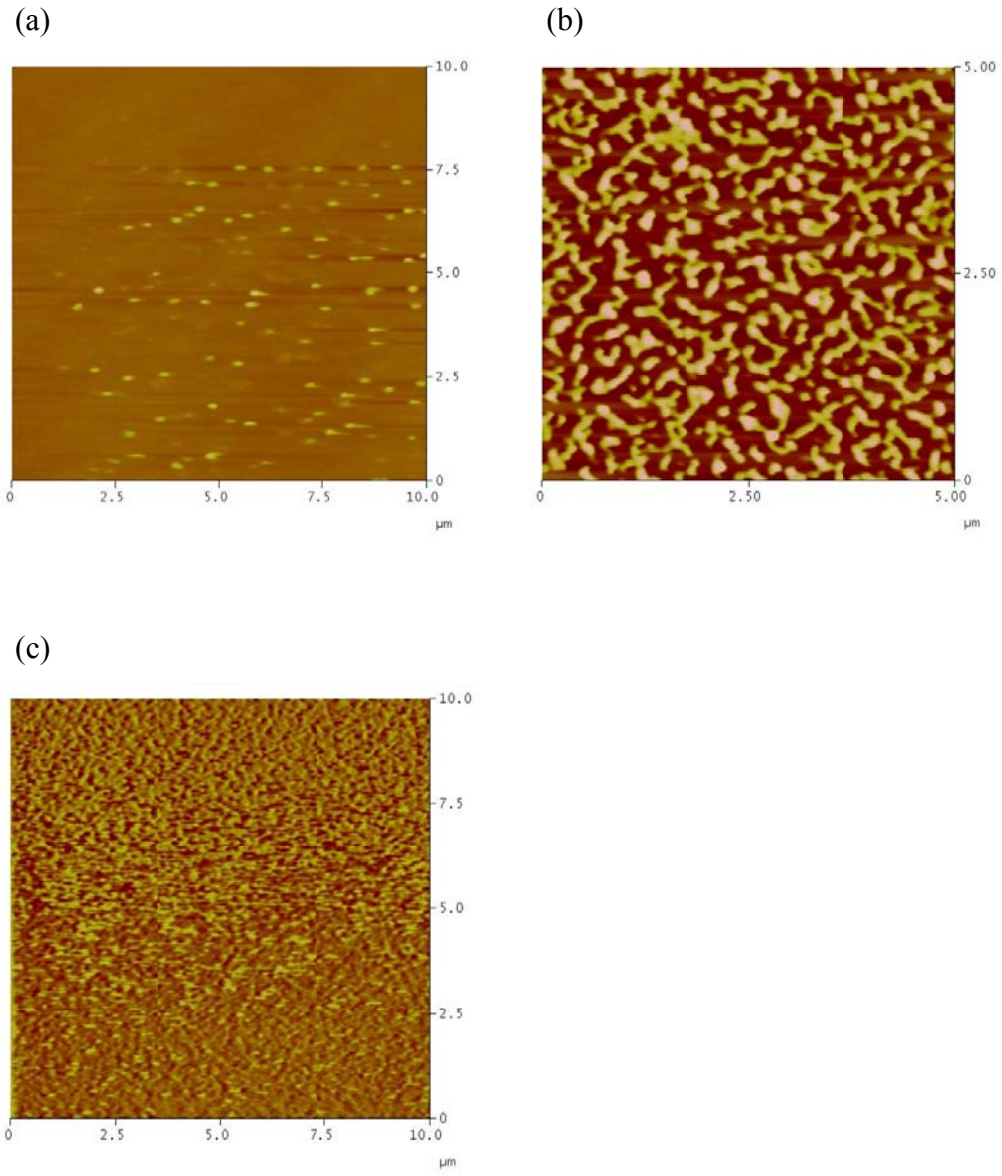

Figure 5. AFM height images of aggregates made from the block copolymer (0.2 (w/v) %): (a) pS_{48}-*b*-pAA_{104}-Cl (**12a**) in 25 % DMF, (b) **12a** in 50 % DMF, (c) **12a** in 100 % DMF.

For D64-PS_{48}-*b*-PAA_{104}-Cl (**12a**) individual aggregates were formed in a 25 (w/w) % DMF (Figure 5a). As the water content is increased to 50 wt %, as shown in Figure 5b, a new morphology started to develop. Both short and long worm-like (or

cylinder) aggregates were found to coexist along with spherical aggregates on the mica surface. These worm-like aggregates seem to be formed by the intermicellar assembly of the individual spherical aggregates. At 100 % DMF, short worm-like aggregates were found to not only be more densely packed but also coexist with spherical aggregates as the concentration of the polymer was increased (Figure 5c).

In the case of D64-PS_{48}-*b*-PAA_{215}-Cl (**12b**), both spherical and worm-like morphologies were observed over the range of water content at 2, 10, 25, 50, and 100 % DMF (Figure 6). At 2 % DMF, individual spherical aggregates appeared monodisperse from the dilute solution (Figure 6a). Meanwhile, the spherical aggregates obtained were also monodisperse and well isolated on the surface at 10 % DMF (Figures 6b-d). A morphological transition from spheres to worm-like aggregates occurred as the water content decreased from 10 % DMF (Figures 6b-d) to 25 % DMF (Figure 6e). The combination of the aggregates having the straight, curved, short, and long aggregates was observed at 25 % DMF. These aggregates might indicate that aggregation of spherical aggregates takes place on the mica surface at this specific condition on drying (Figure 6e). As water content decreased from 25 % DMF to 50 % DMF (Figure 6f), the morphology was again changed from worm-like to spherical aggregates. The spherical aggregates are somewhat monodisperse. Some clusters were formed and coexisted with the spherical aggregates. These clusters might be formed by self-assembly of the spherical aggregates. Spheres and clusters were seen and were rather polydisperse at 100 % DMF (Figures 6g and 6h). As concentration of the polymer increases, more clusters seem to be formed in 100 % DMF.

(a) 2 % DMF

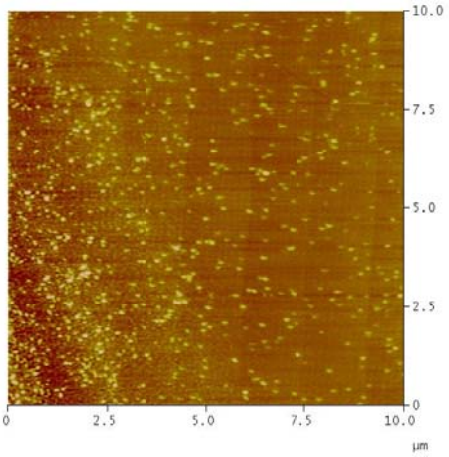

(b) 10 % DMF

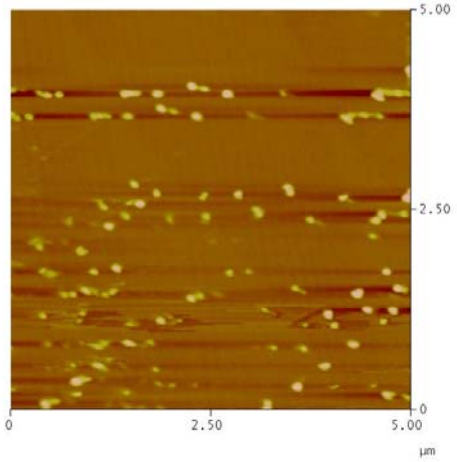

(c) 10 % DMF

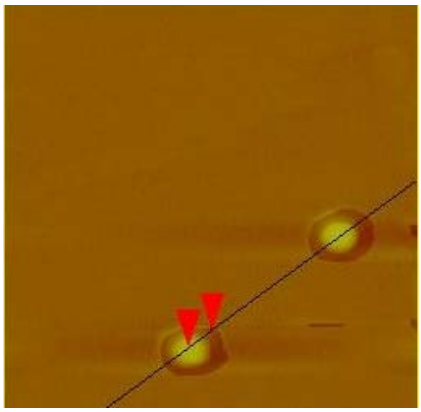

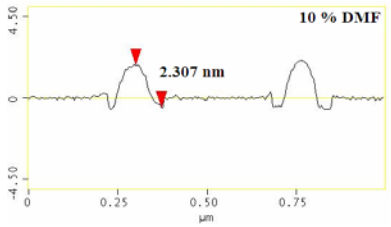

(d) 10 % DMF

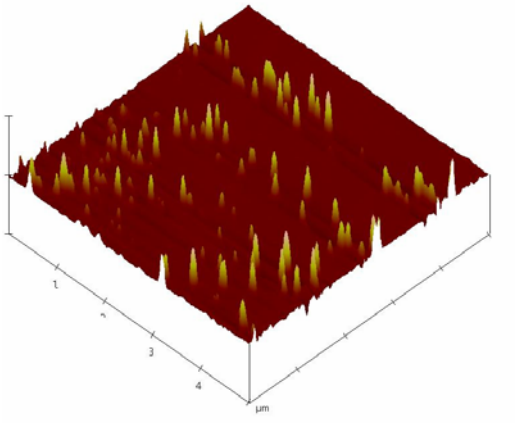

(e) Height Image (25 % DMF)

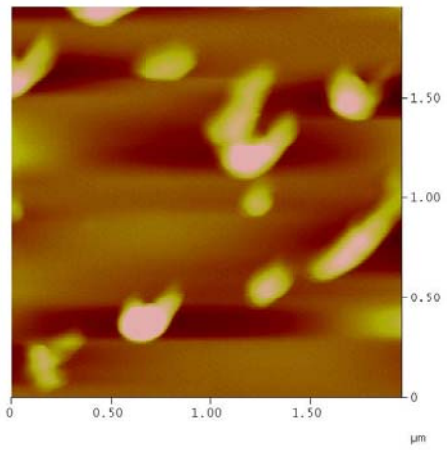

Phase Image (25 % DMF)

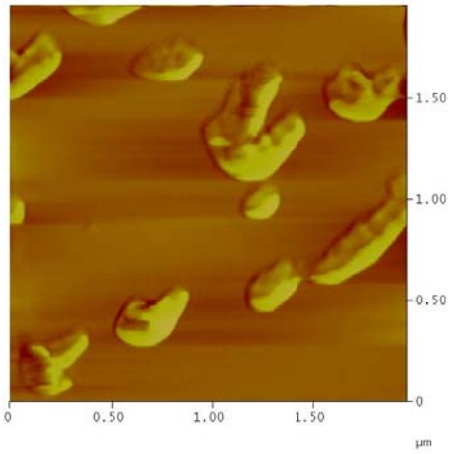

(f) Height Image (50 % DMF)

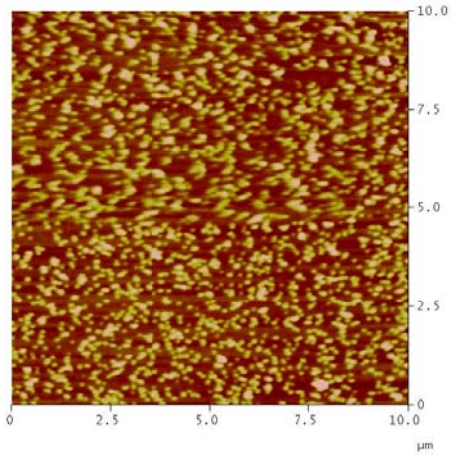

Phase Image (50 % DMF)

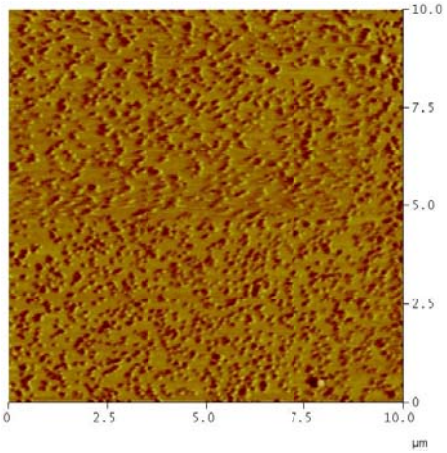

(g) Height Image (100 % DMF) Phase Image (100 % DMF)

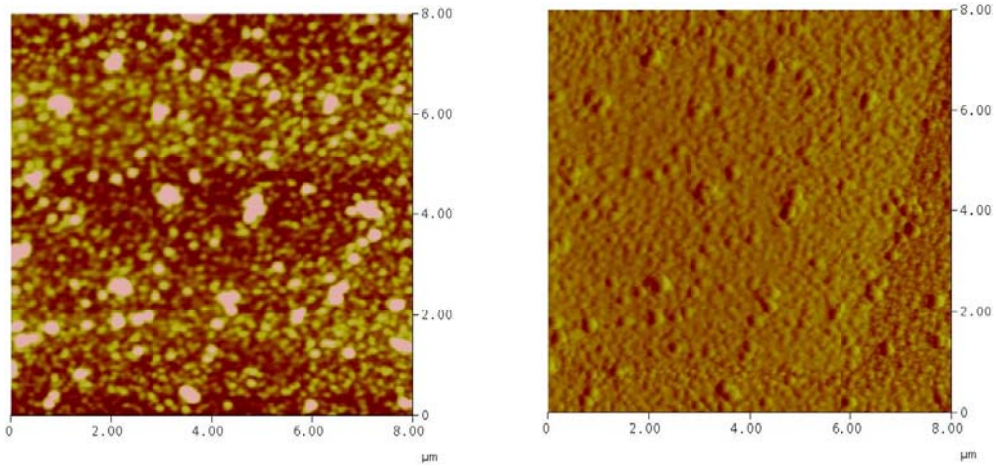

(h) (100 % DMF)

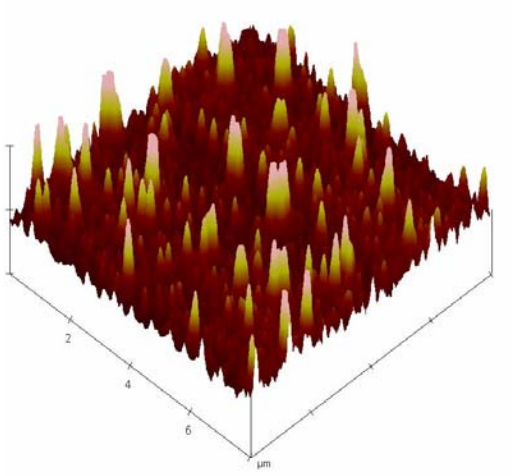

Figure 6. AFM images of aggregates made by spin-coating of the block copolymer (0.2 (w/v)%) in aqueous NaOH at pH~10: (a) height and phase images of pS_{48}-*b*-pAA_{215}-Cl (**12b**) in 2 % DMF, (b) **12b** in 10 % DMF, (c) section analysis of **12b** in 10 % DMF, (d) surface view of **12b** in 10 % DMF, (e) height and phase images of **12b** in 25 % DMF, (f) height and phase images of **12b** in 50 % DMF, (g) height and phase images of **12b** in 100 % DMF, (h) surface view of **12b** in 100 % DMF.

(a) Height Image (25 % DMF)

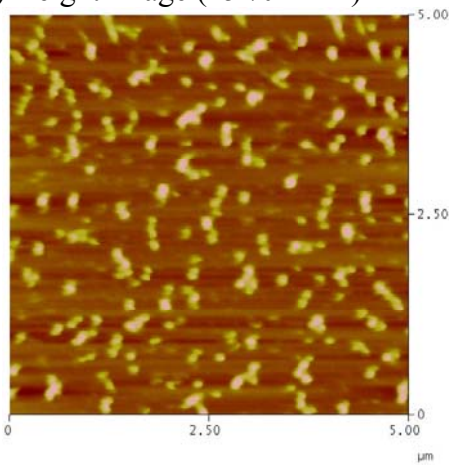

(b) Height Image (50 % DMF)

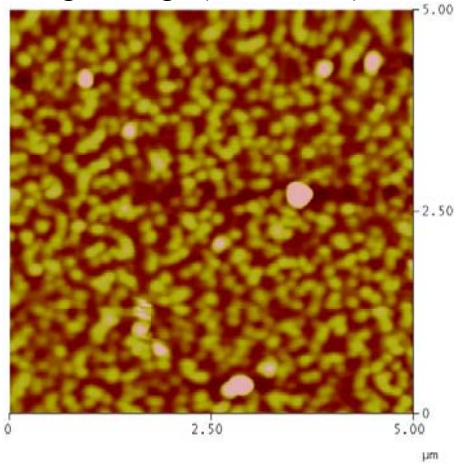

Phase Image (50 % DMF)

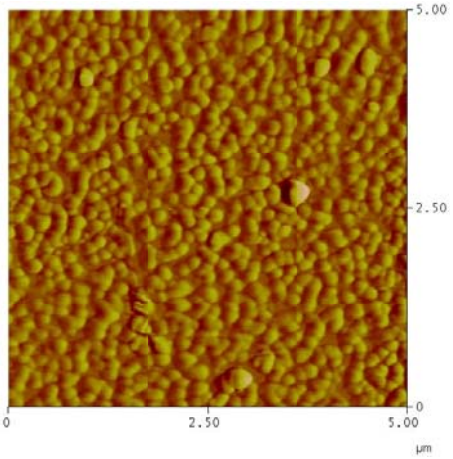

(c) Height Image (100 % DMF)

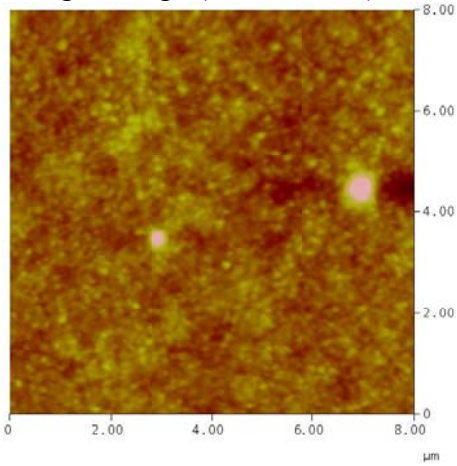

Phase Image (100% DMF)

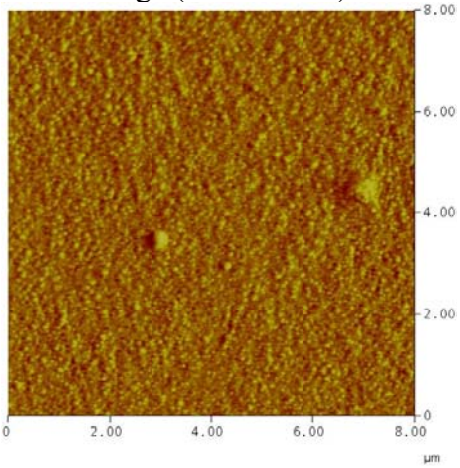

Figure 7. AFM images of aggregates made by spin-coating of the block copolymer pS_{48}-*b*-pAA_{445}-Cl (**12c**) (0.2 (w/v)%): (a) height image of **12c** in 25 % DMF, (b) height and phase images of **12c** in 50 % DMF, (c) height and phase images of **12c** in 100 % DMF.

As for D64-PS_{48}-*b*-PAA_{445}-Cl (**12c**), a transition was observed from spherical to worm-like to spherical as the DMF content increased from 25 % DMF to 50 % DMF to 100 % DMF (Figure 7). At 25 % DMF, spherical aggregates were well isolated and monodispersed (Figure 7a). However, short worm-like aggregates were seen with spherical ones as DMF content increased in 50 % DMF solution (Figure 7b). Worm-like aggregates were back to form spherical ones but more and more densely packed on the surface as concentration of the polymer increased in 100 % DMF solution (Figure 7c). The morphologies of the dendritic PS-*b*-PAA-Cl aggregates in DMF only show spherical aggregates that seem packed densely and are hardly seen in isolated particles on the surface in general. However, there are both spherical and worm-like aggregates as water content increases gradually.

The morphological reversibility was achieved by water addition method. The modified water addition method used for this study was to add the block copolymers in DMF slowly into the basic aqueous solution. In general, the conventional water method is to add water into the polymer solution gradually. Therefore, by selecting the appropriate solvent, one can prepare aggregates whose size or morphology is tunable by, or resistant to, changes in the water concentration. All of the aggregate structures are formed under conditions of kinetic control.

Conclusions

Spin coating of solution of PS-*b*-PAA block copolymers onto mica produced spherical and worm-like aggregates in AFM images. These AFM images show that the materials have aggregation characteristics of amphiphilic PS-PAA linear block copolymers.

From THF solutions the PS_{48} and the PS_{48}-P*t*BA_{104}, THF evaporated faster and the polymers hardened before the polymers had time to spread to a thinner layer during spin coating. The same polymers spin coated from DMF left streaked images, indicating that the polymer spread out to a thinner layer as the DMF evaporated slower.

The transition between spherical and worm-like aggregates is the greatest morphological change seen in the dendritic PS-*b*-PAA-Cl polymers as DMF/water content is varied. When water content is less than 75 %, the morphological transitions are reversible from sphere to worm-like to sphere. It indicates regardless of PAA block lengths that the kinetics of aggregate formation is fast and the formation of aggregates is controlled by thermodynamics of micellization.

Future Work

By maintaining the shorter hydrophilic blocks, an increase in the hydrophobic block length of the dendritic polystyrene-*b*-poly(acrylic acid) should be further studied for the detailed effect of the common solvent on the morphology of the block copolymers. Shorter hydrophobic (PS) blocks and longer hydrophilic (PAA) blocks are also possibly considered. Longer hydrophilic blocks with shorter hydrophobic blocks

with dendritic block copolymers could be much better dispersed in the aqueous solution. In particular, the relationship between the degree of aggregation and the nature of the common solvent as well as the dependence of the aggregate structure on the compositions of the common solvents should be studied. The further study would allow application to the synthesis of the polymer colloids 10-100 nm in diameter that are monodisperse. The amphiphilic poly(styrene-*b*-methacrylic acid) with a dendrimer core could possibly form unimolecular micelles dispersed in aqueous DMF solution. It is important to know what the optimum PS and PAA block lengths of the polymer colloids should be for amphiphilic unimolecular aggregates onto a dendrimer core

Furthermore, the effect of the array of different block lengths in both PS and PAA block on aggregate size and aggregate morphology could be determined. Therefore, one could prepare aggregates on a dendrimer core, whose size is tunable by changes in the water concentration.

Experimental Section

Sample preparation.[6,11,18] A 2 wt % solution of each diblock copolymer was prepared in DMF, which is a common solvent for both polystyrene (PS) and poly(acrylic acid)(PAA) blocks.

Subsequent addition of the polymer/DMF solutions to a basic solution (pH ~10) adjusted by the addition of ca. 0.1 M NaOH (pH ~13), i.e. polymer/DMF to basic water, at a rate of 1 drop every ~5 s with vigorous stirring induced aggregation of the PS blocks.

The addition to water was continued until the desired concentration had been reached: 2, 10, 25, 50, and 100 wt % DMF, respectively.

AFM Experiments.[6,19,20] Samples for AFM analysis were prepared by solvent spin coating at room temperature, starting from a solution of 0.1 to 2 mg of dendritic polymer (PS-PAA) in 1 mL of THF or DMF. The freshly cleaved mica was rinsed with deionized water and dried under a stream of nitrogen gas. Typically, 2 drops of the solution were applied on a 1 x 1 cm^2 piece of the mica. The mica was then spun for 120 sec at a rate of ~1.8 x 10^3 rpm to spread the solution out evenly on the surface of the mica. Samples were analyzed after complete evaporation of solvent at room temperature. The AFM microscope was operated in tapping mode (TM), a procedure that is known to minimize the sample distortion due to mechanical interactions between the AFM tip and the surface. All TM-AFM images were recorded in ambient atmosphere at room temperature with a Nanoscope IIIa (Veeco, Santa Barbara, CA). The probes are commercially available silicon tips with a spring constant of 24-52 N/m, a resonance frequency in the 264-339 kHz range, and a typical radius of curvature of 10-15 nm.

References

(1) Yu, K.; Zhang, L.; Eisenberg, A. *Macromolecules* **1996**, *12*, 5980-5984.

(2) Kang, Y.; Taton, T. A. *Macromolecules* **2005**, *38*, 6115-6121.

(3) Minatti, E.; Viville, P.; Borsali, R.; Schappacher, M.; Deffieux, A.; Lazzaroni, R. *Macromolecules* **2003**, *36*, 4125-4133.

(4) Atanasov, V.; Sinigersky, V.; Klapper, M.; Muellen, K. *Macromolecules* **2005**, *38*, 1672-1683.

(5) Choucair, A.; Lavigueur, C.; Eisenberg, A. *Langmuir* **2004**, *20*, 3894-3900.

(6) Matmour, R.; Lepoittevin, B.; Joncheray, T. J.; El-khouri, R. J.; Taton, D.; Duran, R. S.; Gnanou, Y. *Macromolecules* **2005**, *38*, 5459-5467.

(7) Yu, Y.; Zhang, L.; Eisenberg, A. *Macromolecules* **1998**, *31*, 1144-1154.

(8) Zhang, L.; Eisenberg, A. *Polymers for Advanced Technologies* **1998**, *9*, 677-699.

(9) Zhang, L.; Eisenberg, A. *Macromolecules* **1996**, *29*, 8805-8815.

(10) Burke, S. E.; Eisenberg, A. *Langmuir* **2001**, *17*, 6705-6714.

(11) Zhang, L.; Eisenberg, A. *Journal of the American Chemical Society* **1996**, *118*, 3168-3181.

(12) Choucair, A.; Eisenberg, A. *European Physical Journal E: Soft Matter* **2003**, *10*, 37-44.

(13) Zhang, L.; Shen, H.; Eisenberg, A. *Macromolecules* **1997**, *30*, 1001-1011

(14) Zhang, L.; Eisenberg, A. *Macromolecules* **1999**, *32*, 2239-2249.

(15) Haliloglu, T.; Bahar, I.; Erman, B.; Mattice, W. L. *Macromolecules* **1996**, *29*, 4764-4771.

(16) Choucair, A. A.; Kycia, A. H.; Eisenberg, A. *Langmuir* **2003**, *19*, 1001-1008.

(17) Elbs, H.; Fukunaga, K.; Stadler, R.; Sauer, G.; Magerle, R.; Krausch, G. *Macromolecules* **1999**, *32*, 1204-1211.

(18) Matejicek, P.; Humpolickova, J.; Prochazka, K.; Tuzar, Z.; Spirkova, M.; Hof, M.; Webber, S. E. *Journal of Physical Chemistry B* **2003**, *107*, 8232-8240.

(19) Xu, F. T.; Street, S. C.; Barnard, J. A. *Langmuir* **2003**, *19*, 3066-3070.

(20) Simon, P.; Adhikari, R.; Lichte, H.; Michler, G. H.; Langela, M. *Journal of Applied Polymer Science* **2005**, *96*, 1573-1583.

CHAPTER V

Concluding Remarks

A variety of amphiphilic dendritic molecules have been made using poly(propylene imine) dendrimers (PPI) DAB-*dendr*-$(NH_2)_n$ (n = 8, 32, and 64). These molecules have shown a variety of functionalities at the ends of the dendritic spheres which have allowed for dispersion and determination of the structure of nanomaterials.

Hydrophilic amide dendrimers were synthesized with three different PPI dendrimer generations (G2, G4, and G5) for NMR self-diffusion measurements. Three hydrophilic amide dendrimers show that the self-diffusion coefficients of the dendrimers in aqueous gels of poly(vinyl alcohol) decrease with increasing molecular size of the diffusant, as PVA concentration increases, and as temperature decreases. In NMR relaxation time measurements, the terminal protons are more mobile than the core protons for all the generations of the dendrimers. The mobility for all protons is also slower as dendrimer generation gets larger.

Deuterated tertiary amine dendrimers with hydrophobic chains on every end were synthesized by reductive amination of primary amine PPI dendrimers with $NaBD_4$ in CD_3COOD. This method allows for the reductive ethylation in a one pot reaction. The

synthesis of these dendrimers was an efficient method to complete conversion to tertiary amine dendrimers.

Atom transfer radical polymerization (ATRP) allowed for the synthesis of the monodisperse branched polystyrene with chain lengths of ~50 repeat units from dendrimer chain ends. Amphiphilic poly(styrene-*b*-acrylic acid) with a dendrimer core was synthesized by block copolymerization of styrene and *tert*-butyl acrylate by ATRP followed by hydrolysis of the *tert*-butyl esters to carboxylic acids.

Amphiphilic poly(styrene-*b*-acrylic acid) with a dendrimer core was synthesized for use as a template for small and monodisperse styrene latexes during the seed growth emulsion polymerization. Semi-continuous and surfactant-free emulsion polymerization of styrene with PS-PMAA-shelled dendrimer G2, initiated by KPS, produced particles with diameters of more than 100 nm. More polydisperse latexes with diameters of 45-55 nm were produced when SDS was present. The study of the relation between ionization and aggregation properties at variable pH showed that the branched amphiphlic PS-PMAA and PS-PAA-shelled dendrimers had aggregation characteristics of amphiphilic polystyrene-polyacrylic acid block copolymers.

Amphiphilic poly(styrene-*b*-acrylic acid) formed aggregates in DMF/water mixtures. AFM images showed reversible morphological transitions from spherical to worm-like to spherical when water content was less than 75 %.

VITA

Young Hie Kim

Candidate for the Degree of

Doctor of Philosophy

Thesis: AMPHIPHILIC BLOCK COPOLYMERS ON A DENDRIMER CORE

Major Field: Chemistry

Biographical:

Education: Received Bachelor of Science Degree in Chemistry at Kangwon National University, Korea in February 1984. Received Masters of Science Degree in Organic Chemistry at Kangwon National University, Korea in February 1986. Received Masters of Science Degree in Organic Chemistry at University of Minnesota, Duluth, MN in February 1994. Received Masters of Science Degree in Analytical Chemistry at Purdue University, West Lafayette, IN in February 1997. Completed the requirements for the Doctor of Philosophy with a major in Chemistry at Oklahoma State University, Stillwater, Oklahoma in May 2007.

Experience: Full-time teaching associate, Kangwon National University, Korea 1987 and 1991. Research Assistant, Kangwon National University, Korea 1991-1992. Teaching Assistant, University of Minnesota, Duluth, Minnesota 1992-1994. Special teaching assistant for summer session, University of Minnesota, Duluth, Minnesota 1993. Teaching Assistant and Research Assistant, Purdue University, West Lafayette, Indiana 1994-1997. Teaching Assistant and Research Assistant, Oklahoma State University, Stillwater, Oklahoma 1999-2006

Professional Membership: American Chemical Society

Name: Young Hie Kim. Date of Degree: May, 2007

Institution: Oklahoma State University Location: Stillwater, Oklahoma

Title of Study: Amphiphilic Block Copolymers on a Dendrimer Core

Pages in Study: 119 Candidate for the Degree of Doctor of Philosophy

Major Field: Chemistry

Scope and Method of Study: The purpose of this research was to synthesize amphiphilic block copolymers on a dendrimer core and to use the polymers as templates for styrene latexes at the nanoscale. Materials in this research included amphiphilic dendrimers with both polystyrene/poly(*t*-butyl acrylate) and polystyrene/poly(acrylic acid) at end branches, and dendritic polystyrene latexes. The dendrimers with amphiphilic end branches were for dispersion of nanomaterials and were for use as molecular weight and size standards and hosts for the transport of biologically important guests. Dendritic polystyrene latexes were for applications in nanotechnology.

Findings and Conclusions: The 64-branch poly(propylene imine) (PPI) dendrimer was converted to the dendrimer initiator with 2-bromoisobutyramide end groups. Polystyrene (PS) was grown by atom transfer radical polymerization (ATRP), and poly(*tert*-butyl acrylate) (P*t*BA) was then grown by ATRP. The *tert*-butyl protecting groups of the PS-P*t*BA block copolymers were removed to give poly(styrene-*b*-acrylic acid) (PS-PAA). The measured molecular weights were much less than the calculated molecular weights of star polymers with 64 branches and also larger than the molecular weights calculated for linear PS or P*t*BA. The molecular weights increased as the calculated degree of polymerization of the P*t*BA segment increased, which supported the growth of P*t*BA blocks. The branched amphiphilic PS-PAA block copolymers were stars with small numbers of branches resulting from growth at a small number of initiator sites per dendrimer. Styrene was polymerized in emulsions containing the dendritic PS-PAA. The resulting polystyrene latexes were broader in particle size distribution and 40-60 nm in diameter in the presence of the surfactant sodium dodecyl sulfate (SDS), however, narrower in particle size distribution and over 100 nm in diameter in the absence of SDS. Branched dendritic aggregates of the PS-PAA showed aggregation characteristics of amphiphilic PS-PAA block copolymers.

Advisor's Approval:____Warren T. Ford_____